Photorhabdus virulence factors

Yang, Guowei

Award date:
2005

Awarding institution:
University of Bath

PHOTORHABDUS VIRULENCE FACTORS

Submitted by Guowei Yang
for the degree of Doctor of Philosophy
of the University of Bath
2005

Guowei Yang

ProQuest LLC
789 East Eisenhower Parkway
P.O. Box 1346
Ann Arbor, MI 48106-1346

ABSTRACT

Photorhabdus luminescens is a Gram-negative, bioluminescent bacterium belonging to the *Enterobacteriaceae*. *Photorhabdus* lives in a "symbiosis of pathogens" with entomopathogenic nematodes belonging to the *Heterorhabiditae*. Previous research suggests that *Photorhabdus* genome may contain a large number of novel genes involved either in pathogenicity, symbiosis, or both. These include high molecular weight insecticidal Toxin Complexes, the makes caterpillars floppy toxin (Mcf1), proteases and lipases. In my thesis, I will present some more identified virulent factors including Mcf2, *Photorhabdus* virulence cassettes (PVCs), and some secreted proteins in *Photorhabdus*.

mcf2 was identified as a homologue of *mcf1* within the same *P. luminescens* W14 genome. The predicted amino acid sequence of Mcf2 is similar to Mcf1 but differs at its N-terminus which encodes a HrmA-like domain. Induced Mcf2 carrying *E. coli* kill caterpillars at the same speed as *E. coli* carrying Mcf1-both recombinant bacteria killed 50% of the insects in 60-70 h suggesting that *mcf2* is another virulent factor in *Photorhabdus luminescens*. And the *mcf2*⁻ strain show no difference in killing insects suggests that *Photorhabdus* may employ 'functional redundancy' in toxins capable of killing the insect host.

Two recently sequenced genomes of the insect pathogenic bacterium *Photorhabdus* contain phage related loci encoding putative toxin effector genes, we termed the '*Photorhabdus* virulence cassettes' or PVCs. Comparison of the genomic organization of several PVCs shows that they have a conserved phage-like structure with a variable number of putative anti-insect effectors encoded at one end. Recombinant *E. coli* expressing PVC containing cosmids from *Photorhabdus* have insecticidal activity against moth larvae. Surprisingly, electron microscopy shows that the PVCs are large structures similar to the antibacterial R-type pyocins. However, unlike these bacteriocins, the PVCs of *Photorhabdus* have no demonstrable antibacterial activity. Instead, injection of PVCs destroys the insect's hemocytes, which show dramatic actin cytoskeleton condensation, and then kills the moth larvae itself. Expression of these putative effectors directly inside cultured cells shows that they are capable of re-

arranging the actin cytoskeleton, and suggests their involvement in PVC-associated cell toxicity.

P. asymbiotica has been associated with human infection in the USA and Australia and is not proven to exist as a nematode symbiont (although it is pathogenic to insects). The supernatant of *P. asymbiotica* grown at 30 °C and 37°C were examined via two-dimensional (2D) gel electrophoresis. Visual examination of 2D gels of *P. asymbiotica* at 30 °C and 37°C showed several differences. S15 was identified which expressed at 30 °C but not 37°C. Over-expression S15 in *E. coli* could form *E. coli* cell chains and make nematodes clamping. This phenotype is very similar to aggregation factor in the natural supernatant of *photorhabdus*. PCR mutagenesis analysis reveals that two regions are essential for fibre formation.

The last part of my thesis details of a random knock out library in *P.luminescens* subsp. *laumondii* strain TT01. This library was screened for knock out of specific genes but in general, targeted gene knock out is more efficient.

DEDICATION

For my parents,

Thank you so much for your love, help and support

ACKNOWLEDGEMENTS

Thank to everyone who has helped and support me during my PhD studies.

Thank you to Dr. Nick Waterfield for your enthusiasm, support and technical advice, and to all others in the lab for the same reasons. To Professor Richard ffrench-Constant, my supervisor, a special thank you for giving me the opportunity to undertake this interesting project and for your encouragement and support. I would also like to thank Dr. Susan Joyce and Dr. David Clarke for gene knock out technology, Ursula Potter for her assistance with electron microscopy, Ursula Gerike for running the 2D gel electrophoresis, Jenna Hughes for MALDI-ToF analysis of protein samples, Andrea Dowling and Barbara Reaves for assistance with tissue culture and Paul Wilkinson for all our DNA sequencing.

Finally, a special thanks to Honghong Li, you have always been there for me, it is appreciated so much, and I can not thank you enough.

ABBREVIATIONS

aa	Amino acid
BH3	Bcl homology 3
bp	Base pairs
Bt	*Bacillus thuringiensis*
CFU	Colony forming units
CNF	Cytotoxic necrotizing factor
dH_2O	Distilled water
DMEM	Dulbeccos Modified Eagles Media
GFP	Green fluorescent protein
HPLC	High Performance Liquid Chromatography
IJ	Infective Juvenile
K122	*P. temperate* subsp. *temperate* strain K122
LB	Luria Bertani
Mcf1	Makes caterpillars floppy 1
Mcf2	Makes caterpillars floppy 2
OD	Optical density
ORF	Open reading frame
PAIs	Pathogenicity islands
PBS	Phosphate Buffered Saline
PCR	Polymerase chain reaction
PVC	*Photorhabdus* Virulence Cassettes
RTX	Repeats in toxins
SDS-PAGE	Sodium-dodecyl sulphate polyacrylamide gel electrophoresis
SEM	Scanning Electron Microscopy
TCA	Trichloroacetic acid
Tcs	Toxins complexes
TEM	Transmission electron microscopy
TEMED	N, N, N', N'-tetramethylethylene diamine
TTO1	*P.luminescens* subsp. *laumondii* strain TT01
TTSS	Type III secretion system
W14	*P.luminescens* subsp. *akhurstii* strain W14

CONTENTS

Chapter 2 Materials and Methods

Chapter 3 Identification of *mcf2*

Chapter 4 *Photorhabdus* Virulence Cassettes (PVCs)

Chapter 5 S15- a temperature dependant Secreted Protein in *Photorhabdus*

CHAPTER 1

INTRODUCTION

Photorhabdus is Gram-negative, nematode-associated, insect pathogenic bacteria belonging to the Enterobacteriaceae. *Photorhabdus* was initially identified as *Xenorhabdus luminescens* but DNA-relatedness studies and phenotypic differences resulted in separation into a new genus, *Photorhabdus* (Boemare et al.1993).

1.1 *Photorhabdus* taxonomy

Bacteria associated with entomopathogenic nematodes fall into two genera, *Photorhabdus* and *Xenorhabdus*. The *Photorhabdus* genus was recently split into three species, *P. luminescens*, *P. temperata* and *P. asymbiotica* (Fischer-Le Saux et al. 1999; ffrench-Constant et al. 2003). Two of these genera have also been subdivided into new subspecies. Thus, the *P. luminescens* group has three subspecies, *luminescens*, *akhurstii* and *laumondii*, and the *P. temperata* group has one subspecies, *temperata*. The third species group, *P. asymbiotica*, which consists of isolates from human wounds recovered in the apparent absence of a nematode vector, has not yet been subdivided. However, clinical isolates from America and Australia show very different 16S rRNA sequences, suggesting that they may be distantly related to each other (ffrench-Constant et al. 2003).

Photorhabdus strains used in my research are: *P.luminescens* subsp. *akhurstii* strain W14 (W14), isolated from its nematode symbiont in Florida, USA and *P.luminescens* subsp. *laumondii* strain TT01 isolated from its nematode symbiont from Trinidad; another strain I used is *Photorhabdus asymbiotica* strain ATCC43949-clinical isolates of *Photorhabdus* from human infections in Australia and USA without an apparent nematode vector have been identified (Peel et al. 1999). It is thought that incidence of these infections is most likely underestimated given the unfamiliarity of this pathogen to clinical laboratories identifying the infective bacterium and implicate *P. asymbiotica* as an emerging human pathogen (Gerrard et al. 2004).

1.2*Photorhabdus luminescens* and its host

Pathogenicity and symbiosis are central to bacteria-host interactions. Although several human pathogens have been subjected to a functional genomic analysis, we still understand little about bacteria-invertebrate interactions despite their ecological prevalence (ffrench-Constant et al. 2003). Normally, interactions between bacteria and invertebrates are often intractable and difficult to study in laboratory, but *Photorhabdus luminescens* forms a high tractable system in which the bacteria, their nematode vector and insect host can be readily cultured in the laboratory (Forst et al. 2001).

Photorhabdus lives in a "symbiosis of pathogens" with nematodes that invade insects. That is, it is symbiotic with entomopathogenic nematodes belonging to the Heterorhabiditae (Forst et al. 1997) but becomes pathogenic after release from the nematode into the insect blood system (hemocoel).

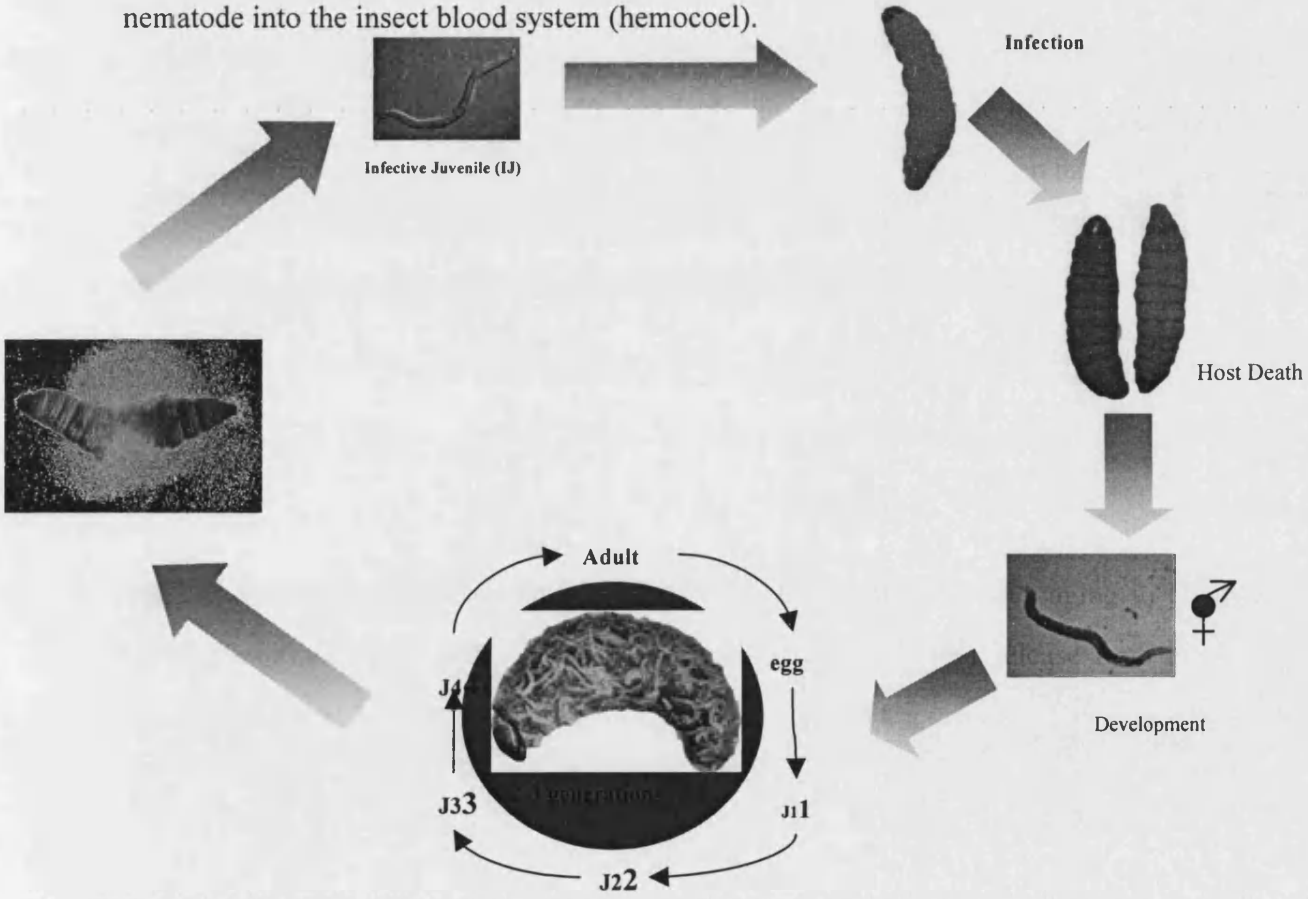

Figure 1.1 The lifecycle of the entomopathogenic nematode and its bacterial symbiont *Photorhabdus* (ffrench-Constant et al. 2003)

The bacteria are found within the gut of the free-living infective form of the nematode called the infective juvenile (IJ). These infective juveniles actively seek out host insects in the soil and attacks by penetrating the cuticle of the insect (Fig 1.1). The nematode achieves entry either via the spiracles, mouth or anus, or physically by using a tooth-like appendage present at the side of the nematode mouth. Upon reaching the open circulatory system of the insect, the bacteria are then regurgitated from the nematode's mouth. Once inside the hemocoel, the bacteria replicate rapidly, secreting a group of high molecular weight toxins complexes (Tcs), alongside a cocktail of other potential virulence factors including; lipases, proteases, lipopolysaccharides, plus broad-spectrum antibiotics, into the haemolymph (Forst et al. 1996; Daborn et al. 2001; Sharma et al. 2002; Silva et al. 2002; Bowen et al. 2003; ffrench-Constant et al. 2003), despite the presence of both a peptide- and cell-mediated insect immune system. Following invasion the immune system is rapidly overcome and death of the insect results in 24 - 48 h, with *Photorhabdus* having successfully evaded both a peptide and cell-mediated insect immune system and avoided phagocytosis (Au et al. 2004). At this stage the cadaver bioluminesces with light produced by the five gene lux operons present in *Photorhabdus*, these lux operons are not present in *Xenorhabdus* (ffrench-Constant et al. 2003). The insect cadaver becomes ideal for reproduction and development; the nematodes feed off of the bacteria, which are bioconverting the cadaver. After several rounds of both bacterial and nematode reproduction, new generations of infective juveniles re-acquire the bacteria and leave the host to colonize new insects (ffrench-Constant et al. 2003).

The entomopathogenic properties of this symbiotic relationship have made the partnership attractive as a crop-protection agent as well as the high molecular weight Tcs produced as potential novel insecticidal agents (ffrench-Constant et al. 1999), especially given the increasing levels of resistance in the field to the Bt toxins from *Bacillus thuringiensis* (McGaughey et al. 1992). These numerous virulence factors, toxins and symbiosis factors produced by *Photorhabdus* have generated interest in

genomic analysis to elucidate the interactions and discover putative virulence factors (ffrench-Constant et al. 2000; Duchaud et al. 2003).

The tobacco hornworm *Manduca sexta* is used as infection model system to research in detail the pattern of infection of an insect by *Photorhabdus luminescens*. It has been used extensively as a model for insect physiology and, although it lacks the genetics of *Drosophlia*, the large size of *Manduca* larvae, and a well-studied immune system, facilitates a ready dissection of bacterial infection. After injection into the insect larva, *P. luminescens* multiplies in both the midgut and haemolymph, only later colonizing the fat body and the remaining tissues of the cadaver (Silva et al. 2002). Bacterial persist by suppressing haemocyte-mediated phagocytosis and culture supernatants grown *in vitro*, as well as plasma from infected insects, suppress phagocytosis of *P. luminescens* (Silva et al. 2002).

1.3 Genomic research in *Photorhabdus luminescens*

A genomic sample sequence of 2,000 random sequencing reads was performed from a *P. luminescens* subsp *akhurstii* strain W14 genomic library to identify the different classes of potential virulence factors. This limited sample sequence reveals ample evidence concerning the types of virulence systems that *P. luminescens* may employ in its complex life cycle. The genome of *P. luminescens* subsp *laumondii* strain TT01 has now been sequenced (Duchaud et al. 2003) and sequencing of *P. asymbiotica* ATCC43949, a clinical isolate, is in progress (www.sanger.ac.uk).

After comparing the sequences obtained to sequences in existing protein and nucleotide databases, many potential virulence factors were found including genes that putatively encode Tc insecticidal toxin complexes, Rtx-like toxins, proteases and lipases, colicin and pyocins, and various antibiotics. And they also include a diverse array of secretion (e.g., type III), iron uptake, and lipopolysaccharide production systems (ffrench-Constant et al. 2000).

These sequences were also compared to the *Escherichia coli* K-12 genome sequence. Although there are many similarities between these two organisms (both are members of the family *Enterobacteriaceae*), the results of this analysis suggest that ~ 53% of the *P. luminescens* W14 genome is clearly distinct from *E. coli* K12. Genome of *P. luminescens* (~5.5Mb) is much larger than typical *E. coli* (4.6Mb). It suggests that this large genome size may reflect the high level of pathogenicity, and possible 'functional redundancy' (e.g. possession of multiple insecticidal toxins with different specificities against different insect groups or different insect tissues), required to kill a diverse range of insect hosts (ffrench-constant et al. 2000). Genomic comparisons may also offer further insight into the evolution of these entomopathogenic bacteria. For example, a genome similarity of over 2,000 orthologous genes exist between *P. luminescens* subsp *laumondii* strain TT01 and *Yersinia pestis*, the causal agent of Plague (Duchaud et al. 2003).

1.4 Bacterial toxins

Pathogenic bacteria produce a vast array of toxins possessing a whole range of different activities to evoke the desired effect on their host target cells. Elucidating the mode of action is the key in understanding the pathogenic processes, invasion and infection caused by the bacteria and the nature of the host–pathogen interaction. The nature of bacterial toxins and mode of action has made them useful tools for elucidating cellular processes and functions given their abilities to either block or activate their specific cellular target molecules. This knowledge can allow us to turn the mode of action of the toxins to our own advantage. Understanding their role in pathogenesis and infection assists in the bid to prevent infection and spread of the bacteria. Further to using the information to target the infection and disease caused by the bacteria, knowledge of toxin mode of action can lead to their use and potential application in therapeutics.

1.41 Type III secreted toxins (TTSS)

Type III secretion systems (TTSSs) were originally documented from pathogens of vertebrates. More recently, however, they have also been found in bacteria either pathogenic to plants or symbiotic with invertebrates. This suggests that TTSSs are not unique vehicles for delivering anti-vertebrate virulence factors but ancient secretion systems for the transport of effector molecules across host membranes, with the potential to play a role in a wide range of bacteria-host cell interactions.

Some Gram-negative bacteria encodes a piece of specialized secretory equipment termed as the Type-III secretion system (TTSS) (Hueck et al. 1998). The bacterial type-III secretion system can be viewed as a 'molecular syringe' where upon contact with the host cell the bacteria are able to 'inject' proteins into the host cytosol (Cornelis et al. 2000). These proteins can instigate internalisation of the bacteria or deliver the toxin/ effector. Apoptosis induced by *Salmonella typhimurium* and *Shigella flexneri* is dependent on entry into host cell. Following internalisation *S. typhimurium* inject SipB (*Salmonella* invasion protein B) and *S. flexneri* inject IpaB (Invasion plasmid antigen B) proteins, along with other proteins, into the cytosol. SipB and IpaB proteins bind to and activate caspase-1, which goes on to mediate apoptosis of the host cell. Although the mechanism for this and the downstream pathways following caspase-1 activation are still unclear (Hilbi et al. 1998; Jarvelainen et al. 2003). Some views are that they are inducing a cytolytic from of cell death – oncosis rather than apoptosis (Nonaka et al. 1999; Boise et al. 2001). Oncosis is associated with cell swelling, plasma membrane leakage and leads to inflammation.

Yersiniae express and deliver *Yersinia* outer proteins (Yops) via their type-III secretion system, YopP (*Y. enterocolitica*) or YopJ (*Y. pestis* and *Y. pseudotuberculosis*) induce apoptosis in macrophages. *Yersiniae* are able to induce apoptosis from the outside of the cell (Weinrauch et al. 1999; DeLeo et al. 2004). The proteins act to inhibit pro-survival proteins and activate pro-apoptotic proteins. YopP/J block NFkB, MAP-kinase (MAPK) and MAPKK inhibiting the survival pathways maintained by

these. YopP/J directly bind to MAPKK and block phosphorylation preventing activation and thus downstream activation of NFκB preventing nuclear translocation of this pro-survival factor (Grassme et al. 2001). YopP/J belong to the family of cysteine proteases and are also possibly capable of activating apoptosis by directly cleaving caspases upstream of Bid and initiating the translocation of Bid to the mitochondria (Denecher et al. 2001).

1.42 Pyocin

Pyocins are produced by more than 90% of *Pseudomonas aeruginosa* strains and each strain may synthesise several pyocins. The pyocin genes are located on the *P. aeruginosa* chromosome and their activities are inducible by mutagenic agents such as mitomycin C. The synthesis of pyocins starts when a mutagen increases the expression of the *recA* gene and activates the RecA protein, which cleaves the repressor PrtR, liberating the expression of the protein activator gene *prtN*. (Michel-Briand et al. 2002)

There are three types of pyocins (i) R-type pyocins resemble non-flexible and contractile tails of bacteriophages. They provoke a depolarization of the cytoplasmic membrane in relation with pore formation. (ii) F-type pyocins also resemble phage tails, but with a flexible and non-contractile rod-like structure. (iii) S-type pyocins are colicin-like, protease-sensitive proteins. They are constituted of two components. The large component carries the killing activity (DNase activity for pyocins S1, S2, S3, AP41; tRNase for pyocin S4; channel-forming activity for pyocin S5). It interacts with the small component (immunity protein) (Michel-Briand et al. 2002).

R-type pyocins have bactericidal activity. Immediately after adsorption, all R-type pyocins arrest the synthesis of macromolecules in sensitive cells and release intracellular material, which is followed by cell death within 20 min (Kageyama 1964; Ohsumi et al. 1980). The cell death results from a depolarization of the cytoplasmic membrane (of at least 90 mV), in relation with pore formation (Uratani et al. 1984).

1.43 A-B toxins

A-B toxins consist of two different moieties often produced as a monomeric protein. Activity is normally associated with the amino-terminus of the protein (A-moiety) and ability to bind to the target host cell is generally associated with the B-moiety. Activation of the toxin generally requires proteolytic cleavage; either the toxin is cleaved away from the bacteria by a protease, or the toxin is cleaved and activated by a protease native to the host cell e.g. furin (Falnes et al. 2000). Another form of A-B toxin is the binary toxins. The structure of binary toxins is such that the enzyme (active) component and cell-binding component are individually synthesized proteins that assemble together on the target cell (Hofmann et al. 1997; Barbieri et al. 2002). Examples of intracellular targets of the A-moiety include ribosomes, actin and small GTP-binding proteins like Rho (Falnes et al. 2000).

Modification of the actin cytoskeleton is a target for many bacterial toxins as alterations can allow the bacteria pathogenic advantages such as evasion of phagocytosis, invasion of target cells and allow spread of infection (Barbieri et al. 2002; Fiorentini et al. 2003). Rho GTPases belong to the Ras family of monomeric GTP binding proteins (Etienne-Manneville et al. 2002). Small GTPases include Ras, Rap, Ral which are involved in signal transduction, and members of the Rho family: Rho, Rac and Cdc42, which are involved in actin cytoskeleton remodeling and in a variety of cell functions such as cell cycle progression and gene transcription. The three major classes are Rho, Rac and Cdc42 all of which are involved in the organization of the actin cytoskeleton and have been implicated in both pro- and anti-apoptotic signaling as well as directly in the apoptotic process itself (Coleman et al. 2002).

1.5 Pathogenicity factors in *Photorhabdus luminescens*

Pathogenicity islands (PAIs) were first described from *E. coli* strains pathogenic to man (Hacker et al. 2000). Although their role and function are well documented in

anti-vertebrate pathogenicity, their role and origins in invertebrate pathogenesis and their potential evolutionary link to vertebrate pathogenesis are less clear (Waterfield et al. 2002). PAIs often show shifts in GC contents and tRNA linkage. Numerous factors have been implicated in the anti-insect virulence of *Photorhabdus* by biochemical analysis and intervention strategies. Sample sequencing of the *Photorhabdus* W14 genome and the recent complete sequencing of the TT01 genome has also revealed a plethora of further candidate virulence factors.

The genome of *Photorhabdus* strain W14 is packed with candidate insect virulence factors and potential symbiosis genes. The dramatic shifts in GC content spanning some of the genomic islands in the W14 genome suggest that some of these factors have been recently acquired from other bacteria some of which are pathogenic to man. Sequencing of these genomic islands within insect pathogens should allow us to begin to understand the interrelationship between anti-invertebrate and anti-vertebrate virulence factors (Waterfield et al. 2002).

1.5.1 *tc*-islands

The *Photorhabdus* Tc's are the best characterized of the *Photorhabdus* toxins and were first purified in the late 1990s (Bowen et al. 1998). They retrieved a protein complex estimated to be 1,000,000 MW from the supernatant of peptone broth in which *Photorhabdus* had been grown. The high molecular weight complex proved to be lethal when injected into the haemolymph of, or orally ingested by the lepidopteran *Manduca sexta* (tobacco hornworm) larvae and a number of other insects. The denatured complex was analyzed using sodium dodecyl sulphate polyacrylamide gel electrophoresis (SDS-PAGE) and was discovered to consist of multiple protein subunits ranging from 30 – 200 kDa. The complex was separated using native gel electrophoresis and the purified native toxin complex was subsequently shown to be active in nanogram concentrations against four insect orders (Bowen et al. 1998).

Further to this, the high molecular weight fraction, from *P. luminescens* subsp

akhurstii strain W14, was separated using High Performance Liquid Chromatography (HPLC) into four Tcs: Tca, Tcb, Tcc and Tcd (Bowen et al. 1998). Originally it was thought that these were encoded for by four *toxin complex* (*tc*) loci: *tca, tcb, tcc* and *tcd,* but subsequent extended sequencing of the *tc* loci has shown the presence of additional *tc*-like sequences and other genes which may encode putative virulence factors such as a lipase, colicin and pyocin like loci and photopexin (a supposed iron scavenger). These surround the *tc* loci indicating that they may be on pathogenicity islands, there are four putative pathogenicity islands in W14 one of which carries multiple tandemly repeated copies of *tcdA* and *tcdB*-like genes as well as multiple copies of *tccC*-like genes (ffrench-Constant et al. 2000; ffrench-Constant et al. 2002).

It is interesting that *tc* homologues have been identified in other Gram-negative bacteria including *Xenorhabdus* (ffrench-Constant et al. 2000; Morgan et al. 2001; Joo Lee et al. 2004), *Serratia entomophila* the causal agent of amber disease in New Zealand grass grub *Costelytra zealandica* (Hurst et al. 2000) and *Y. pestis*, the causal agent of plague (Parkhill et al. 2001), even *Pseudomonas syringae* pv. tomato, a plant pathogen, has not been documented to associate with insects. The origins and spread of *tc*-like genes, their relationship with phage, and the phenotypes they confer upon the bacteria within which they are found, all clearly warrant further investigation (ffrench-Constant et al. 2003)

1.5.1.1 Oral toxicity

The *tc* genes encode high molecular weight insecticidal toxin complexes, which destroy the insect midgut and render the infected host incapable of further feeding (Bowen et al. 1998, Waterfield et al. 2001). The *tcd*-island, inserted at an AspV tRNA, carries multiple copies of *tc* genes including *tcdA*-like genes, *tcdB*-like genes and *tccC*-like genes (Waterfield et al. 2002).

It was determined that Tca was responsible for most oral activity against *M. sexta*, having a median lethal dose of 875 ng/cm^2 of artificial diet, and significant weight

reducing effects at 40 ng/cm^2 (Bowen et al. 1998). The cause of oral toxicity was investigated by deleting or disrupting each of the *tc* loci from *P. luminescens* strain W14, generating the knockout strains: *tca*$^-$, *tcb*$^-$, *tcc*$^-$ and *tcd*$^-$ (Bowen et al. 1998). It was observed from oral toxicity bioassays that knocking out either *tca* or *tcd* significantly reduced the toxic effects of W14 on *M. sexta*, and that knocking out both together in a single strain eliminated oral toxicity altogether. Indicating that the toxins Tca and Tcd encoded by these loci (Tca: *tcaA1, tcaB1, tcaC1* and Tcd: *tcdA1 and tcdB1*) were responsible for high levels of oral toxicity to *M. sexta*. The knockout experiment also indicated that complex interactions between the gene products might be taking place which may have a bearing on their toxicity, for example Tca may require Tcd for enhancement of toxicity (Bowen et al. 1998).

The non-orally toxic strain *P. temperata* subsp *temperata* strain K122 has been used to recombinantly express the tripartite Tcd toxin via *tcdA1B1* with *tccC1*, and Tca via *tcaA1B1C1* operons from W14. Both of which confer oral toxicity to *M. sexta* onto the supernatant of K122 (Waterfield et al. 2001). A truncated plasmid containing only *tcdA1B1*, without *tccC1*, was also capable of conferring potent levels of oral toxicity onto supernatants of K122 expressing the plasmid. Expression of oral toxicity in *E. coli* was subsequently achieved using a plasmid containing the full tripartite complement of Tcd: *tcdAB* with *tccC* (Waterfield et al. 2001). In addition, to achieve full levels of oral toxicity, mitomycin C needs to be added to the growth medium or the culture must be allowed to stand for 48h. This may be because the toxin complex is surface associated and the environmental stresses of aging/mitomycin C may initiate their detachment or even may initiate expression (Waterfield et al. 2001).

Transmission Electron Microscopy of high molecular weight particulate toxin preparations from *P. luminescens* strain W14, recombinant K122 expressing TcaABC and *E. coli* expressing either TcdAB or TcdAB and TccC show the presence of supramolecular 'head and tail' like complexes approximately 25nm long. Although *E. coli* expressing just TcdAB forms these structures it is not orally toxic, requiring the

co-expression of TccC. Hypotheses raised surrounding this suggest that TccC may activate the TcdAB complex,(Waterfield et al. 2001) or that it may be the active toxin component itself, with TcdAB providing the delivery system (Waterfield et al. 2001).

The oral activity of the Tcs' is unexpected given the route of attack via the cuticle and haemocoel of the host larvae by the entomopathogenic nematodes vectoring *Photorhabdus*. The Tcs are now thought to be encoded by ancestral *tc* genes acquired by *Photorhabdus* and are normally employed as active toxins on the haemocoel side of the gut (Waterfield et al. 2005).

Recently TcdA has been expressed in transgenic plants, although expression levels were low and the lethal dose required was much higher for TcdA purified from transgenic plants than that of the native toxin (Liu et al. 2003). It has now been shown that increased levels of activity of TcdA expressed in *E. coli* is potentiated by two other proteins, TcdB and TccC, and most enhanced by co-expression in the same *E. coli*. TcdB and TccC are also capable of increasing toxicity when co-expressed with TcaAB suggesting some form of modifying or targeting abilities increasing lethal efficacy. Expression within cells reveals nuclear translocation of TcdB suggesting a potential targeting activity, while the other proteins (e.g. TcdA) may carry active sites. However, the site of action along with the exact role and mechanism of the various component proteins remains to be elucidated (Waterfield et al. 2005).

1.5.2 *mcf*-island

The Mcf toxin (Makes caterpillars floppy) was discovered upon screening 300 individual clones from a cosmid library, constructed from *P. subsp. akhurstii* strain W14 genomic DNA, for injectable activity against *M. sexta*. A 33kb cosmid was isolated which permitted the persistence of *E. coli* in the insect hemocoel, and caused a loss of body turgor at ~12h termed the 'floppy' phenotype, followed by death at ~24h. It was determined that an 8.8kb gene consisting of a single open reading frame was responsible for enabling both the persistence of *E. coli* within, and the

death of, the *M. sexta* via transposon mutagenesis. The Mcf protein is predicted to be 324 kDa in size. (Daborn et al. 2002)

mcf1 lies in a Pathogenicity island inserted at a Phe tRNA, which encodes the novel toxin "makes caterpillars floppy"-Mcf, a large toxin with little similarity to known proteins but carries a BH3 domain and triggers apoptosis in both insect hemocytes and the midgut epithelium (Daborn et al. 2002). It is striking that this single gene is sufficient to allow *E. coli* to persist within and kill insects. Database searches for protein homology revealed only three areas of similarity with known proteins, these include a consensus sequence for a BH3 domain, with > 80% homology, found in a Prosite search. There is also a 20% identity to a region in *C. difficile* toxin B (CdtB) putatively involved in translocation/ endocytosis, cytotoxic activity of this CdtB has been unequivocally linked with the N-terminus of the holotoxin (Hofmann et al. 1997). Similarity is present in the predicted C-terminus to the export domain of apxIVA, an RTX-like toxin (cytolytic toxin) from *Actinobacillus pleuropneumoniae* (Schaller et al. 1999).

Southern analysis of three other strains: *P. luminescens subsp.temperata* strain K122, *subsp. laumondii* strain TTO1 and *P. asymbiotica* strain ATCC43949 – a clinical isolate (Peel et al. 1999), demonstrated the presence of homologs to *mcf* in all of these different strains, suggesting that it may be a critical pathogenic factor (Daborn et al. 2002).

This region carries genes encoding proteins from the Sh1A/HecA/FhaA hemagglutinin-like family and a fragment of a CP4-like integrase. The same Phe tRNA is also associated with the She PAI from *Shigella flexneri* 2a and O-island 122 from *E. coli* O157, which also carry CP4-like integrases, suggesting a common mechanism of acquisition (Waterfield et al. 2002).

1.5.3 *cnf*-island and the *Photorhabdus* Virulence Cassettes (PVC)

A third recently described PAI (PAI III) from W14 encodes a homolog of a cytonecrosis-like toxin (*cnt*-like) designated *pnf*. These gene products belong to a large family of binary toxins, which include the Cyto Necrosis Factor genes of *E. coli*, CNF1 and CNF2. The CNF1 protein from uropathogenic *E. coli* is a Rho-GTPaseactivating toxin. It is an A-B toxin divided into three domains, each implicated in the three steps of the intoxication process; binding to the cell receptor; internalization and transport to late endosomes; and release from the endosome and entry into the target cell cytoplasm. The carboxy-terminal domain is an enzyme that deamidates Rho-GTP-binding proteins leading to profound reorganization of the actin cytoskeleton of the host cell (Flatau et al. 1997; Sugai et al. 1999). Although the specific role of the Pnf toxin in *Photorhabdus* virulence remains to be tested, it is interesting that the C-terminal portion of the putative protein is highly conserved with other members of the family and contains the active site (Buetow et al. 2001), whereas the normally variable cell targeting and translocation domains are absent entirely. This suggests the protein may be directly delivered into a target cell by either type IV or type III secretion systems. The region sequenced shows no predicted tRNA genes or any flanking core sequence, making it difficult to suggest an insertion site for PAI III in strain W14. However, overall, this region contains genes, some of which are phage related, with similarity to a region of the genome from the *cyanobacterium* Nostoc sp. PCC 7120, supporting the description of this region as a putative PAI. Interestingly, a comparison of this region with the fully sequenced genomes of *P. luminescens* TT01 and the gapped genome of *P. asymbiotica* ATCC43949 has revealed that this region appears to represent a novel group of mobile elements that we designate the *Photorhabdus* Virulence Cassettes (PVC). These regions show that *pnf* and other putative virulence factors are all encoded in a 'carriage' region adjacent to the conserved putative mobile PVC unit. We speculate that the tightly linked type IV pilus operon is responsible for the conjugative transfer of these elements (Waterfield et al. 2004).

1.5.4 Bacteriocins and phage

Phage and phage-related derivatives are important and widespread members of bacterial genomes. Phage and their relatives have been implicated in the acquisition and spread of virulence factors and toxins, and phage derived elements such as bacteriocins form important protein antibiotics (Parret et al. 2002). A limited number of phage-related structures have been previously reported from *Xenorhabdus* and *Photorhabdus* (Boemare et al. 1992; Thaler et al. 1995). The analysis of the *Photorhabdus* W14 and K122 genomic sample sequences has confirmed the presence of many sequences similar to genes of the P2, lambdoid and Mu-like phages.

1.5.4.1 Bacteriocins

1.5.4.1.1 R-type pyocins: photorhabdicin

Pyocins are phage-related bacteriocins from *P. aeruginosa* that can be divided into R-, F- and S-types. The R-type (e.g. R2 pyocins) and F-type pyocins are derived from phage tails and the R2 pyocin is thought to have derived from a common ancestor of phage P2 and pyocin F2 of phage lambda. A phage tail-like bacteriocin structure similar in appearance to an R-type pyocin has been documented in *X. nematophilus* and termed 'xenorhabdicin' (Thaler et al. 1995). These structures were produced after mitomycin induction, along with phage head-like particles, and xenorhabdicin was shown to have antimicrobial activity against closely related bacteria. Similar structures are also observed, which in turn termed 'photorhabdicins', after mitomycin induction of both *Photorhabdus* W14 and K122 cultures (ffrench-Constant et al. 2003). Transmission electron micrographs of negatively stained preparations of particulate material from culture supernatants revealed photorhabdicins in both the 'contracted' and 'relaxed' forms, suggesting that these structures are functional. Estimates of the lengths of the photorhabdicins were made by taking an average of measurements made from both contracted and relaxed forms from multiple TEM images. The K122 photorhabdicins closely resemble R-type pyocins while the longer and thinner W14 equivalents are more similar to the F-type pyocins. Furthermore,

particulate preps from *Photorhabdus* W14 supernatants, which are enriched for photorhabdicins, do show antimicrobial activity against both *E. coli* and other *Photorhabdus* strains (ffrench-Constant et al. 2003).

1.5.4.1.2 S-type pyocins: lumicins

The S-type pyocins are also secreted by the *P. aeruginosa* type strain PAO1 and can break down cellular DNA in susceptible cells. A novel class of similar bacteriocins from *Photorhabdus* W14 is recently described, which termed the 'lumicins' (Sharma et al. 2002). The lumicin loci are capable of killing other *Photorhabdus* strains and even other *E. coli* strains when expressed in a common *E. coli* host. These novel bacteriocins may not only play a role in protecting the *Photorhabdus* infection from invading or native bacteria, but the observation that the lumicins share similarity with *usp* from *E. coli* has a further important implication.

1.5.4.2 Phage

The presence of phage, as well as bacteriocins, has been documented after treatment of *X. nematophilus* strains with mitomycin or high temperature (Boemare et al.1992) and their presence in the genome of *Xenorhabdus* has been conformed by DNA hybridization. Numerous phagelike sequences are detected in the *Photorhabdus* W14 sample sequence and in other extended sequences of this and other strains. Tailed phage can be seen under the electron microscope in high molecular mass preparations from the supernatant of W14, and partial sequences of phage genomes have been obtained from genomic libraries made from this strain (ffrench-Constant et al. 2003).

1.6 Virulence factor secretion

The W14 sample sequence shows a wide range of candidate secretion systems for virulence factors (Figure 1.2) (ffrench-Constant et al. 2003).

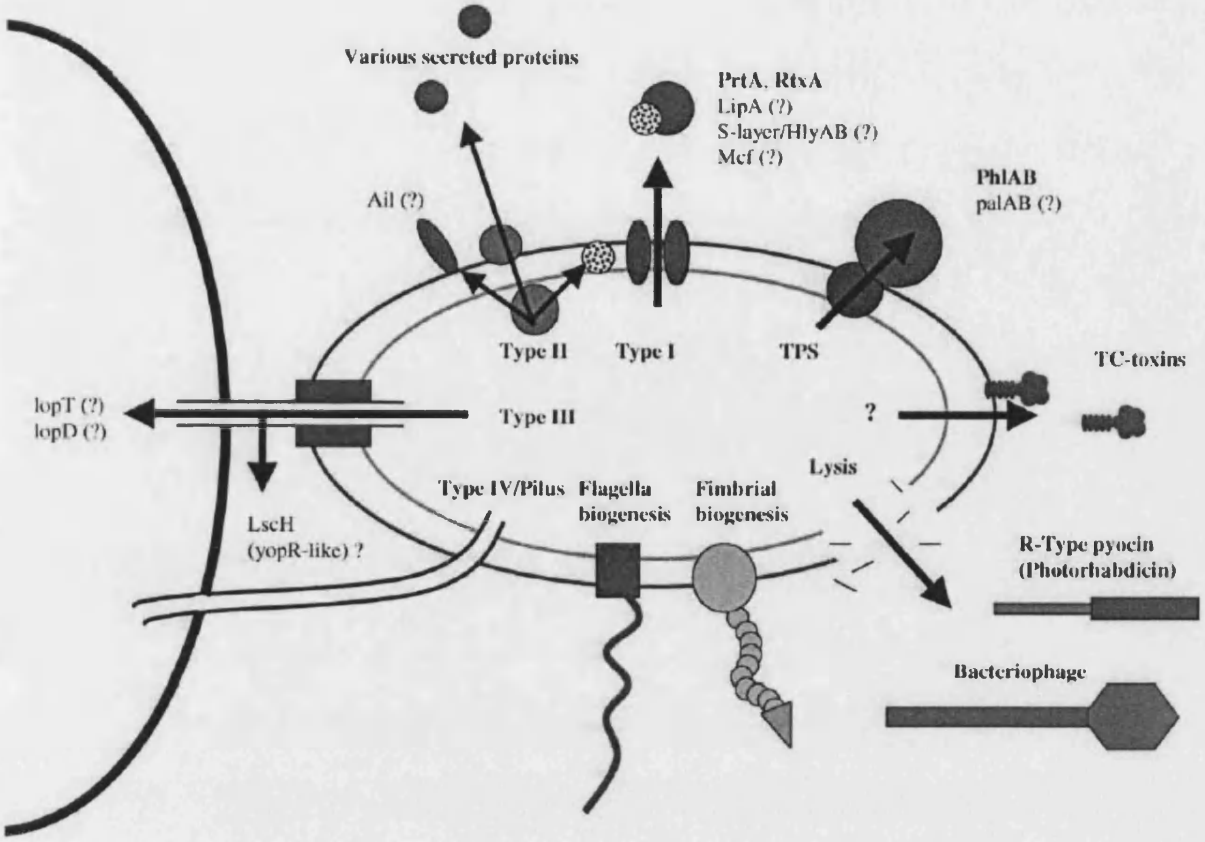

Figure1.2 Summary of known and predicted secretion mechanisms that *Photorhabdus* may use to deliver proteins involved in pathogenicity and symbiosis. Proteins shown in bold have been documented as being secreted, whereas other proteins (followed by ?) have not. Alongside the conventional type I, II, III and IV secretion systems, we infer that host cell lysis is important in the release of high molecular mass factors such as pyocins and phage (ffrench-Constant et al. 2003).

1.6.1 Type I and TPS secretion.

The PrtA protease of strain W14 can be secreted from *E. coli* expressing clones carrying the complete *prtAIBCD* operon. This is because *prtBCD* encodes a type I secretion system capable of secreting PrtA from the recombinant cells. In fact deletions of any part of the secretion system stop the formation of zones of clearing or 'halos' in gelatin overlays (Valens et al. 2002). This system is similar to protease-encoding genes described from *Erwinia*, *Pseudomonas* and *Serratia*, except

that in some other bacteria the type I secretion system for the protease is found elsewhere in the genome. Type I secretion systems are also found in the genome of *Photorhabdus* W14, adjacent to homologs of the RtxA toxin from *Vibrio cholerae*, but again the role of the RtxA-like protein in insect infection remains undocumented (ffrench-Constant et al. 2003).

1.6.2 Type III and type IV secretion

The first TTSS found in *Photorhabdus* W14 shows a similar order of gene homologs to that found in *Y. pestis* but differs from the gene order in *Pseudomonas aeruginosa*, as the pscU-exsB block of genes is inverted (Figure 1.3) (Waterfield et al. 2004). The *Photorhabdus* W14 TTSS predicts proteins similar to YopBD and YopR, which in *Y. pestis* are secreted proteins necessary for infection in the mouse model, possibly forming the actual translocon pore. Further the *Photorhabdus* TTSS also encodes a homolog of LcrV. Antibodies raised against *Y. pestis* LcrV play a protective role in mice against infection by plague (Fields et al. 1999). This raises the possibility that LcrV-like proteins may important in the interaction of *Photorhabdus* with the cells of either of its invertebrate hosts.

It is likely that *Photorhabdus* also employs a type IV secretion system. This system is closely related to the plasmid conjugation and T-DNA transfer system of *Agrobacterium*. Within the W14 sample sequence homologs to type IV pilus biogenesis genes, including those encoding prepilin peptidase and the structural assembly proteins PilA and PilB, have been identified (ffrench-Constant 2003).

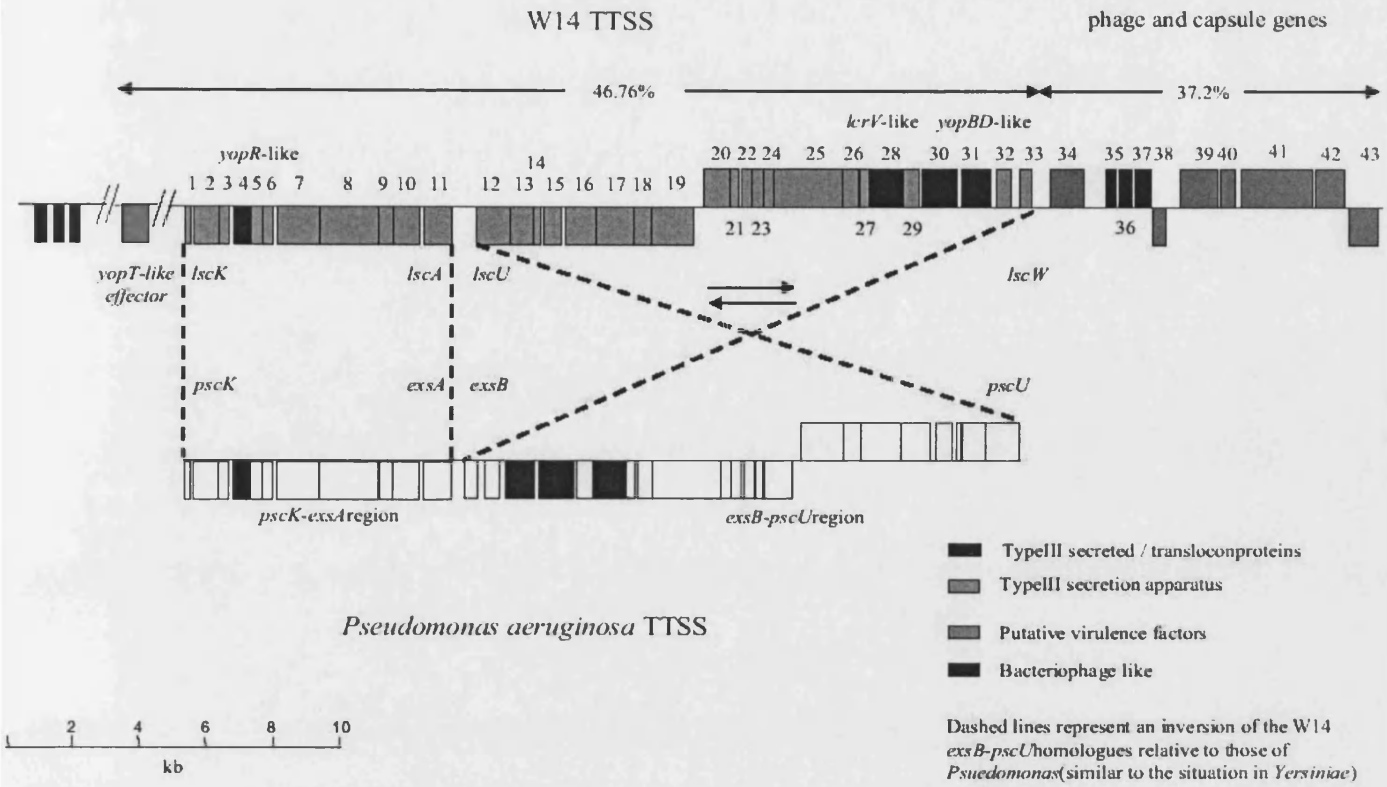

Figure1.3 A region of the *Photorhabdus* genome, termed pathogenicity island (PAI) IV, encoding a Type Three Secretion System (TTSS) (GenBank accession AY144117). The open reading frames (ORFs) of the TTSS predict proteins most similar to secreted proteins from a range of bacteria, including YopR (ORF 4) and YopBD (ORF 30 and 31). The TTSS-island is linked to a region containing phage and capsule genes (ORFs 34–43), suggesting that these may have been involved in its transfer into the *Photorhabdus luminescens* genome. The order of predicted ORFs in the *Photorhabdus* TTSS is compared with that found in the TTSS of *Photorhabdus aeruginosa* (GenBank accessions AF010149 and AF010150) (Waterfield et al. 2004).

1.7 AIMS OF THESIS

Many insecticidal toxins have been identified in *Photorhabdus*, such as Tc toxins, Mcf1. However recently sequenced genomes of the insect pathogenic bacterium *Photorhabdus* (strain TT01, *asymbiotica* ATCC43949 and genome sample sequence of strain W14) reveals many potential virulence factors including *mcf2*, PVCs, and TTSS. The aim of my thesis was to characterize novel insecticidal toxins of *photorhabdus*. The first step of identification is based on genome sequence and several potential virulence factors were found. Further shifting from genotype to phenotype: gene expression, bioassay and gene knock out are used to investigate their function.

CHAPTER 2

MATERIALS AND METHODS

2.1 DNA plasmid

Plasmids used during this thesis are as follows: pBAD30, pLOF, pWEB, PDS132 and pRK5myc for cloning, over-expression and knock-out.

2.1.1 pBAD30

pBAD30 vector contains the P_{BAD} promoter of the arabinose operon and its regulatory gene, *araC* (figure 2.1) (Guzman et al. 1995). The AraC protein is both a positive and a negative regulator. In the presence of arabinose, transcription from the P_{BAD} promoter is turned on; in its absence, transcription occurs at very low levels. So the target gene expression can be modulated over a wide range of inducer (arabinose) concentrations and reduced to extremely low levels by the presence of glucose, which represses expression (Guzman et al. 1995).

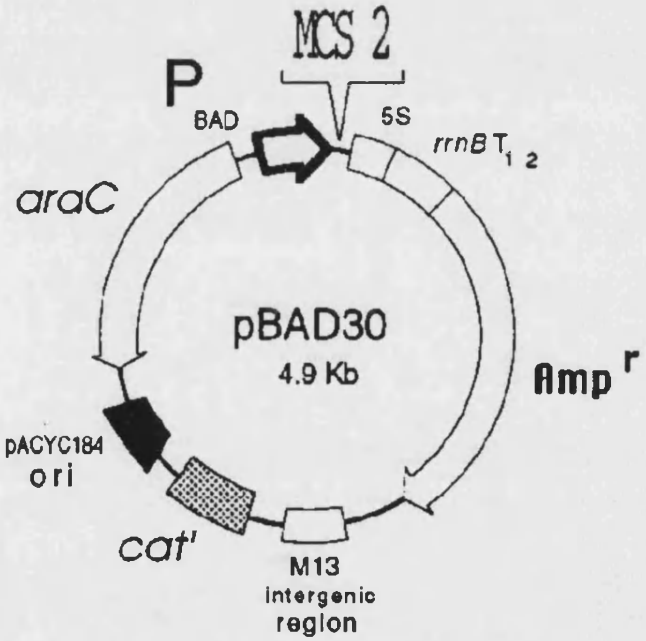

Figure2.1 Map of arabinose inducible vector-pBAD30 (Guzman et al. 1995)

2.1.2 pLOF

The pLOF series vectors have been developed as versatile tools for the genetic analysis and genetic engineering of a wide variety of gram-negative bacteria (figure 2.2) (Herrero et al. 1990). It could be maintained only in donor host strains that produce the R6K-specified protein, which is an essential replication protein for R6K and plasmids derived therefrom. The availability of the functionally distinct Tn10- and Tn5-based vectors on the broad-transfer-range suicide delivery system should diminish problems of hot spots for insertion and transposon host range that may be encountered in some target organisms. (Herrero et al. 1990).

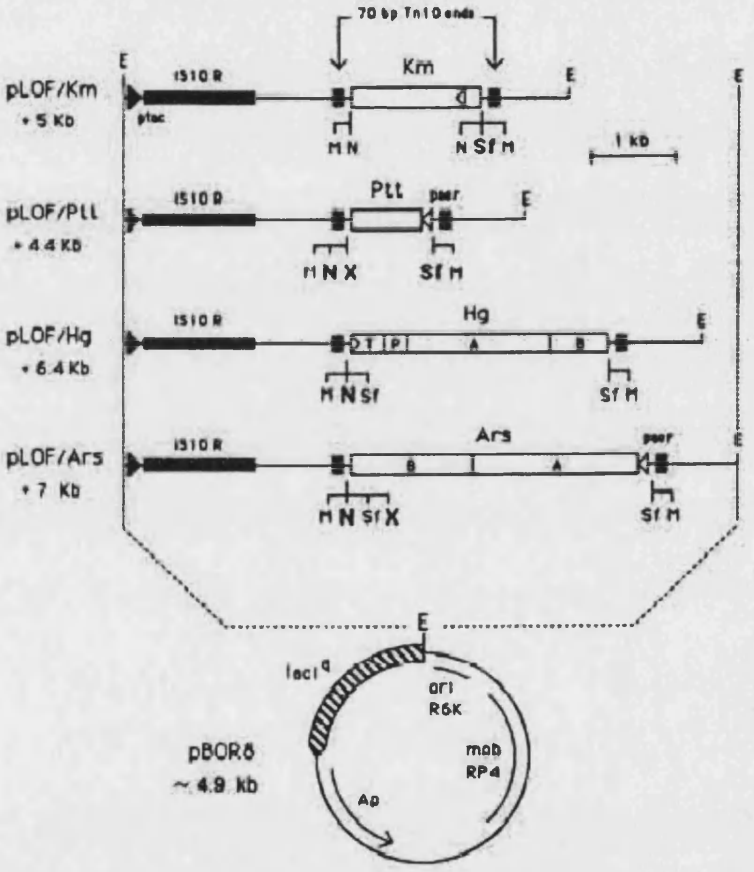

Figure2.2 Map of suicide vector-pLOF (Herrero et al. 1990)

2.1.3 pWEB

The pWEB Vector is a derivative of pWE15 which has a number of features that make it well suited for use in cosmid cloning. pWEB contains a unique *Sma* I site for

the cloning of blunt-ended genomic DNA. This site is flanked by rare cutting *Not* I sites for the subsequent excision of insert DNA. The vector contains a col E1 origin of replication and Ampicillin resistance for growth in *E. coli*, and an SV40 origin of replication and neomycin resistance for selection in eukaryotic cells. The vector contains M13 forward and T7 promoter primer binding sites that can be used for sequencing insert ends and generating probes for chromosome walking. Restriction mapping of insert DNA can be performed using lambda terminase and labeled oligonucleotides complementary to the cos sites (ON-R and ON-L). The pWEB Vector is conveniently supplied as a *Sma* I-linearized dephosphorylated vector.

2.1.4 pDM4

pDM4 are derivatives of pNQ705 that contain the sacBR genes from *Bacillus subtilis* (Debra et al. 1996), and could made chromosomal insertions by integrating a plasmid into the target gene, As a suicide plasmids containing R6K to be maintained in *P. luminescens* after conjugal transfer from *E. coli*, they must have integrated into the chromosome, most likely within the complementary target gene. This integration was required for generating the insertional mutations. Transconjugants were selected by utilizing the chloramphenicol resistance gene located on the suicide plasmid.

2.1.5 pDS132

pDS132 is a derivative of the well-described suicide plasmid pCVD442 (Donnenberg et al. 1991), which carries R6K ori, the replication origin of plasmid R6K, the mob (plasmid mobilisation region) and the *sacB* gene of *B. subtilis*. pCVD442 is modified by removal of IS*1* element and replaced bla by the cat gene conferring chloramphenicol resistance (N. Philippe et al. 2004) (Figure 2.3). This suicide vector is able to replicate only in strains producing the π protein, the product of the *pir* gene. Integration of the plasmids into the chromosome is selected by an antibiotic resistance marker and in a *pir*$^-$ background. Excision of the integrated plasmid for allelic exchange is selected with counter-selectable markers: if the

plasmid is still integrated in the chromosome, the cell will die in the presence of the counter-selective compound. The *Bacillus subtilis sacB* gene encodes levane saccharase, which is lethal in most gram-negative bacteria in the presence of sucrose (Gay et al. 1983). Plasmid excision in the cells can therefore be selected by growth in a sucrose-containing medium.

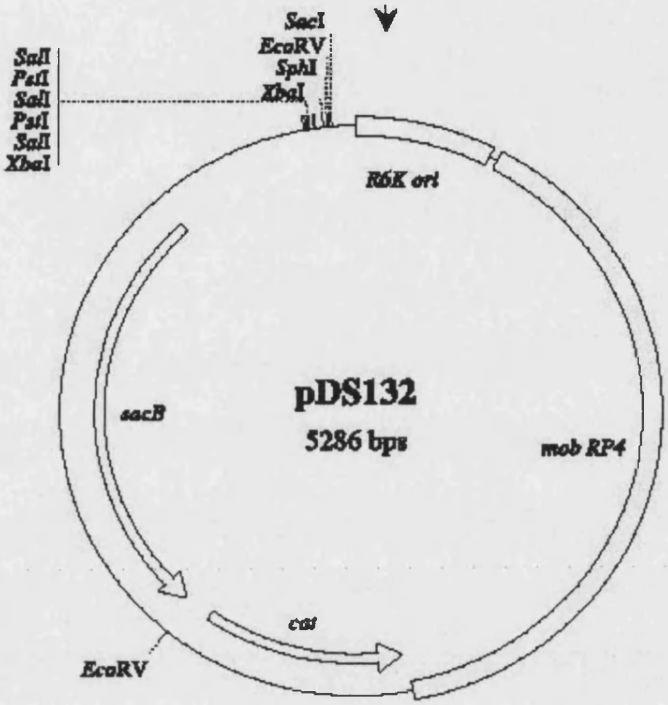

Figure2.3 Map of suicide vector-pDS132 (N. Philippe et al. 2004)

2.1.6 pRK5myc and pEGFP-Actin

pRK5myc is a mammalian expression vector which expresses the c-Myc epitope tag and was used as a cloning vector to express some PVC putative effectors- Pnf, LopT and Sepc-like as a Myc-fusion protein. To assist in the observation of cell morphology of NIH 3T3 cells expressing the constructs they were co-transfected with pEGFP-actin (Clontech). pEGFP-actin, a mammalian expression vector which expresses the EGFP-Actin fusion protein of the human codon optimized variant of green fluorescent protein (EGFP) and the gene encoding human cytoplasmic β-actin (Clontech, UK). Cells expressing the empty pRK5myc vector and pEGFP-actin

alone retain a normal cellular morphology and faint diffuse cytoplasmic expression of Myc detected by immunostaining.

2.2 Cloning

2.2.1 PCR

Add the following to a microfuge tube: 10ul reaction buffer, 1ul 15uM forward primer, 1ul 15uM reverse primer, 1ul template DNA, 5ul 2mM dNTPs, 8ul 25mM $MgCl_2$, water to make up to 100ul. Start the PCR cycles according the following schemes: a) denaturation - 95 ° C, 30sec (for rTth 93° C). b) annealing - 55 °C 0.5-2 min. c) extension - 72 °C (for rTth 68° C, time depends on length of PCR product and enzyme used), repeat cycles 30 times. Add a final extension step of 10 min. to fill in any uncompleted polymerisation. Then cooled down to 4- 25 °C.

Genomic fragments (~500 bp) upstream and downstream from the target gene to be inactivated were amplified by PCR using 1, 3 primers and 2, 4 primers (Primer 3 is designed to bind at the ATG start site of the target gene to amplify at least 500 nt into the flanking gene and which contains the TAA termination codon of the target gene and 15 nt homology to the flanking gene following the target gene and TAA codon; Primer 4 is designed to bind at the TAA termination codon site of the target gene to amplify at least 500 nt into the flanking gene and which contains the ATG start codon of the target gene and 15 nt homology to the flanking gene following the target gene and ATG codon (Figure 2.4). Anneals the two 500nt fragments in the presence of *Taq* DNA polymerase but no primers (2 min at 95 ° C; 10 cycles of 30 s at 95 ° C, 30 s at 50° C, 2 min at 72 ° C; 10 min at 72 ° C). In order to amplify the resulting fusion product, 10 ul of the reaction mixture was added to a 50 ul PCR reaction mixture containing the 1 and 2 primers (Lionel et al. 2004). The long range PCR was performed using *rtth* DNA polymerase, with the following amplification conditions: 2 min at 93 ° C; 30 cycles of 30 s at 93 ° C, 30 s at 55 ° C, 3 min at 68 ° C, 10 min at 68

° C. The PCR product was digested with *Xba* I and *Sac* I to clone into the suicide vector-pDS132.

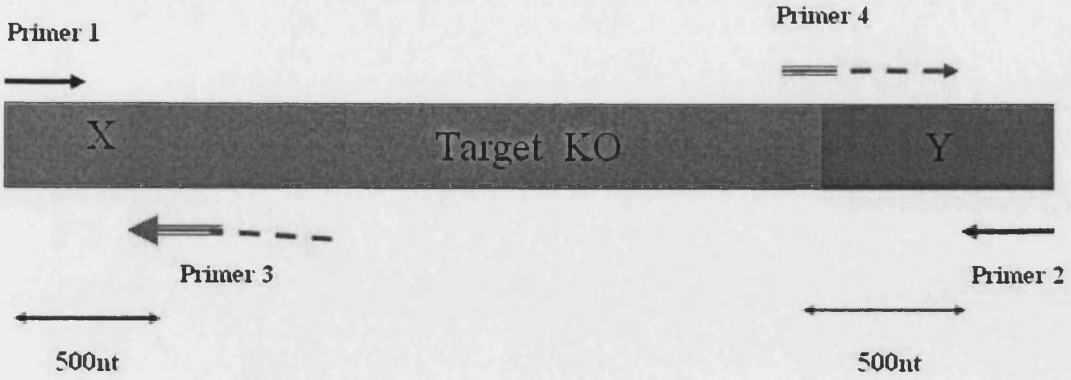

Figure2.4 Primers used for cloning DNA fragment into pDS132

2.2.2 Ligation

Ligations were conducted using LigaFast™ Rapid DNA Ligation System (Promega, UK) with a 3:1 insert: vector ratio of DNA concentration. Appropriate amounts enzyme digested plasmid template DNA is added to a 10ul reaction mix containing 0.5mM ATP, 5x reaction buffer, appropriate amounts of digested PCR-generated insert, and 1ul of T4 DNA ligase (4 U/ul). The reaction is incubated at 25°C for 15min. 3ul is removed and used to transform *E. coli*.

2.2.3 Transformation of electrocompetent *Escherichia coli*

2.2.3.1 Generation of electrocompetent *E. coli*

E. coli strains DH5-α and EC100 were used. 1 in 100 dilution of overnight bacterial culture was added to a flask containing 400 ml autoclaved LB and grown until an Optical Density (OD) at 600nm of between 0.4- 0.6 was reached. The culture was then chilled on ice for 15 minutes prior to centrifugation at 10,000 rpm for 30 minutes. Following centrifugation the supernatant was gently decanted and the pellet resuspended in 400 ml of chilled autoclaved distilled water before repeating the centrifugation again. The supernatant was decanted and cell pellet resuspended in 50 ml chilled 10 % (v/v) autoclaved glycerol and centrifuged at 13,000 rpm for 30

minutes, this step is repeated once. The final pellet was resuspended in 1 in 400 of the original volume of culture (1 ml) chilled 10% glycerol, divided into 40 µl aliquots before snap-freezing in liquid nitrogen and storage at –80 °C.

2.2.3.2 Electroporation

Plasmids were transformed into the electrocompetent *E. coli* using a Bio-rad Gene Pulser II (Bio-rad, UK), set at 2.5 kV, 200 Ω. Following electroporation the cells were recovered using LB and incubated at 37°C for 1 h before plating out on LB agar containing the suitable antibiotic for the selection marker on the plasmid.

2.2.3.3 DNA preparation and purification

DNA was prepared for transformation, restriction digests and ligations using Qiagen miniprep kit (according to manufacturer's instructions, Qiagen, UK). Larger scale DNA preparations for transfection into mammalian cells were made using Qiagen Midiprep kits.

To purify *P. luminescens* genomic DNA, overnight culture of *P. luminescens* equivalent to 5OD is centrifuged in an Eppendorf, resuspended in 561 µl TE buffer, add 30 µl 10% (w/v) SDS, 6 µl 20mg/ml proteinase K and 3 µl 10 mg/ml RNase to incubate at 37°C for 90 min. Add 100 µl 5M NaCl and 80 µl CATB buffer (10% CATB- Hexadecyltrimethyl ammonium bromide and 0.7 M NaCl in water), mix well but gently, incubate at 65°C for 10 min. Extrate with 700 µl phenol+chloroform: isoamyl alcohol (25:24:1), shake to mix and centrifuge. Remove aqueous phase to a fresh tube and extract with 500 µl chloroform: isoamyl alcohol (24:1), centrifuge and precipitate genomic DNA with a 0.6 vol of isopropanol. Centrifuge to collect DNA and wash with 70% ethanol.

2.3 Cosmid library preparation

The cosmid library was prepared from *P. luminescens* subsp. *akhurstii* strain W14

genomic DNA by MWG Biotech (Munich). DNA was physically sheared, size selected for fragments of ≈30 kb, and then cloned into pWEB. The average insert size (≈32 kb) was determined by restriction analysis of a random selection of clones.

2.4 Sequencing and assemble of cosmids

We used insertional mutagenesis with a EZ::TN<TET1> transposon (Epicentre) to sequence the cosmid containing the target gene. Transposon mutants were used as entry points in nucleotide sequencing of the target cosmid. Cosmid DNA was prepared on a RoboPrep plasmid preparation robot (MWG Biotech) and sequenced on an ABI3700 nucleotide sequencer (Applied Biosystems). The LASERGENE software package (DNASTAR, Madison, WI) was used to assemble and analysis sequences (Figure 2.5).

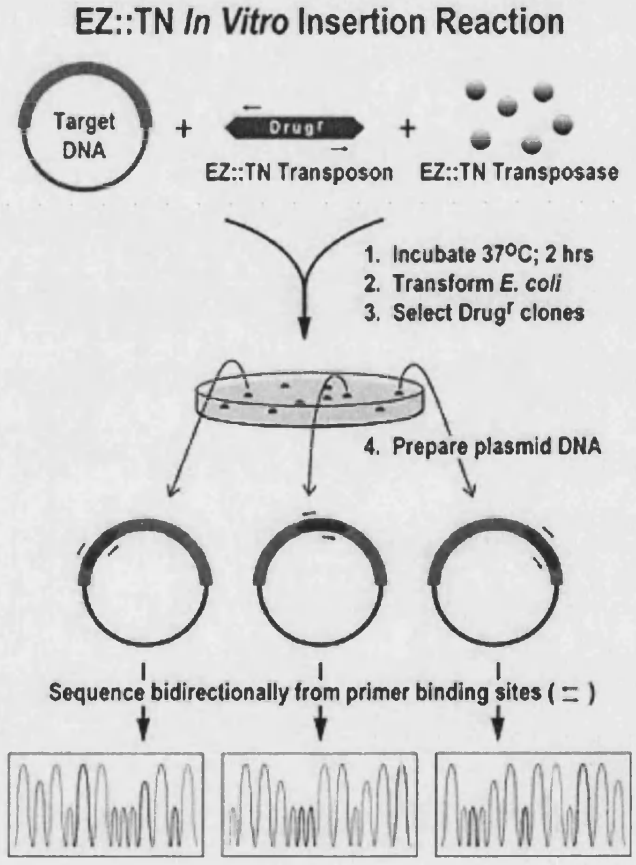

Figure2.5 Insertional mutagenesis with a EZ::TN<TET1>

2.5 Over-expression in pBAD30

Bacterial cultures were grown up in Luria broth (LB) with 100 μg ml^{-1} ampicillin and 0.2% glucose, at 37°C overnight in a shaking incubator. The induction culture was started with a 1 in 100 dilution of the overnight culture. The cultures were grown to OD600 of 0.6, 0.2% arabinose (w/v) (from 20%stock made in distilled water and filter sterilised through a 0.22 μm filter) was added and aliquots taken following induction at 1, 3, 6 h and overnight, OD readings made at each point and the pellets frozen. Pellets were prepared for SDS-PAGE.

2.6 TCA precipitation

Add 1/10 volume of 100% TCA (Trichloroacetic acid) into culture supernatant and leave it on ice for 1 to 2 hours. After spin tube in microcentrifuge at 14K rpm, 10 min, remove supernatant, leaving protein pellet intact and wash pellet with 200μl cold acetone. Dry pellet and, add sample buffer for SDS-PAGE gel.

2.7 Denaturing SDS-PAGE

Samples were diluted as required in 1, 2 or 5 X SDS-PAGE sample buffer (5X sample buffer: 10% sodium dodecyl sulphate (SDS), 50 % glycerol, 0.2 M Tris-HCl pH 6.8, 5 % β-mercaptoethanol, 0.1 % Bromophenol blue) and heated at 100 °C for 10 minutes. Equivalent amounts of protein at either 10 or 15 μg per sample (depending on experimental requirements) were loaded onto a vertical SDS-polyacrylamide gel, the Bio-rad Mini-Protean system was used for all applications. Either 8 % or 12 % SDS-PAGE gels were used to give resolution as required 8%: 0.375 M Tris pH 8.8, 8 % acrylamide mix, 0.1 % SDS w/v, 0.1 % ammonium persulphate w/v, 0.06 % TEMED v/v, and 12 % as for 8 % except: 12 % acrylamide mix, 0.04 % TEMED (Sambrook et al. 1989). All gels had a 5 % stacking gel layer (0.125 M Tris pH 6.8, 5 % acrylamide mix, 0.1 % SDS w/v, 0.1 % ammonium persulphate w/v, 0.01 % TEMED v/v) into which a comb was inserted creating wells to load the samples. SDS-PAGE was conducted at 120 V in electrophoresis buffer (25 mM Tris, 0.1 % SDS, 192 mM glycine) for approximately

90 minutes. Protein standard markers used were either Precision Plus Protein standards (Bio-rad) or Prestained Protein Marker, broad range (NEB). Gels were stained in coomassie brilliant blue (Sigma) or prepared for western blotting (Section 2.7). Staining in coomassie brilliant blue was carried out overnight on a shaking platform at room temperature, followed by several rinses in destain solution (3:1:6 methanol: glacial acetic acid: H_2O) for visualisation of the protein bands. Gels were dried using the DryEase Gel Drying System (Invitrogen, UK).

2.8 Injection and bioassay

10 µl (for *Manduca sexta*, use 30 µl)contained $1.0U10^7$ colony forming units (CFU) for the target gene was injected into individual *G. mellonella* larvae, as determined by plating dilutions onto LB antibiotics agar plates. Mortality, defined as an inability to react to poking with a needle, was scored as regular intervals.

2.9 Gene knock-out

2.9.1 Conjugation

Donor and recipient strains were grown in LB until late log phase (OD600 nm= 0.8). Cells were then mixed at a 1:4 ratio and mixed onto a LB plate. After 6 h of conjugation at 30 °C, cells were recovered by washing the plate with LB and plated on the appropriate selective medium to eliminate the donor strain and to select for plasmid integration into the chromosome. EC100 *λpir* was used as the donor strain to allow efficient replication of the R6K ori-based suicide plasmid. The recipient strain does not contain the *pir* gene, therefore preventing relication of the plasmid.

2.9.2 Allelic exchange

The first step of allelic exchange was selection of plasmid integration into the recipient chromosome (which does not carry the *pir* gene) by plating cells on chloramphenicol-LB plates. For conjugation experiments, the donor strain SM10 λpir was eliminated by adding streptomycin in the medium. After overnight growth at 30 °C, one colony was picked, diluted in 10mM MgSO4, and serial dilutions were plated

on LB agar plates with 5% sucrose and without NaCl. This plating step allowed selection of plasmid excision from the chromosome by a second cross-over. After overnight incubation at 30 °C, 100 clones were streaked on chloramphenicol-containing LB agar plates and on LB agar with 5% sucrose and without NaCl. Suc^R Cam^S clones were stored in a glycerol suspension at 80 °C.

2.10 Cell line growth, maintenance and transfection

2.10.1 Cell lines and culture conditions

The mammalian cell lines NIH 3T3 was obtained from the European Collection of Animal Cell Cultures (ECACC, Porton Down, Salisbury, UK). It was cultured in Dulbeccos Modified Eagles Media, (DMEM) plus Glutamax I (Gibco BRL) supplemented with 10 % calf serum , 2 % of 100X penicillin and streptomycin solution, and 1 % non essential amino acids (Sigma-Aldrich, UK), Cells were grown at 37 °C, 95 % air /5 % carbon dioxide (v/v) and were subcultured every three to four days at a 1 in 5 dilution.

Cell lines were grown as monolayer cultures and subcultured at 80-95 % confluence. For subculture, 25 cm^2 (T25) flasks (Falcon, Becton Dickinson, Basel, Switzerland – as are all tissue culture flasks and plates used) containing monolayers were washed with sterile PBS and then incubated with 0.75 ml 1X trypsin-EDTA (Sigma) for approximately 5 minutes. Detached cells were diluted to 5 ml with complete culture medium and 1 ml of this suspension was added to 7 ml fresh culture medium in a new T25 flask.

2.10.2 Transient transfection of mammalian cell lines with GeneJuice

Cells were transfected with mammalian expression constructs using GeneJuice (Novagen, Merck Biosciences, UK) as manufacturer's instructions. In brief cell viability counts were conducted as described (Section 2.3.2) and approximately 10^5 were seeded into the required flask or plate and grown for 24 h before transfection, at

around 50 % confluence. For six well plates a quantity of 3 µl per 100 µl OptiMEM (Gibco BRL, UK), for each well to be transfected, was vortexed and incubated at room temperature for 5 minutes. High purity plasmid DNA prepared by maxi-prepping was added at a quantity of 1 µg of DNA per 3 µl GeneJuice, mixed gently and incubated at room temperature for approximately 15 minutes. The mixture was then added drop wise to the cells and mixed into the cell culture media by gently rocking. Cells were left growing for 24- 48 h before preparing for immunofluorescent staining or another desired application. Volumes of GeneJuice, OptiMEM and DNA were scaled up for transfections of larger numbers of cells.

2.11 Fluorescence and confocal microscopy

2.11.1 Fixation of cells

Coverslips were washed by immersing three times in sterile PBS and touched dry on tissue. The samples were fixed by covering with 4 % paraformaldehyde (w/v) in PBS. 4% paraformaldehyde solution was made by dissolving in PBS in a waterbath at approximately 60 °C for 3 - 4 h. Coverslips were incubated for 15 minutes at room temperature followed by washing as before. At this stage coverslips were either stained immediately or stored in sterile PBS at 4 °C for no longer than 48 h.

2.11.2 Immunofluorescence

Cells were immunostained in various experiments with the following primary antibodies: monoclonal mouse anti c-Myc (Invitrogen, UK), mouse monoclonal anti -cytochrome c (BDBiosciences, Pharmingen, UK), polyclonal rabbit anti-Gpp130 (Covance Research Products) – a transmembrane protein localised to the *cis*-Golgi.

For immunofluorescent staining of cells, coverslips were fixed as described above and permeabilised by covering with 0.2 % Triton X-100 in PBS for 15 minutes at room temperature. Following permeabilisation the coverslips were washed with 1X PBS and then blocked in as solution of PBS containing 0.2 % BSA or 10 % normal

donkey serum for 60 minutes. The coverslips were then inverted onto 60 µl of 1 in 200 primary antibody diluted in blocking solution (1in 100 in the case of anti-Gpp130) and incubated for 90 minutes at room temperature. Following the primary incubation the coverslips were washed three times for 5 minutes in blocking solution before being inverted onto 60 µl of either Cy3-conjugated donkey anti-mouse or Cy5-conjugated donkey anti-rabbit secondary antibodies (Jackson ImmunoResearch Laboratories, Inc) diluted 1 in 300 in blocking solution and incubated in the dark for 45 minutes at room temperature. The coverslips were then washed three times for 5 minutes in PBS with the second wash containing 0.12 µg μl^{-1} Hoechst 33258 (Sigma) if nuclear staining was required. A final wash by brief immersion twice in distilled water was made and coverslips mounted onto slides using one droplet of Dako Fluorescence Mounting medium (Dako Cytomation).

2.11.3 Fluorescence and confocal imaging

Fluorescence images of the samples were obtained using a Zeiss LSM-510 confocal laser-scanning microscope (Zeiss LSM-510 system with inverted Axiovert 100M microscope) equipped with a krypton-argon laser and helium-neon lasers. Green fluorescent protein (GFP) was imaged with excitation at 488 nm and emission from 515 to 540 nm. Cy3 (indocarbocyanine) conjugated secondary antibodies were imaged with excitation at 568 nm and emission at 590 nm. Cy5 (indodicarbocyanine) conjugated secondary antibodies were excited at 633 or 647 nm and emission at 670 nm far-red detection visualised using the confocal imaging system. Fluorescence microscopy was conducted on a Nikon Eclipse TE2000-U, with a Lambda 10-2 filter unit (Sutter Co) and a Hamamatsu ORCA-ER camera controller. Imaging was done using Ultraview software package.

2.12 PVC DEAE-sepharose purification

Overnight cultures of *E. coli* containing PVC-encoding cosmids were grown overnight in LB medium at 30°C with aeration. Cultures were centrifuged at 8000 rpm in a GS3 rotor for 30 min. at 4°C. The supernatant was decanted to remove the cell

pellet and the centrifugation was repeated to remove any remaining cells. The cell free supernatant was then centrifuged at 150, 000 g for 90 minutes at 4°C in a Sorval ultra centrifuge to harvest particulate material. The supernatants were then discarded and the pellets washed by gentle resuspension in 1xPBS before a second centrifugation at 150, 000 g for 90 minutes at 4°C to pellet particulate material. The pellet was finally resuspended in 500 µl of ice cold PBS and stored at 4°C. As a second step in PVC purification the particulate preparations were further separated by DEAE-sepharose chromatography. For DEAE-sepharose chromatography, the particulate material recovered after the first high speed centrifugation described above was re-suspended in 10 ml of ice cold Phosphate Buffered Saline (PBS) and an equivalent volume of DEAE Sepharose CL-6B anion exchanger (in PBS) was added. This was incubated at room temperature for 15 minutes. The Sepharose resin was harvested by centrifugation (3000g), and the supernatant discarded. The resin was re-suspended in 40 ml of ice cold PBS and again harvested by centrifugation. This wash was repeated a further 3 times and the resin finally re-suspended in 10 ml of elution buffer [0.5M NaCl, 50mM phosphate-buffer at pH 7.4]. The resin was removed by centrifugation and the supernatant containing the PVCs was again centrifuged at 150, 000 g for 90 minutes at 4°C to pellet particulate material. Particulate material was finally re-suspended in 600 µl of ice cold PBS and stored at 4°C.

2.13 Transmission electron microscopy (TEM)

Pioloform covered 300 mesh copper grids, coated with a fine layer of carbon, were used as substrates for the protein fractions in the TEM. Four different aqueous negative stains were tested with the protein samples: 1% uranyl acetate, 3% ammonium molybdate, 3% methylamine tungstate and 2% sodium silicotungstate. The preferred stain, 3% methylamine tungstate, produced acceptable contrast and minimum artifacts and was subsequently used for all samples viewed in the TEM. The coated grids were exposed to UV light for 16 hours immediately prior to use to ensure adequate wetting of the substrate. A 10 µl drop was applied to the TEM grid and the protein allowed to settle for five minutes. Liquid was absorbed by filter paper

from the edge of the grid and substituted immediately with 10 μl of filtered negative stain. This drop was partially removed with filter paper and the grids allowed to air dry thoroughly before viewing in a Jeol 1200EX transmission electron microscope (Jeol, Tokyo Japan) operating at 80KV.

2.14 Hemocyte counts and actin staining

Injected *Galleria* were bled onto microscope slides by piercing the larval cuticle. Four animals were bled per treatment and hemocytes were counted in four random microscopic fields of view per slide. This provided an estimate of recoverable (circulating) hemocyte number. A TRITC-phalloidin conjugate was used to stain the hemocyte cytoskeleton. Briefly, pre-injected *Galleria* larvae were bled onto coverslips, and the hemocytes allowed to attach to the glass surface by incubation at room temperature for 20 min. after which they were fixed and stained with TRITC-phalloidin.

2.15 Southern blot

Digest an appropriate amount of genomic DNA by *Bgl*II and *Sph*I for 1 hour and load genomic DNA onto 1.0% gel in TAE. After electrophoresis, stain the gel with EB and photograph it. Place a transparent ruler alongside the gel so that the distance of migration of the DNA bands can be read directly from the photograph. Wash gel in 0.25 M HCl for 5 min to depurinate DNA fragments, in (0.5 M NaOH, 1.5 M NaCl) for 20min and in (0.5 M Tris pH 7.0, 3.0 M NaCl) for 20min to denature and neutralize DNA. Capillary transfer the gel to the positively charged nylon filter: Cut nylon membrane (MSI 0.45 micron #N04HY00010) and several pieces of blotting (e.g. Schleicher and Schuell GB002) paper to the same size as the gel. Wet the nylon with dH20, then soak in 5x SSC. Assemble sandwich: a. Large sheet of plastic wrap; b. Two pieces blot paper (precut to same size as gel) soaked in 20x SSC(1x SSC is 0.15 M sodium chloride plus 0.015 M sodium citrate); c. Gel (wells-side down); d. Presoaked nylon; e. One piece blot paper soaked in 5x SSC; f. 10-15 pieces of dry blot paper; h. Wrap whole sandwich in the plastic wrap; i. Place glass plate and

weight on top and let transfer >3 hr. The DNA was cross-linked to the filter by UV irradiation.

Partial fragment in the middle of *mcf2* cloned into pDM4 was used as the probe. Mix 25ng of DNA template to be labelled, 21μl water and 10 μl random oligonucleotide primers and heat at 100 ° C for 5 min; Add 10 μl 5x primer buffer, 5 μl labelled nucleotide and 1 μl Exo(-) Klenow enzyme, incubate at 37 ° C for 10 min and stop the reaction by adding 2 μl of stop mix.

The prehybridization and hybridization solutions were the same (2x SSC, 5x Denhardt's solution (0.5 g of Ficoll, 0.5 g of polyvinylpyrrolidone, 0.5 g of bovine serum albumin, and water to 500 ml), 0.5% sodium dodecyl sulfate (SDS), and 100 mg of denatured, fragmented salmon sperm DNA per ml). Prehybridization was done for 1 to 2 h at 55 ° C, and hybridization was done for 16 to 20 h at the same temperature. After hybridization, the filters were washed at 55 ° C for 15 min with 1x SSC and 0.1% SDS. The filters were then autoradiographed.

2.16 PCR mutagenesis

The random PCR products are amplified using Random Mutagenesis Kit (STRATAGENE). It is a blend of two error prone PCR polymerases- Mutazyme I DNA polymerases and a novel *Taq* DNA polymerase mutant that exhibits increased misinsertion and misextension frequencies compared to wild type *Taq*. This combination produce a less biased mutational spectrum with equivalent mutation rates as A's and T's vs. G's and C's. The mutation rate is 1-16 mutations per kb by using a single set of buffer conditions optimized for high product yield.

Start the PCR cycles according the following schemes: a) denaturation - 95 ° C, 30 sec. b) annealing - 55 °C 30 sec. c) extension - 72 °C 1min, repeat cycles 30 times. Add a final extension step of 10 min. to fill in any uncompleted polymerisation. Then cooled down to 4- 25 °C. Three DNA template concentrations are used to optimize the

mutation frequency. Then cloning PCR products into pBAD30 and sequence.

2.17 2D gel electrophoresis and protein identification

Supernatant proteins from *E. coli* EC100 carrying either the c4DF10 cosmid (which encodes PaPVCpnf) or the control vector pWEB, were phenol precipitated and protein resuspended in 150µl CDU (9M Urea, 4% Chaps, 130mM DTT, 1 x HALT™ protease Inhibitor Cocktail Mix, Pierce) and incubated for 2h at room temperature. Samples were then centrifuged for 30 min. at 88,760 g. For protein quantification, the RediPlate Protein Quantitation Kit (Molecular Probes) was used. For 2D gel electrophoresis, the Multiphor II system (GE Healthcare) was used for isoelectric focusing and horizontal SDS polyacrylamide gel electrophoresis with Immobiline DryStrip gels and precast 12.5% homogenous SDS gels (GE Healthcare). Briefly, Immobiline Dry strip gels were rehydrated over night in rehydration buffer consisting of 8 M Urea, 2% CHAPS, 0.002 % bromphenolblue, 18mM DTT and 0.5 % IPG buffer containing 15 µg of the protein sample. Isoelectric focusing was performed at 20°C. For the IPG strip 3-10 the upper limits for current and power were set to 2mA and 2W, respectively. In phase 1 the voltage was kept at 300V for 1Vh, in phase 2 the voltage was increased to 3500V over 2900Vh, in the third phase the Voltage was kept at 3500V for 7100Vh. The resulting strips were then frozen at –80°C for subsequent analysis. Before SDS gel electrophoresis, strips were equilibrated for 15 min. in 50mM Tris pH8.8, 6M urea, 30% glycerol, 2% SDS, 0.002 % bromphenolblue and 65 mM DTT. In a second equilibration step, 65 mM DTT was replaced with 135 mM iodoacetamide. The Immobiline DryStrip gel was then transferred onto the SDS polyacrylamide gel and electrophoresed. Before staining, gels were washed over night in fixation solution containing 40% ethanol and 10 % acetic acid. Silver staining was performed according to the protocol of the PlusOne silver staining kit (GE Healthcare), omitting glutaraldehyde from the sensitising solution and formaldehyde from the silver nitrate solution. Protein spots from silver stained gels were cut from

the acylamide and sent to the protein sequencing facility at the University of the West of England. MALDI analysis of trypsin-digested protein samples was used to generate a spectrum, which was compared to all proteins in the database and also to a database of predicted proteins from the *P. asymbiotica* ATCC43949 genome.

Chapter 3

MAKES CATERPILLARS FLOPPY 2(Mcf2)

IN *PHOTORHABDUS LUMINESCENS*

3.1 INTRODUCTION:

The Mcf toxin (Makes caterpillars floppy) was discovered upon screening 300 individual clones from a cosmid library constructed from *P. luminescens* subsp. *akhurstii* strain W14 genomic DNA, for injectable activity against *M. sexta*. A 33 kb cosmid was isolated which permitted the persistence of *E. coli* in the insect haemocoel, and caused a loss of body turgor at ~12 h termed the 'floppy' phenotype, followed by death at ~24 h. It was determined that an 8.8 kb gene consisting of a single open reading frame was responsible for enabling both the persistence of *E. coli* within, and the death of, *M. sexta* via transposon mutagenesis. The Mcf protein is predicted to be 324 kDa in size (Daborn et al. 2002).

Here the discovery of a *mcf1* homologue, *mcf2*, will be described within the same *P. luminescens* W14 genome. The predicted N-terminal domain of Mcf2 lacks a BH3-like motif but instead has a region of similarity to the HrmA type-III secreted effector from the plant pathogen *Pseudomonas syringae* pv. *syringae*, which is a plant avirulence protein (Heu et al. 1993). Plant cell death induced by recognition of HrmA triggers localised cell death, which limits bacterial infection, and confers avirulence on the virulent bacterium *P. syringae* pv. *tabaci* in all tobacco cultivars examined (Alfano et al. 1997). The avirulence function of *hrmA* is dependent on the hypersensitive response and pathogenicity (*hrp*) genes, some of which are involved in the regulation and assembly of the bacterial type-III secretion system or TTSS (Alfano et al. 2000). HrmA is secreted by the TTSS directly into plant cells and transient expression of HrmA in tobacco cells results in cell death (Alfano et al. 1997). Here we show that, like Mcf1, expression of *Photorhabdus* Mcf2 in *E. coli* is sufficient to kill caterpillars.

3.2 RESULTS:

3.2.1 Gene sequence analysis

After identification of Mcf1 in *P. luminescens* W14 genomic sample sequence, a cosmid was found containing partial *mcf1*-like gene during random end-sequencing of a *P. luminescens* W14 cosmid library. The sequence derived from this *mcf1*-like gene containing cosmid assembled with *mcf1* sequences (Lasergene, Madison, WI, USA) but was clearly different at the nucleotide level. Following identification of the *mcf2* gene, the cosmid library was re-screened using polymerase chain reaction (PCR) primers to isolate a cosmid W14-1C-G1 carrying the complete *mcf2* ORF. The complete nucleotide sequence of this cosmid was then determined using transposon mutagenesis using an EZ-Tet transposon sequencing primers within the transposon (EpiCenter). After assemble, we got an ORF-encoding a *mcf1*-like gene, and termed it *mcf2*. The length of it is 7218 bp. Upstream of *mcf2*, there are three RTX-like genes, encoding *RtxB*, membrane-fusion protein and toxin secretion transporter separately. This region' G+C content is higher (53.7%) than the rest of the genome of *Photorhabdus luminescens* (42%) (Figure 3.1). It suggests that this region may be containing a new PAI.

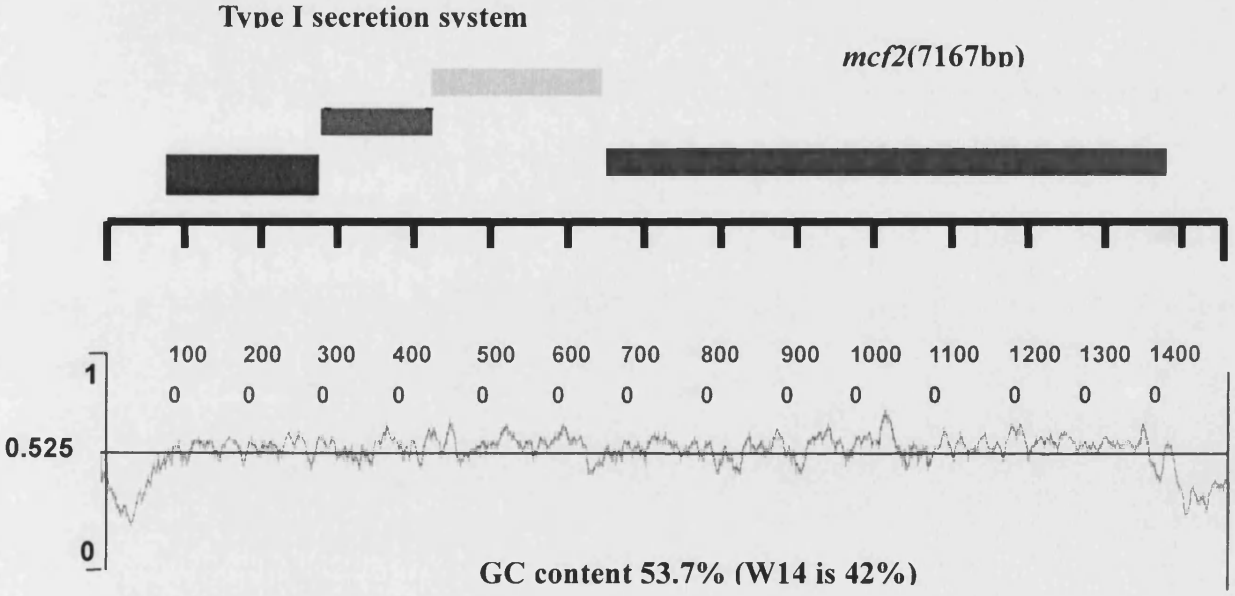

Figure 3.1 upstream of *mcf2* are three RTX genes, this region's GC content is much higher than the whole genome of W14

The *mcf2* gene predicts another large (262 kDa) protein. Like Mcf1, amino acids 1015-1548 of Mcf2 are 39% similar and 20% identical to amino acids 867-1368 of *C. difficile* toxin B, but Mcf2 lacks the similarity to the C-terminus of an RTX-like toxin from *Actinobacillus pleuropneumoniae* carried by the C-terminus of Mcf1 (Figure 3.2A). Since the original description of the Mcf1 gene, a new entry in Genbank shows that both Mcf1 and Mcf2 also show a second region of homology to an RTX-like cytotoxin (gene VVA1030) from Vibrio vulnificus strain YJ016 (amino acids 695-914 of Mcf2 are 30% identical and 48% similar to amino acids 3250-3496 of VVA1030). The predicted N-terminal domain of Mcf2 is shorter than that of Mcf1 and lacks a BH3-like domain (Figure 3.3). Instead, the N-terminus carries a region with significant similarity (54% similarity and 40% identity) to the C-terminus of the plant avirulence protein HrmA from *P. syringae pv. syringae* (Figure 3.2B).

Further examination of unfinished genome sequences shows that Mcf1 and Mcf2 are part of a family of toxins including two undescribed homologues from *Pseudomonas fluorescens* strain Pf01, ORFs 4315 and 4316, which are 28% identical and 46% similar to each other. A comparison of these predicted proteins with the *Photorhabdus* Mcf1 and Mcf2 proteins shows that the N-terminal domain is variable in this family of proteins, predicting a glycosyltransferase domain in the *P. fluorescens* proteins. The *mcf2* gene lies in an operon adjacent to three genes encoding a type-I secretion apparatus, which is conserved in the two different *Photorhabdus* strains examined-strain W14 and TTO1 (Figure 3.4).

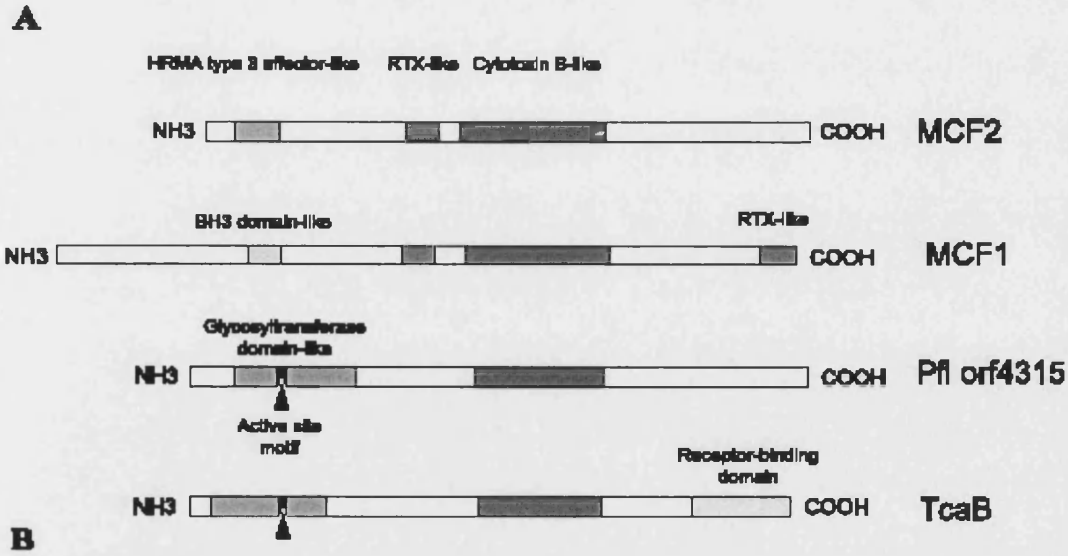

B

```
Mcf2:  199 QQQKMLERALESNAYWRYSNDRPVGISRLDKSEQQAFVSYIKTLATRITTI--DILVQGN 372
           ++ + L R  E   Y  Y  D P   + ++ +EQ+ ++  ++ L  +   I    +
HrmA:  135 EKAEALGRDTEIGIYMIYKRDTP-DTTPMNAAEQEHYLETLQALDNEKNLIIRPQIHDDR 193

Mcf2:  373 EKTALELQ---TDDALNNAEAFRMLPKDFAQRYGTRGKLGARLTINVMKAHFNLLARALP 543
           E+  L L     +D        FRM+PKD       G    RLTI V   +   LA A+
HrmA:  194 EESELDLGRYIAEDRNARTGFFRMVPKDQRAPETNSG----RLTIGVEPKYGAQLALAMA 249

Mcf2:  544 QLFNDNNRGWLEQAKIMGPKNLGSRTDQAVIYLSKAGIEHAQTISEKLSEL--LPATAFV 717
            L + +    + Q K++GP   G +TD A++Y++   +  A  + EKL +L  +P   FV
HrmA:  250 TLMDKHKS--VTQGKVVGPAKYGQQTDSAILYIN-GDLAKAVKLGEKLKKLSGIPPEGFV 306

Mcf2:  718 EHTPTGMYRVGKGISYSETAAGGSSSHGQSRAQLIAAAGTQSLLTDIPIEKTLTHTLQTR 897
           EHTP  M   G G+SY+E+  G  SSHGQ+R  +I  A    L    P+E  L   L  R
HrmA:  307 EHTPLSMQSTGLGLSYAESVEGQPSSHGQARTHVIMDA----LKGQGPMENRLKMALAER 362

Mcf2:  898 GYDVENPAL 924
           GYD  NPAL
HrmA:  363 GYDPENPAL 371
```

Figure 3.2 Similarity of Mcf2 to other toxins and to the HrmA plant avirulence gene. A: Predicted structure of the Mcf2 protein compared to Mcf1 and other members of the same toxin family. All these high molecular mass toxins carry a central domain with similarity to *C. diffcile* toxin B but vary at their N- and C-termini. Both Mcf1 and Mcf2 are encoded within the genomes of *P. luminescens* W14 and TT01. Mcf2 predicts a region within its N-terminus with similarity to the type-III effector HrmA whilst Mcf1 shows similarity to a consensus sequence for a BH3 (pro-apoptotic) domain. TcaB from *C. diffcile* and a novel homologue from *P. fluorescens* (ORF 4315) both carry a putative glycosyltransferase domain. The C-termini of Mcf1 carries an RTX-like export domain whereas the C-terminus of TcaB carries a receptor-binding domain. Note that *P. fluorescens* ORF 4316 is not shown for brevity but that it is 28% identical to and 46% similar to ORF 4315. B: Alignment of part of the N-terminus of Mcf2 with the C-terminus of the HrmA type-III effector protein from *P. syringae pv. syringae*.

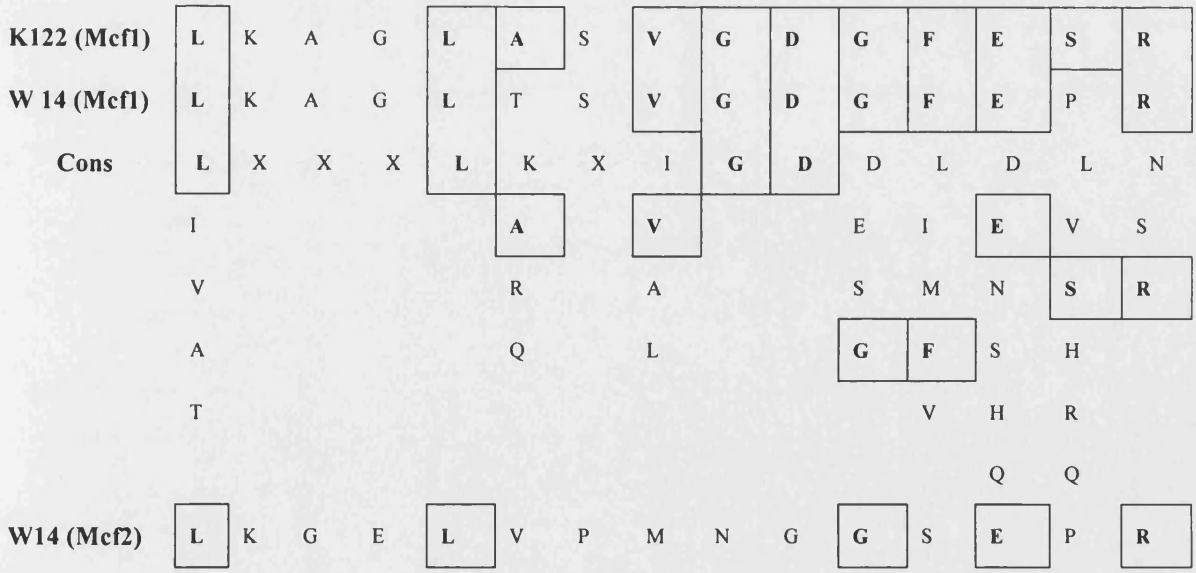

Figure 3.3 Match to the BH3 domain consensus sequence for Mcf1 and Mcf2

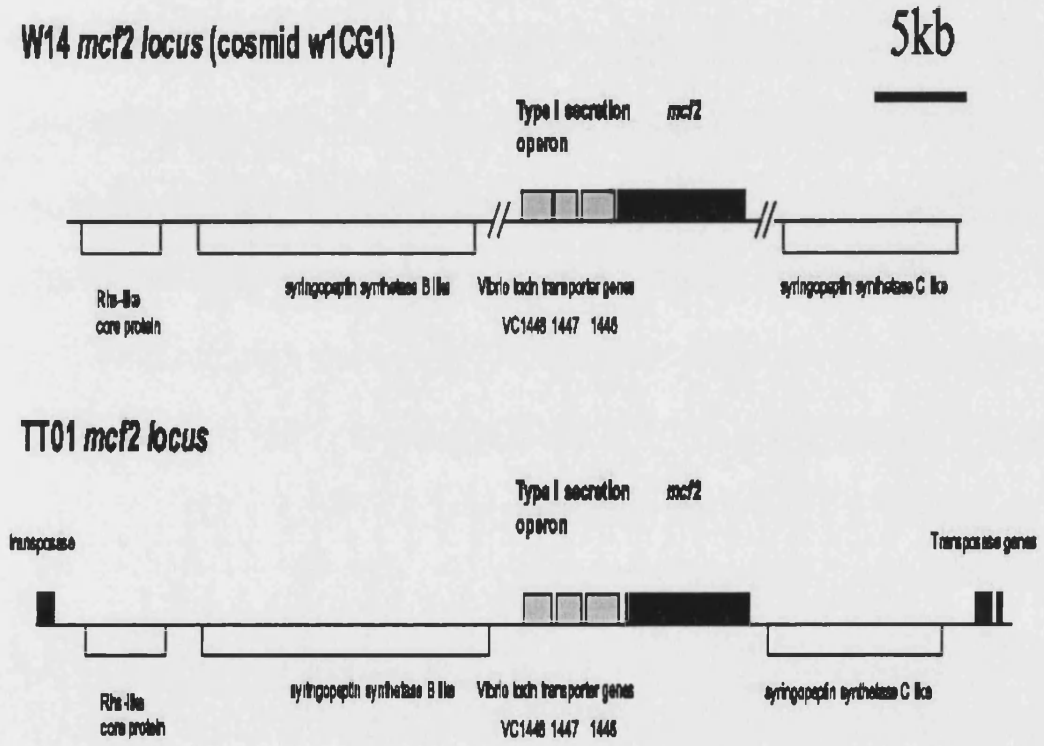

Figure 3.4 Genomic organisation of the *mcf2* locus in the *P. luminescens* strain W14 and TT01 genomes. Note that the *mcf2* gene lies within an operon containing three candidate type-I secretion genes. The double bars in the W14 *mcf2* locus mark regions not currently assembled due to the presence of numerous repeats.

3.2.2 Cosmid injection

Two cosmids were found containing whole *mcf2*(1C-G1 and 2D-D9), and the SDS-PAGE gel reveals the presence of a single protein with the predicted molecular weight-262kD (Figure3.5).

E. coli carrying the Mcf2 expressing cosmids was injected into *Manduca sexta* caterpillars, and like *E. coli* expressing Mcf1, these cosmid also caused caterpillars to die with a 'floppy' phenotype (Figure 3.6), confirms that Mcf2 is real virulence factor that can kill *M. sexta*.

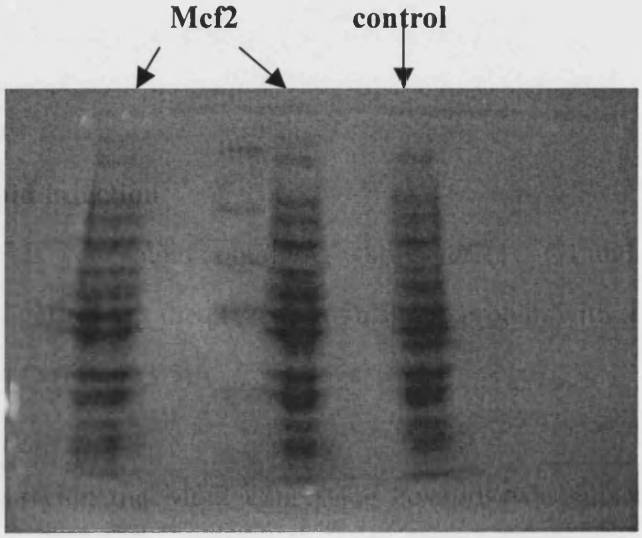

Figure 3.5 SDS-PAGE for cosmid containing *mcf2*, control is empty pWEB

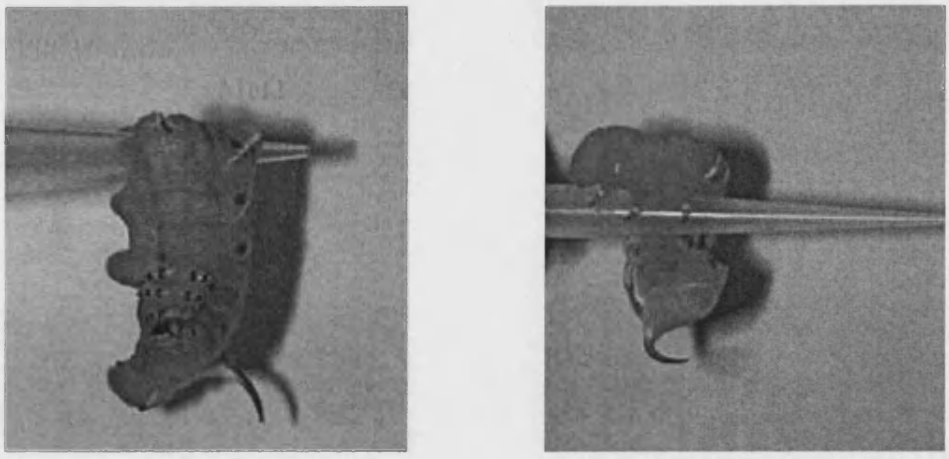

Figure 3.6 Assay for caterpillar death. The right one is control- injected with *E. coli* containing just pWEB, it still keeps turgor.

3.2.3 Comparison of the toxicity of Mcf1 and Mcf2

In order to better compare the toxicity of Mcf1 and Mcf2, both genes were cloned into the arabinose-inducible and tightly regulated vector -pBAD30. Previous attempts to clone either gene away from their own native promoters into 'leaky' expression plasmids consistently failed, suggesting that both proteins may be detrimental to *E. coli*. The *mcf1* gene was cloned into pBAD30 as a PCR product using the primers 5'-AATATGAGCTCTTGCCTTTGACCCGATCAT-3' and 5'-ATCAGTCTAGACTAGATGGCCCAAGGCAGC-3'. The *mcf2* gene was also cloned into pBAD30 in the same fashion, using the primers 5'-AATATGAGCTCGTAAATACCAAAG-3' and 5'-ATCAGTCTAGATTAGGACAGCGATG-3'. Examination of cultures of *E. coli* expressing Mcf1 and Mcf2 by SDS- PAGE analysis showed Mcf2 to be a high molecular mass protein migrating faster than Mcf1, as expected (Figure 3.7). However, the Mcf2 protein shows a ladder of bands on the gel, suggesting either that it is degraded or that it may exist in a number of different post-translationally modified forms.

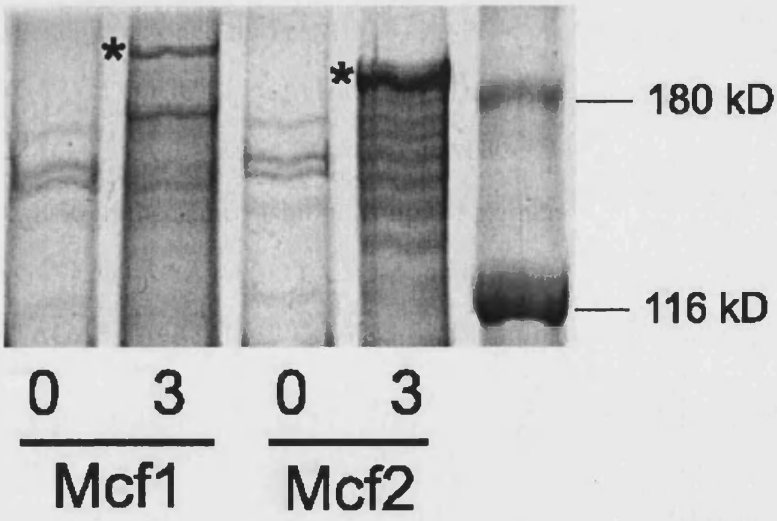

Figure 3.7 SDS-PAGE gel of Mcf1 and Mcf2 expressed in pBAD30 under arabinose induction (asterix in each lane) and stained with Coomassie brilliant blue. Lanes are uninduced (0) and 3 h after induction with arabinose (3)

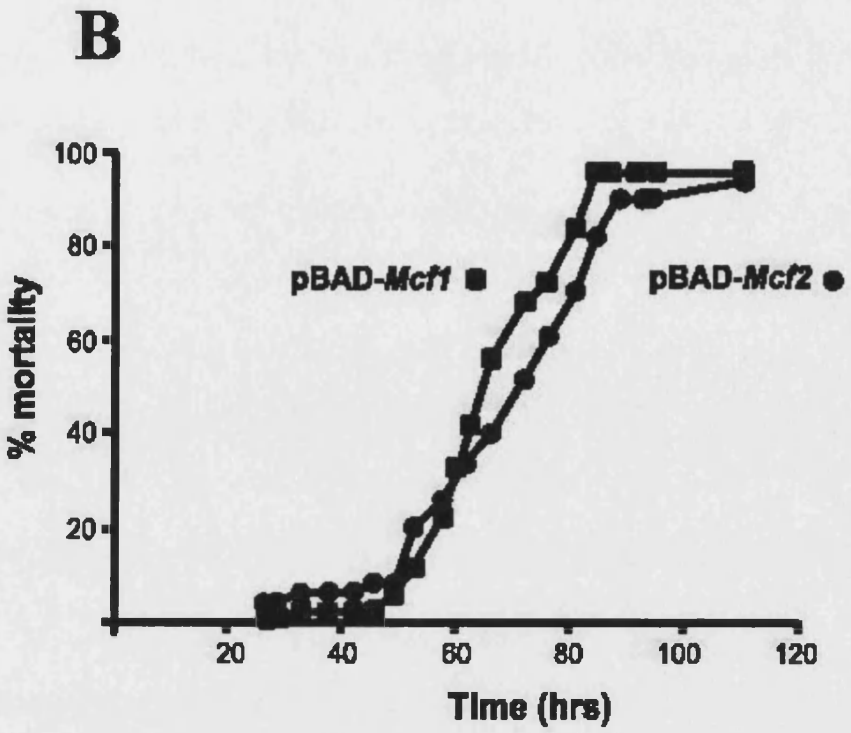

Figure 3.8 Time taken to kill *G. mellonella* larvae after injection of a fixed dose of Mcf1 and Mcf2 expressing *E. coli*.

Injection of $1.5X10^7$ arabinose-induced pBAD-*mcf2 E. coli* into *G. mellonella* caterpillars resulted in 50% mortality within 70 h. Similar results were achieved with $1.0 X10^7$ arabinose-induced pBAD-*mcf1 E. coli*. Thus induced Mcf2 carrying *E. coli* kill caterpillars at the same speed as *E. coli* carrying *mcf1*-both recombinant bacteria killed 50% of the insects in 60-70 h (Figure 3.8).

3.2.4 *mcf2* knock out using pDM4

3.2.4.1 Knock out using pDM4

In order to investigate the function of *mcf2* further, *mcf2* was knocked out in *Photorhabdus luminescens* TTO1 Rif^+ strain. Deletion in the *mcf2* gene was achieved by cloning the modified PCR product (partial fragment in the middle of *mcf2*, about 700 bp) into a suicide vector- pDM4. The partial fragment was PCR amplified from the genome DNA using the rTth DNA polymerise kit (Perkin-Elmer). Primers were

synthesised by MWG biotech [primer sequences 5' to 3'.forward: CGG AGA TCT TGG CGA CAA GTT GAC CCC TAT CT reverse: GGT AGA TCT CAC CGC CTT CTG TAC ATC GTT CTC]. The resulting PCR product was purified with a QIAquick Gel Extraction kit (Qiagen), digested with *BglII* (primers contained *BglII* site), purified again with the QIAquick Gel Extraction kit and ligated into *BglII*-linearized pDM4. After ligation the recombinant plasmid was electrotransformed into *E. coli* S17λ*pir* and Cm^+ colonies were screened on AGAR plates (Cm^+).

Recombinant pDM4-*mcf2* was conjugated into genome of TTO1 Rif^+. As *P. luminescens* does not encode the Pir protein, the only Cm^+/ Rif^+ colonies were those in which homologous recombination had occurred. After the second homologous recombination, clones were checked for their sensitivity to chloramphenicol (screening on arga plate Cm^+/ Rif^+). The deleted clone was finally verified by southernblot (Figure 3.9).

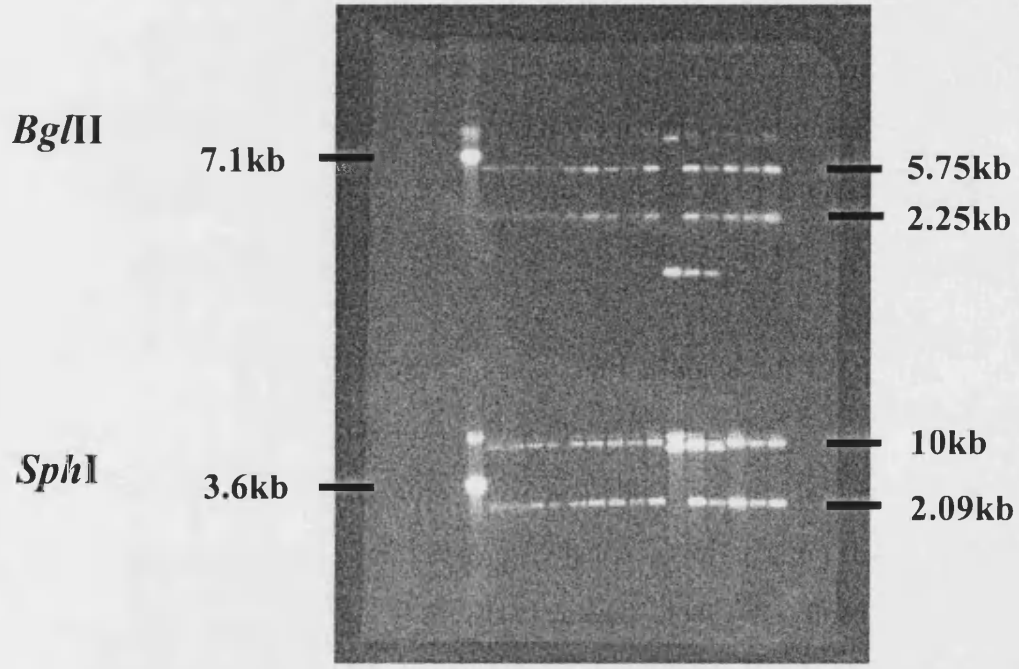

Figure 3.9 Southern analysis of chromosomal DNA of TTO1 and TTO1 *mcf2*⁻. Approximate fragment sizes were calculated from the agarose gel. Lanes 1 wild type TTO1(negative control), partial fragment in the middle of *mcf2* was used as the probe.

3.2.4.2 Bioassay of TTO1 *mcf2*⁻ strain

After injection of TTO1 wild strain and *mcf2*⁻ strain into *G. mellonella* and *Manduca sexta*, we found no significant different between them with survival time (Figure 3.10).

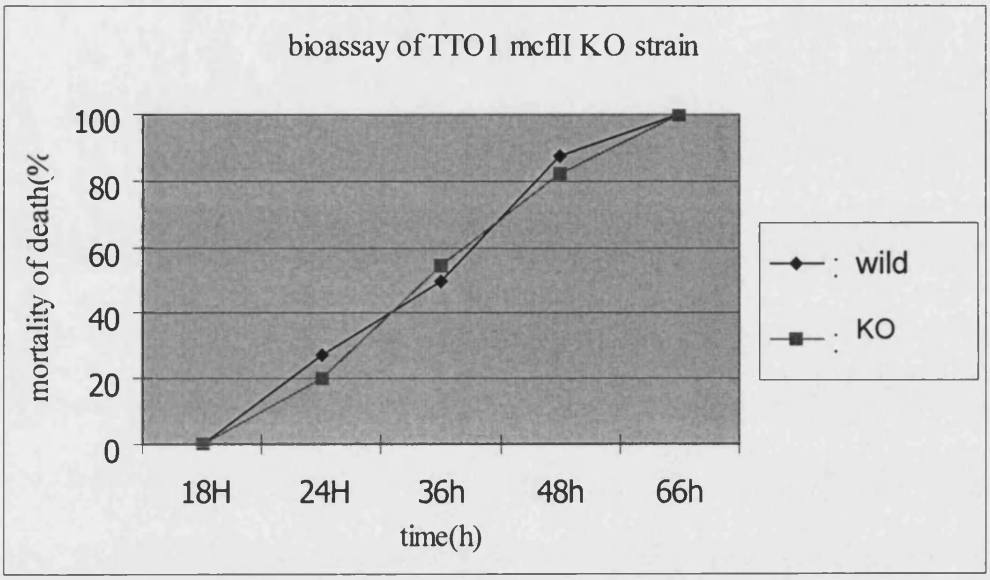

Figure 3.10 Injection results of TTO1 wild strain and *mcf2*⁻ strain into *Manduca sexta*. 1X (Mcf1)=2.6X10^6 cells/ 30 μ l, 1X (Mcf2)=2.4X10^6 cells/ 30 μ l.

3.3 Conclusion

Here described the identification of a homologue of *mcf1*, termed *mcf2*, within the *P. luminescens* genome. The predicted amino acid sequence of Mcf2 is similar to Mcf1 but differs at its N-terminus. The genomic context of *mcf2*, in an operon with type-I secretion machinery, suggests secretion of Mcf2 via the type-I pathway. It is interesting to note that HrmA is secreted by the type-III pathway in *P. syringae pv. syringae* and therefore that the HrmA-like domain of Mcf2 may effectively be a fusion of a type-III effector with the high molecular mass Mcf1-like toxin.

Considering the function of Mcf1 in *Photorhabdus*, it is therefore unexpected that *Photorhabdus* strains, including W14 and TT01, should require a second potent toxin also possessing the same properties. There are several potential explanations for this

observation. First, as insect death is a prerequisite for the lifecycle of *Photorhabdus*, they encode more than one toxin capable of killing the insect host. Secondly, Mcf1 and Mcf2 may have activities against different types of insects. Finally, and alternatively, Mcf1 and Mcf2 may have very different sites of action within the insect. The Mcf1 toxin can destroy the insect gut and hemocytes by triggering massive programmed cell death. However, the site and mode of action of Mcf2 is unknown and is currently under investigation. The knock out of both Mcf homologues is under investigating.

CHARPTER 4

PHOTORHABDUS VIRULENCE CASSETTES (PVCs)

4.1 Introduction

Phage-like loci within bacterial genomes can encode bacterial effectors subsequently secreted by secretion machinery encoded elsewhere in the genome (Ehrbar et al. 2005; Boyd et al. 2002). For example the *Salmonella* outer protein E (SopE) is encoded within a prophage (Mirold et al. 1999) but is then subsequently secreted into host cells via the Type Three Secretion System (TTSS) encoded elsewhere (Wood et al. 1996). However the expression of such effector carrying prophage within recombinant *Esherichia coli* is not sufficient for effector secretion and delivery in the absence of the independently encoded TTSS. In *S. entomophila*, the 120 kb pADAP plasmid confers 'amber disease', a disease associated with 'clearing' of midgut of the New Zealand Grass grub (Hurst et al. 2000). The pADAP plasmid contains genes encoding both homologs of the insecticidal *toxin complex* (*tc*) genes (ffrench-Constant et al. 2004), termed *sepA*, *sepB* and *sepC* (Hurst et al. 2000), which are responsible for insect gut clearance, and also a prophage-like locus responsible for a separate 'anti-feeding' effect (Hurst et al. 2004). This pADAP prophage-like locus contains 18 putative open reading frames predicting proteins with high similarity to phage tail and base plate proteins as well as a putative effector protein, putatively responsible for the anti-feeding activity against the grass grub (Hurst et al. 2004).

Similarly the genomes of two recently sequenced species of *Photorhabdus*, *P. luminescens* strain TT01 (Hurst et al. 2004; Waterfield et al. 2004) and *P. asymbiotica* strain ATCC43949, contain numerous copies of these prophage-like loci each encoding different putative effector proteins (Figure 4.1). Some of these putative effectors show predicted amino acid similarity to parts of known multi-domain toxins such as the Mcf cytotoxin from *P. luminescens* (Daborn et al. 2002), Toxin A from *Clostridium difficile* (Dove et al. 1990), YopT from *Yersinia enterocolitica* (Zumbihl et al. 1999), or the active site of Cytotoxic Necrosis Factor, CNF1, from *E. coli*

(Landraud et al. 2004). Others show no predicted similarity to known effectors and so may represent novel effectors with novel modes of action.

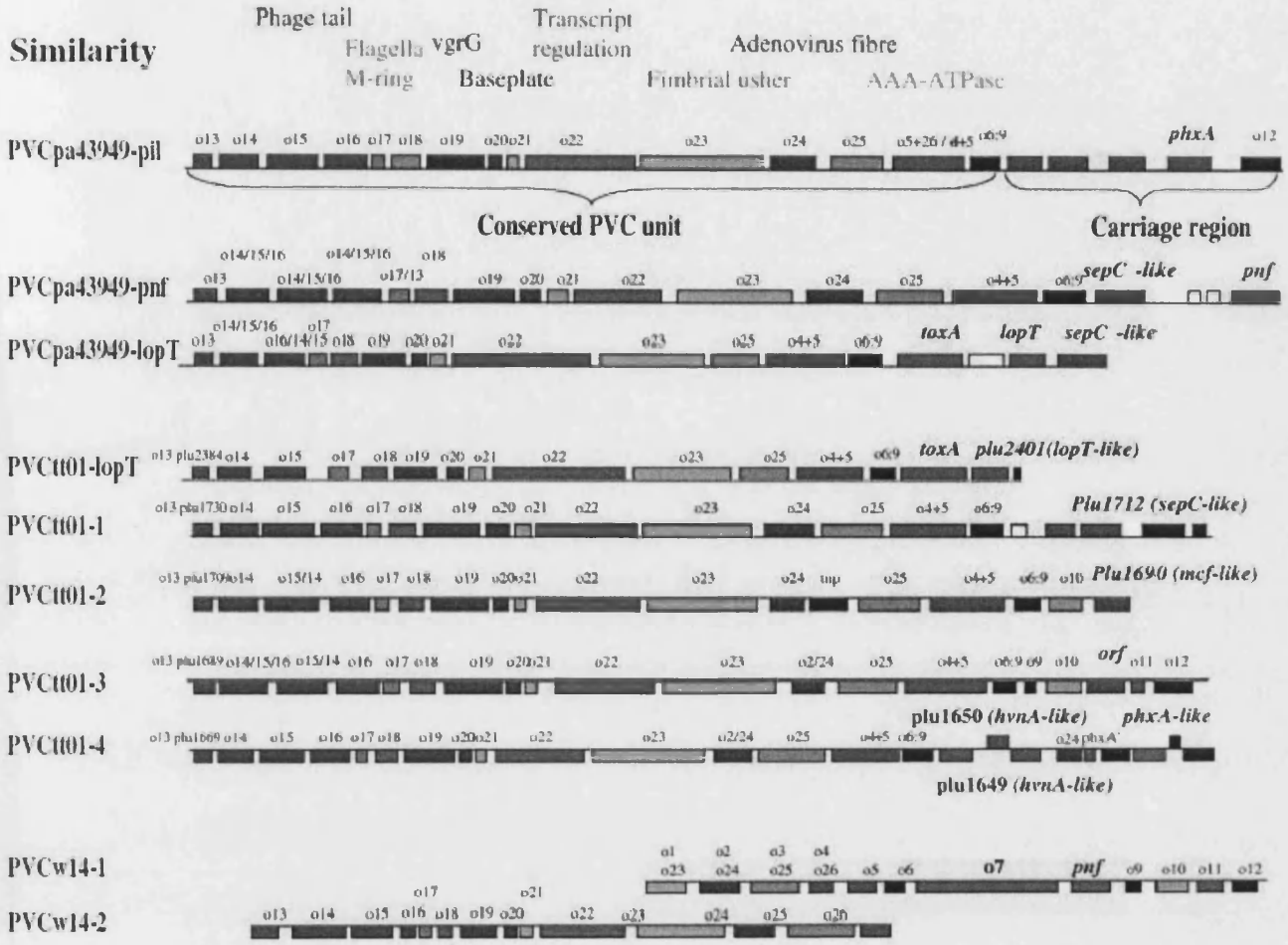

Figure 4.1 Diagrammatic summary of the different PVC units in *Photorhabdus*. Homologous genes are colour-matched. Genes in red represent potentially mobilized genes encoded in the 'carriage' region of the PVC. Many of these open reading frames (ORFs) show similarity to virulence factors from other pathogens. These include not only the pnf gene (necrosis factor), but also the *yopT*-like type III effector *(lopT)*, the dermonecrosis toxins (*toxA* and *dnt*) and genes similar to the variable-tail region of the Serratia entomophila *tccC* homologue, *sepC*. In addition to severalge nes of unknown function, homologues of the putative heme-binding protein PhxA and halovibrin (HvnA) are seen, the latter of which is essential for symbiosis between *Vibrio sp.* and squid. ORFs are designated an o-number based on similarity to the previously published *pnf* loci, which is encoded on PVC regions of *P. luminescens* strainW14 (GenBank accession number AY144118).

In order to determine if the *Photorhabdus* PVCs have insecticidal activity, as suggested by the anti-feeding activity of the pADAP PVC locus in *S. entomophila*, here PVCs' injectable activity against larvae of the waxmoth *Galleria mellonela* will be described. Not only *E. coli* expressing PVC containing cosmids are toxic to larvae on injection but also these same *E. coli* produce structures similar to one type of bacteriocin, the R-type pyocins. Unexpectedly, the PVCs have no anti-bacterial activity but trigger rapid destruction of insect phagocytes following injection. This hemocyte destruction is associated with actin condensation, an effect that can be re-capitulated by expressing putative effector proteins from the PVCs directly in tissue culture cells. These results are consistent with a hypothesis that pyocin-like structures in *Photorhabdus* have been co-opted from use against bacteria to a novel use against insect phagocytes.

4.2 RESULTS:

4.2.1 Genomic organization of the PVCs

To determine the genomic organization of the PVCs within different *Photorhabdus* species, PVCs from *P. luminescens* strain TT01 (Duchaud et al. 2003), *P. temperata* strain K122 and *P. asymbiotica* ATCC43949 were identified and compared. PVC loci are found distributed around the genome, in both *P. asymbiotica* ATCC43949 and *P. luminescens*. However in the case of *P. luminescens*, four PVC elements are also clustered in a tandem array between a type IV DNA conjugation pilus operon and a *mukB* replicon partitioning gene. In *P. asymbiotica* only one of these PVC elements is present at this locus, while in *P. temperata* this PVC cassette is replaced with a Mu-like phage, suggesting a common insertion site for mobile elements. Detailed comparison of the different predicted open reading frames within the different PVCs shows their phage-like structure. Thus each PVC unit is predicted to encode 15 to 20 proteins, each with predicted similarity to phage tail, phage base plate assembly, fimbrial usher and putative effector proteins from other pathogenic bacteria (Figure 4.2). It is interesting to note that each PVC unit carries different putative effector

sequences but always in the equivalent position, as documented for other prophage (Boyd et al. 2002). The different PVC effectors are also often flanked by transposons, suggesting a possible mechanism for their insertion into the PVC or their movement between different PVCs. Importantly, the presence of multiple effectors within a single cassette, or indeed multiple PVCs at a single locus suggests that a single PVC containing locus may be able to confer several different phenotypes via the array of multiple effectors present. Finally, one PVC element is consistently inserted adjacent to the *mukB* locus, a locus involved in plasmid maintenance and stability (Weitao et al. 2000). This suggests that *mukB* may either be a communal insertion point for these phage-like elements or that it may regulate the insertion of plasmids containing these elements. Interestingly, a type IV DNA conjugation pilus operon is found immediately 5' to this PVC element insertion site. A similar operon is also found on the pADAP plasmid where it is responsible for conjugative transfer of the plasmid. It is therefore temping to speculate that this operon in *Photorhabdus* is involved in horizontal movement of the PVC elements. One model element from *P. asymbiotica* designated PaPVCpnf was selected for detailed investigation.

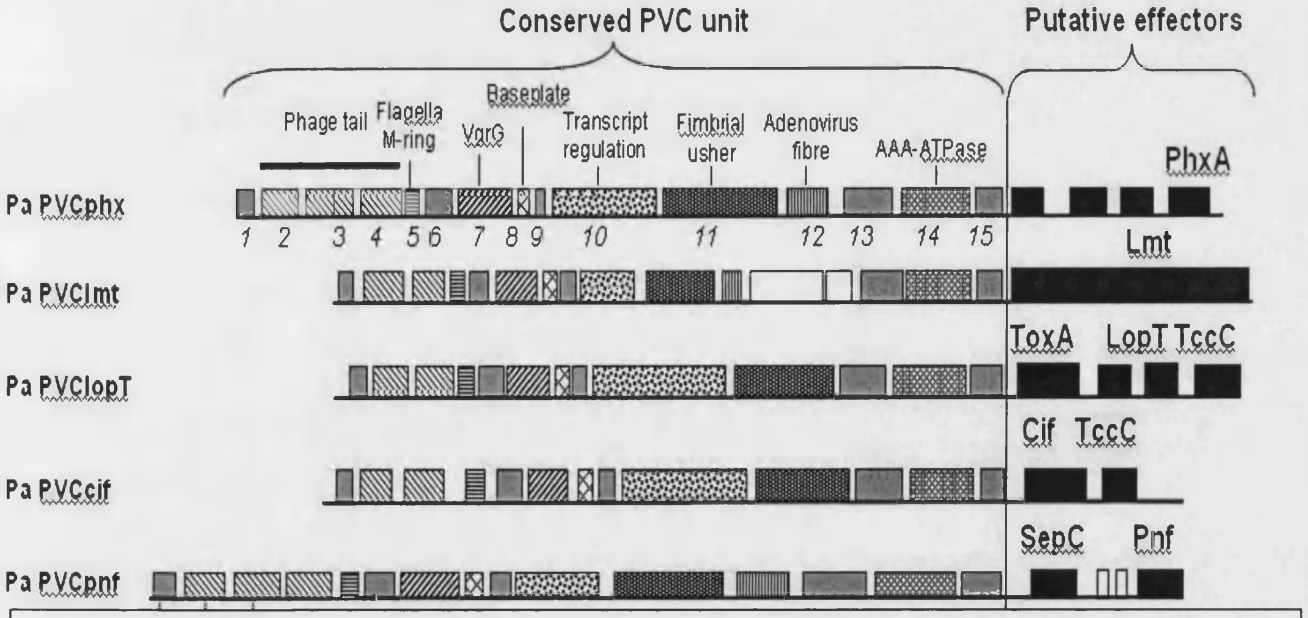

Figure 4.2 The *Photorhabdus* Virulence Cassette (PVC) encoding loci of *P. asymbiotica* .The conserved PVC unit of 13-15 ORFs predicted proteins with high similarity to different phage components. Note the variable number of putative effector proteins encoded at one end of each PVC locus. These effectors are either unnamed or bear the name of the protein to which they bear the most similarity in a BlastX search

Although the specific role of the putative effector in *Photorhabdus* virulence remains to be tested, it is interesting that the C-terminal portion of the putative (CNF-like) toxin designated Pnf is highly conserved with other members of the family and contains the active site (Buetow et al. 2001), whereas the normally variable cell targeting and translocation domains are absent entirely (Figure 4.3). This suggests the protein may be directly delivered into a target cell by either type IV, type III or a novel secretion systems.

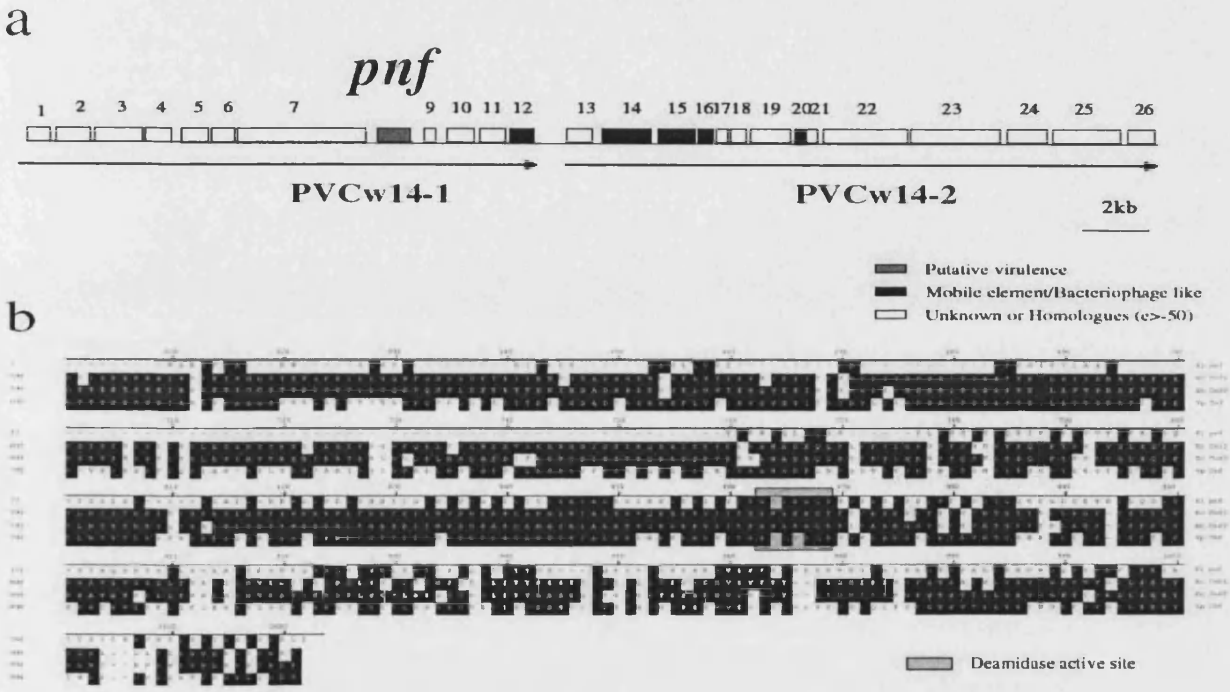

Figure 4.3 A region of the *P. luminescens* W14 genome, showing similarity to the genome of a *Nostoc sp.* cyanobacterium (GenBank accession number NC_003272) and encoding a Cnf-like toxin, pnf. (A, lower panel). Note that a number of ORFs in this region are either bacteriophage-like (14–16 and 20) or putative transposases (ORF 12), and that two large repeats flank the sequenced region itself encompassing ORFs 1–4 and 23–26 (broken arrows below ORF map). Within the region sequenced, no tRNA was found. ORFs have been colour-coded based on their likely functions as predicted from BlastX searches (see key). The predicted amino acid sequence of the Pnf protein from *Photorhabdus* can be aligned with the C-terminal domains of other Cnf homologues showing conservation of the Rho-deamidase active site (boxed). Predicted amino acid sequences for *E. coli* CNF1, CNF2 and *Yersinia pseudotuberculosis* CNF were derived from accession numbers AAA85196, AAA18229 and AAG46433, respectively.

4.2.2 PVC expression and structure

The supernatant of PaPVCpnf cosmid containing *E. coli* was examined via two-dimensional (2D) gel electrophoresis and subsequent MALDI-TOF analysis of expressed *Photorhabdus* proteins (Figure 4.4). Visual examination of 2D gels of *E. coli* with and without PVC carrying cosmids showed several differences. Subsequent MALDI-TOF analysis of trypsin digests of proteins present only in the PVC expressing *E. coli* and subsequent interrogation of a database of predicted PVC proteins, confirmed that three of the most abundant differentially expressed proteins were of PVC origin and correspond to the first three predicted open reading frames in the PVC locus (Orf1, Orf2, Orf3) (Figure 4.2 and Figure 4.4).

High speed centrifugation confirmed that PVCs activity was 'particulated'. To determine the structure of the final exported PVC we examined supernatants of PaPVCpnf expressing recombinant *E. coli* via TEM. Electron microscopy revealed the presence of structures highly reminiscent of R-type pyocins (Michel-Briand et al. 2002). These structures are approximately 30nm in width and of variable length, with some example exceeding 800nm in length (Figure 4.5). They comprise a rigid contractile outer sheath and thin hollow inner "needle" structure (approximately 6nm wide) analogous with R-type pyocins. Examples of both 'contracted' and 'relaxed' forms were seen. Although the precise mode of action of R-type pyocins themselves is not known, it is suggested that their antibacterial activity is achieved by injection of the needle into bacterial cells via the contraction of the sheath (Michel-Briand et al. 2002).

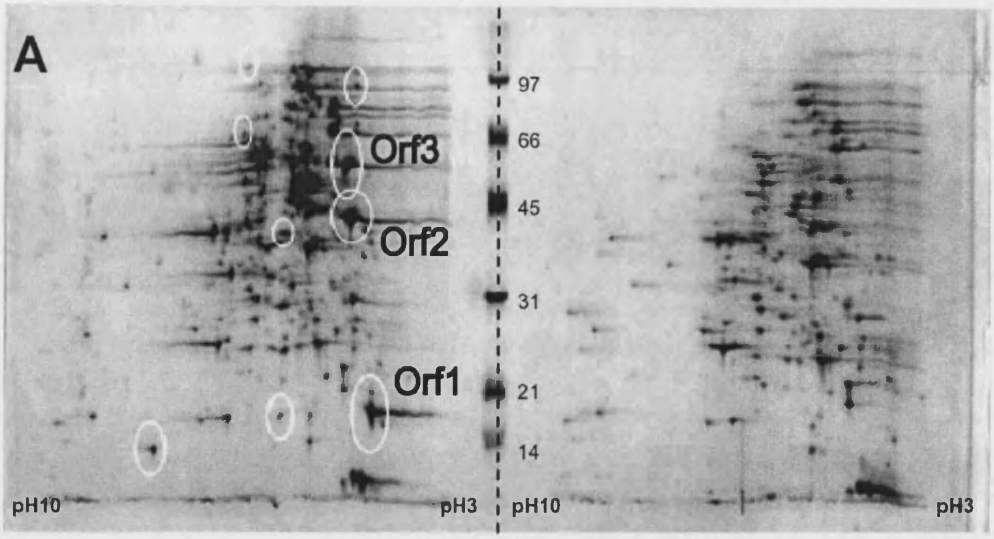

Figure 4.4 Two dimensional gels of *E. coli* proteins prepared from recombinant bacteria with (left panel) and without (right panel) PaPVCpnf. Circled proteins are unique to the PaPVCpnf expressing *E. coli* and three of the most abundant of these proteins were confirmed as PVC encoded proteins by picking the spots from the gel, analysis by MALDI-TOF and subsequent matching predicted tryptic digests of all PVC encoded proteins. Orf's 1, 2 and 3 correspond to the first three open reading frames in the PaPVCpnf unit

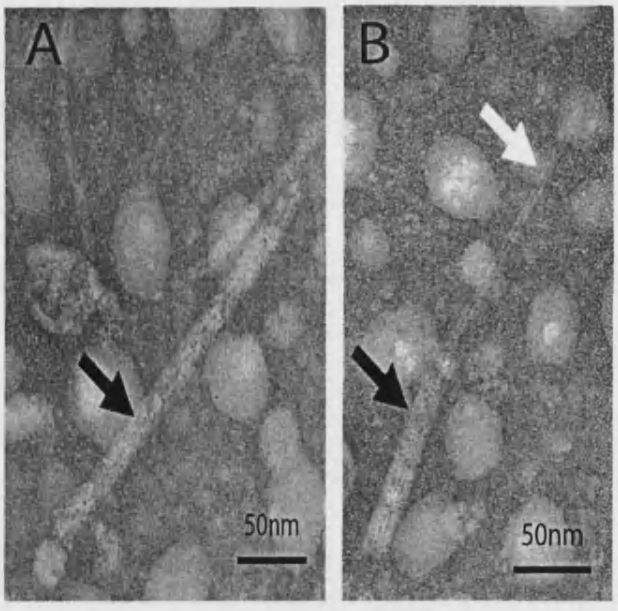

Figure 4.5 Transmission electron micrograph of PVCs showing their similarity to R-type pyocins. (*A*) Relaxed PVC showing only the outer sheath (filled arrow). (*B*) Contracted PVC showing extrusion of inner needle (open arrow) from outer sheath (closed arrow).

4.2.3 Growth of PVCs carrying *E. coli*

To test if the release of PVC effectors from the recombinant bacteria was mediated via simple lysis of the host *E. coli* cells, PVC carrying *E. coli* grown overnight in 3ml LB(Amp), and 1:100 dilute to check optical density every one hour and plate LB(Amp) plates every two hours to count survival cells. The results show that PVC carrying *E. coli* grow slower than pWEB carrying *E. coli* (Figure 4.6), while cells viability data shows that only about 10 percent of the cells survive after 7 hours' growth. This confirms that PVC elements are toxic to *E. coli* (Figure 4.7).

Thin sections of PVC carrying *E. coli* were also examined using transmission electron microscopy (TEM). Although *E. coli* cells expressing PVCs show abnormal morphology, with extensive vacuoles present that are absent from *E. coli* carrying non-PVC containing cosmids (Figure 4.8 B, C), their periplasms are intact and that they show no signs of lysis (Figure 4.8 B).

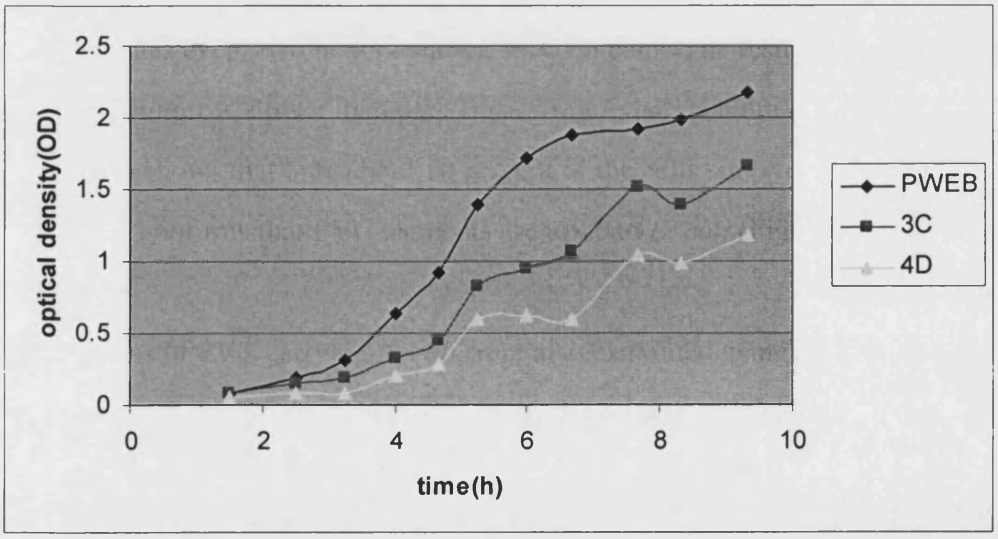

Figure 4.6 Time-elapsed optical density curve of recombinant *E. coli* carrying PWEB, PVCs (3C and 4D)

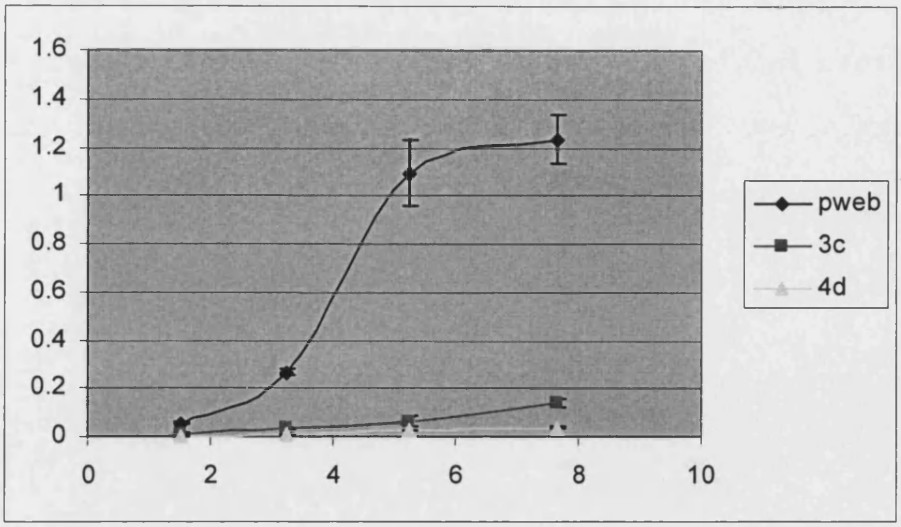

Figure 4.7 Time-elapsed cell survival curve of recombinant *E. coli* carrying PWEB, PVCs (3C and 4D) (1=0.5x10^9)

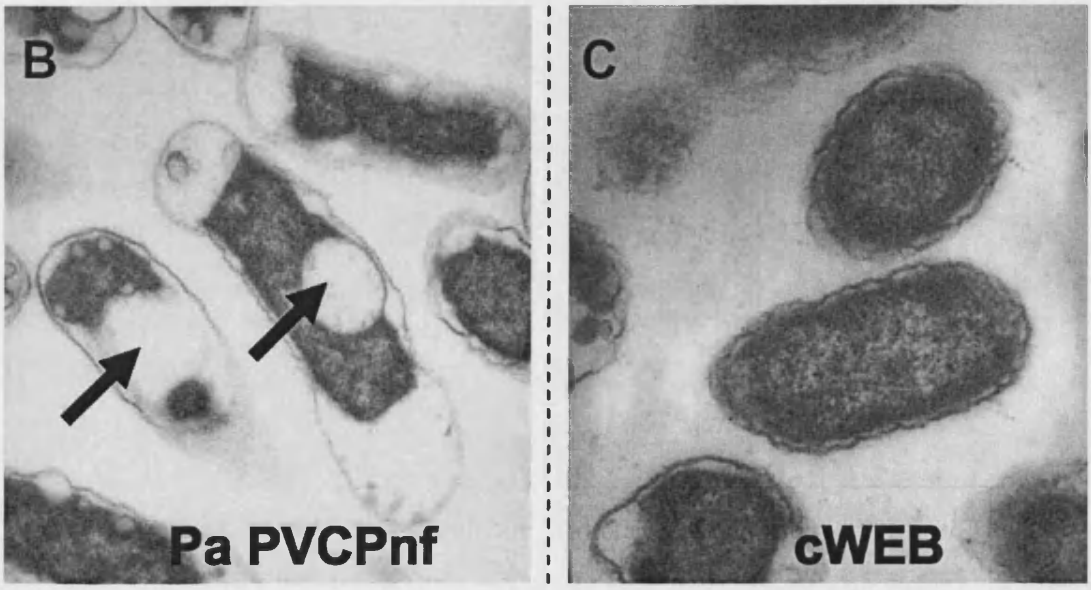

Figure 4.8 Transmission electron micrograph of a thin section through recombinant *E. coli* expressing PaPVCpnf. Note the large vacuoles within the bacteria expressing a PVC, suggesting that the cells are dying. However note also that the bacterial periplasm is still intact and that no bacterial lysis is apparent. Control section of recombinant *E. coli* carrying the cosmid vector only. Note the absence of vacuoles.

4.2.4 Insecticidal activity of the PVCs

Although R-type pyocins are bacteriocins with well documented anti-bacterial activity (Michel-Briand et al. 2002), it is still unable to demonstrate any PVCs' activity against *E. coli* or *Micrococcus Luteus*. Therefore PVCs' insecticidal activity was tested.

E. coli K12 EC100 carrying individual PVC containing cosmids was injected into larvae of the waxmoth. Following injection of whole cultures of PVC expressing *E. coli*, larvae died within 24 h (Figure 4.9). For *E. coli* expressing PaPVCpnf, larvae injected with cell free supernatant alone became black and moribund 15 min. post injection (Figure 4.10). This injectable activity within the supernatant from PaPVCpnf expressing *E. coli* was eliminated by heat treatment prior to injection (Figure 4.10). Comparison of mortality data from injection of *E. coli* carrying PVCs from different *Photorhabdus* species suggests that PVCs from human pathogen *P. asymbiotica* (Gerrard et al. 2004), show higher toxicity to insects than those derived from the insect pathogen, *P. luminescens* TT01 (Duchaud et al. 2003).

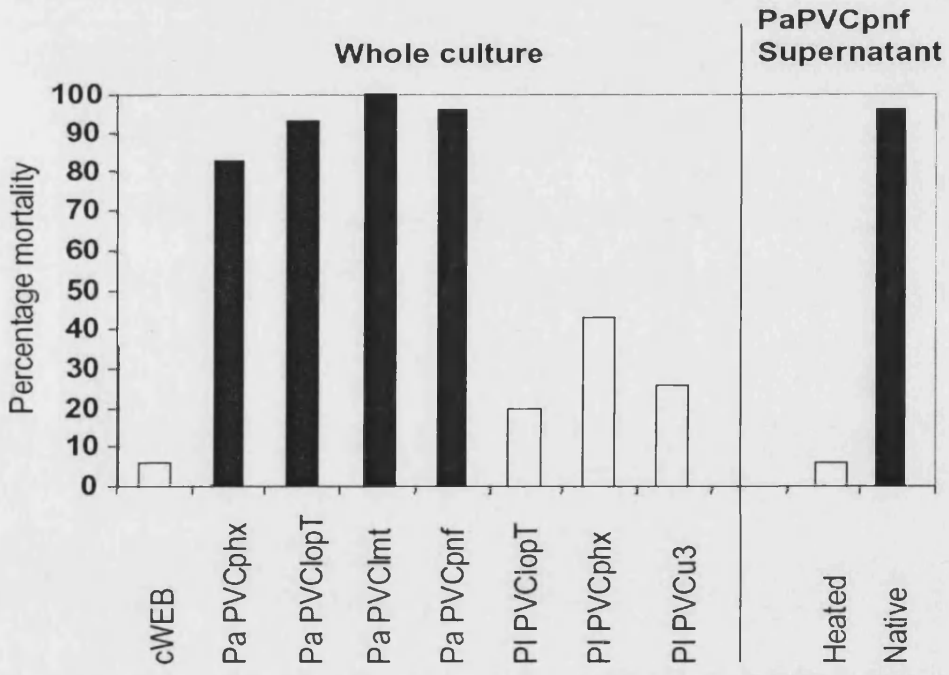

Figure 4.9 Percentage of larvae showing blackening after 24 h after injection with either whole PVC expressing *E. coli* cultures (left) or the culture supernatant of PaPVCpnf alone. Note that all the PVC expressing cosmids from *P. asymbiotica* (PaPVC) caused blackening in 80-100% of larvae whereas those from *P. luminescens* (PlPVC) only showed a phenotype in 10-40% of larvae.

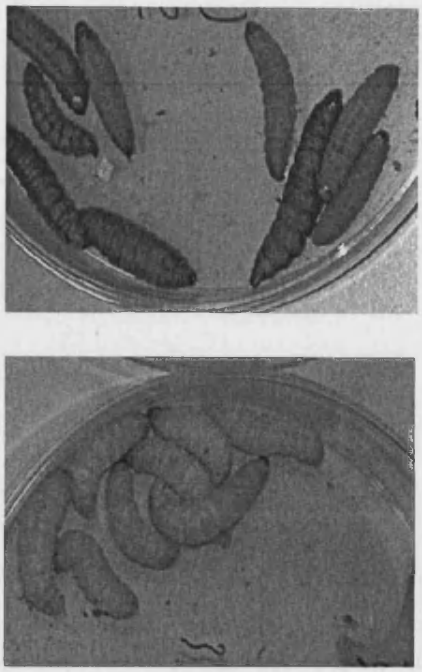

Figure 4.10 Larvae injected with supernatants from *E. coli* expressing PaPVCpnf show rapid blackening and death within 30 minutes. Control larvae injected with *E. coli* heated supernatants from *E. coli* expressing PaPVCpnf show no effects

4.2.5 Over-expression of PVCs effectors alone shows no effect on insects

To test the effect of the PVC encoded effectors in isolation, the *lopT*-like and *pnf*-like genes from Pa PVClopT and PaPVCpnf were PCR amplified from *P. asymbiotica* strain ATCC43949 genomic DNA using the following primer pairs; lopTF= TAAgagctcAATTATAATCTAAAGGTAAT; paLopT_R=ATGAAGcTtTTAGGGATAGTTGTGA; paPNF_F=AATgAATTCAACCATCACGGAGA and paPNF_R=TGGGCAAgcTTATAACAACCGTT. These PCR products were purified and cloned into the arabinose inducible expression plasmid pBAD30. The resulting clones were sequenced to confirm their identity. Despite the fact that abundant recombinant protein is detectable in cytosolic preparations of recombinant *E. coli* carrying these plasmids (Figure 4.11), injection of recombinant cytosolic preparations directly into *Galleria* larvae showed no effects, suggesting that these effectors cannot act on their own within insects.

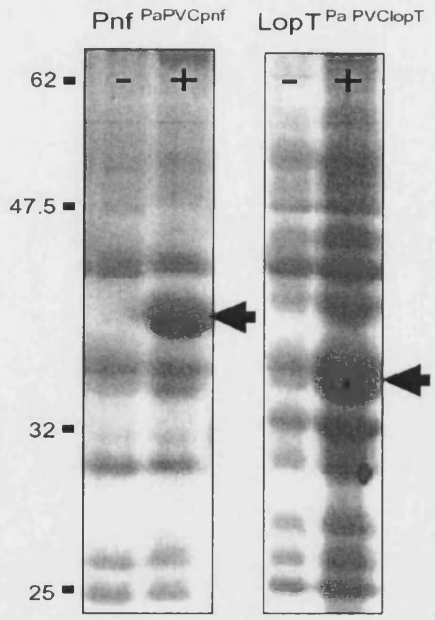

Figure 4.11 Expression of putative PVC effectors within *E. coli*. Showing lysates of recombinant *E. coli* with (+) and without (-) plasmids expressing two different cloned effector proteins, Pnf and LopT.

4.2.6 PVCs destroy hemocytes and re-arrange actin

Following injection of *E. coli* K12 EC100 not expressing any bacterial virulence factors, the insect immune system normally clears the infecting *E. coli* via a combination of antibacterial peptide production and via the phagocyotosis and nodulation reactions associated with insect hemocytes (Gillespie et al. 1997).

Therefore, in order to understand why PVC expressing *E. coli* are not successfully neutralised by the insect immune system, we bled Galleria larvae 30 min. post-injection with PaPVCpnf supernatants and examined their hemocytes. Simple counts of recoverable hemocytes revealed a dramatic decrease in insect hemocytes 30 min. post injection (Figure 4.12). Further staining of these few remaining hemocytes with TRITC-phalloidin revealed that their actin cytoskeletons are compressed within their residual cell bodies (Figure 4.13). This dramatic decrease in recoverable hemocytes from infected insects as little as 30 min. post injection, helps explain how PVC expressing *E. coli* can persist in the presence of the insect phagocytes or hemocytes.

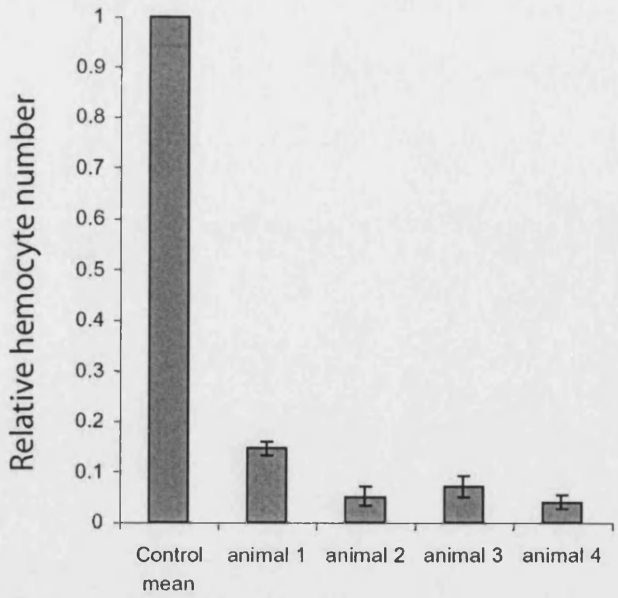

Figure 4.12 Drop in recoverable hemocytes associated with injection of PVC expressing *E. coli*. Histogram comparing the number of hemocytes recovered 30 min. After injection with heat treated PaPVCpnf supernatants (left column) compared to the number recovered after injection of native supernatant. Note the dramatic decrease in the number of recoverable hemocytes following injection with the native supernatant from PVC expressing *E. coli*.

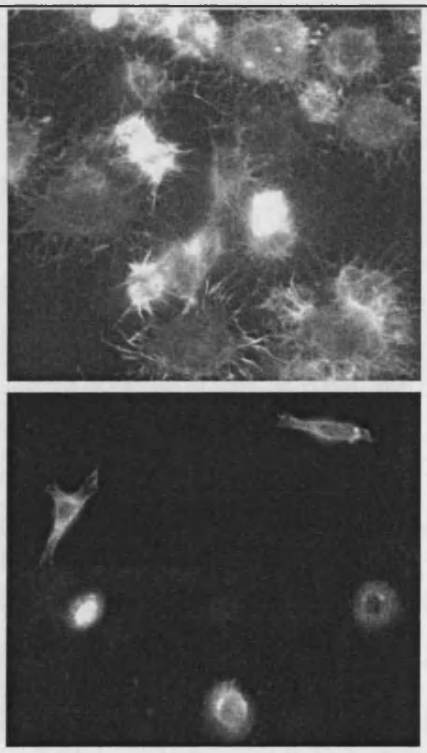

Figure 4.13 Injection of PVC expressing *E. coli*' effect on hemocytes actin cytoskeleton. Control hemocytes stained with TRITC-phalloidin. Note the numerous actin rich projections in healthy *Galleria* hemocytes. Hemocytes recovered from *Galleria* injected with *E. coli* carrying a cosmid expressing PaPVCpnf. Note the marked condensation of the cell body and the remnant bundle of condensed actin in the remaining dead hemocytes.

To examine the different effects of different PVC encoded effectors on the actin cytoskeleton, the *pnf*-like and *sepC*-like genes of PaPVCpnf were PCR amplified from *P. asymbiotica* genomic DNA using the following primers (5' to 3'); papnfrk5FbamH1=TTAggatccTTAAAATATGCTAATCCT; papnfrk5Rpst1=TGCCCTCATTctGCAgAATTATAACA; pasepCrk5FbamH1=TTTAggatccCCTAGATATGCTAATTAT and pasepCrk5Rpst1=TATTCTgCaGATGACATGAAAATCCA. The *plu1690* PlPVCmcf-encoded gene was PCR amplified using; plu1690FbamH1=AATggatccCCAAACAGCAAATATAGT and plu1690Rpst1= AATCTgcaGGGTATATATTAATTGT. The resulting PCR products were restriction digested and DNA-ligated (New England Biolabs) into the equivalent sites of mammalian expression vector pRK5myc. Representative clones were fully sequenced to confirm the correct sequence of the cloned ORF.

This mammalian expression vector pRK5myc expresses each effector as a fusion protein with Myc, allowing for its detection in transfected cells using an anti-Myc antibody (Dowling et al. 2004). To assess the subsequent integrity of the actin cytoskeleton we co-transfected the same cells with a construct expressing EGFP actin (Figure 4.14). Consistent with its dramatic effect on insect hemocytes, the effector showing similarity to Pnf, encoded by PaPVCpnf, dramatically reduced the cell bodies of transfected cells, leaving only a bundle of condensed actin (Figure 4.14C). Interestingly, a second putative effector also encoded on the PaPVCpnf element, which shows similarity to the C-terminal region of the SepC toxin, produced long arms of actin rich filaments in transfected cells (Figure 4.14D). Finally, a third effector, encoded by plu1690, which shows similarity to part of the *P. luminescens* cytotoxin Mcf (Daborn et al. 2002), also reduced the cell bodies of transfected cells, leaving an intact nucleus surrounded by several actin rich bundles (Figure 4.14B). Together these data suggest that the PVC encoded effectors are capable of rearranging the actin cytoskeleton of host cells. Furthermore, we have also demonstrated that when heterologously expressed in *E. coli* (independent of the rest of the PVC

element), that the putative effectors Pnf and lopT show no injectable toxicity to insects. This suggests that in order to be toxic to cells, these effectors must be delivered into the host cytoplasm. However, again, the mechanism by which they might enter host cells remains obscure. We note that only a small proportion of the potential effector sequences identified have been tested in current study, and that the majority of putative effectors remain untested. The PVCs may therefore be a rich source of bacterial effectors with novel modes of action.

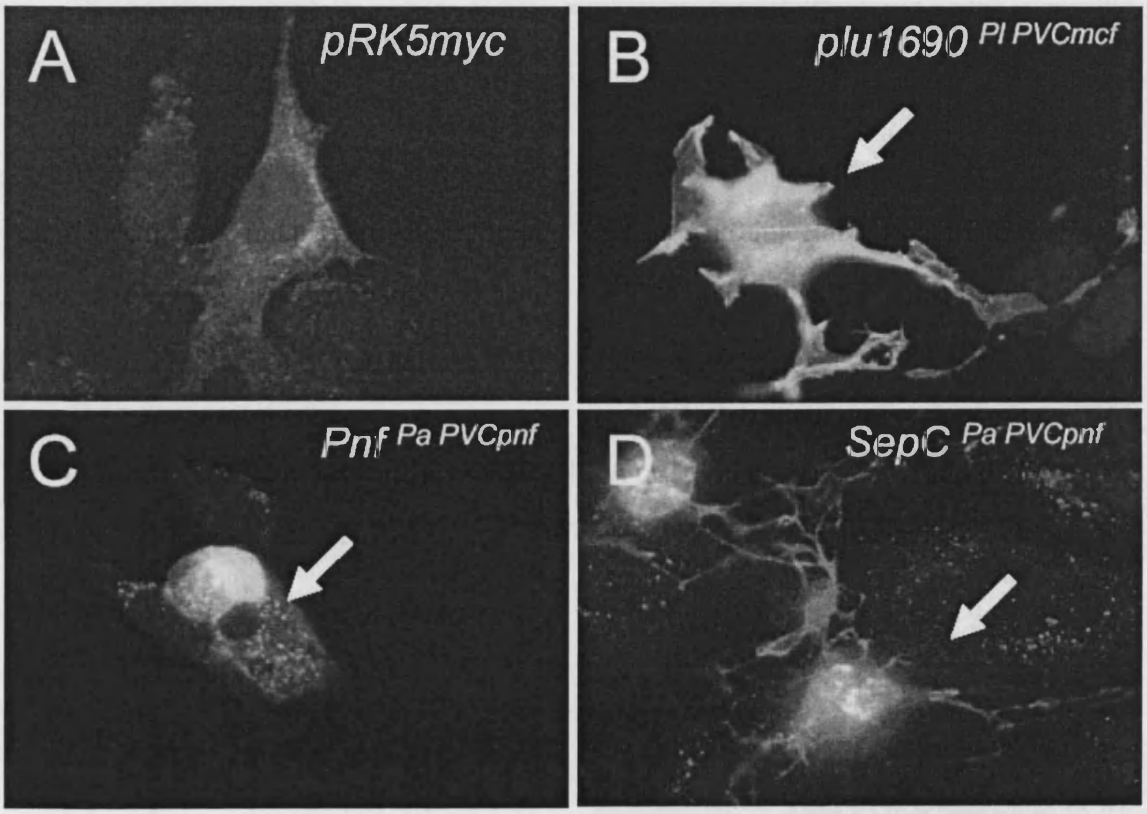

Figure 4.14 Expression of PVC effectors within mammalian tissue culture cells.
(*A*) NIH 3T3 cells transfected with the pRK5myc (red) vector alone and co-tranfected with a second construct expressing actin-EGFP (green) show a normal actin cytoskeleton. Nuclei are stained with DAPI (blue). (*B*) Cells transfected with pRK5myc expressing the Mcf-like effector Plu1690 show only fragments of successfully transfected cells which again show actin condensation. (*C*) Cells transfected with pRK5myc expressing the Pnf-like effector show contracted cell bodies and condensed actin. (*D*) Cells transfected with pRK5myc expressing the SepC-like effector show remarkable actin rich cabling, a phenotype never seen in cells from the pRK5myc transfected controls.

4.3 Conclusion

Here the first functional studies on phage-like PVC structures found as repetitive cassettes in two different species of entomopathogenic bacteria, *Photorhabdus* was described (Waterfield et al. 2004). Each of these different virulence cassettes carries one or more different putative effector sequences suggesting it may be a virulence factor. The genomic organization of the PVC loci in different *Photorhabdus* genomes were examined and tested if PVC containing cosmids were toxic to *Galleria* via injection.

Examination of supernatants of PaPVCpnf expressing recombinant *E. coli* via TEM show that these loci encode particles similar in structure to R-type pycocins. However, unlike R-type pyocins the PVCs have no demonstrable antibiotic activity, but have injectable activity against larvae of the waxmoth. Despite the unknown mechanism whereby the PVCs kill injected insects, there is a dramatic decrease in recoverable hemocytes from infected insects as little as 30 min. post injection. This observation helps explain how PVC expressing *E. coli* can persist in the presence of the insect phagocytes or hemocytes. Moreover the fact that the actin cytoskeletons of the remnant hemocytes are severely altered is consistent with the phenotypes observed upon direct expression of several different potential effector sequences directly inside mammalian cells. Finally, although the mechanism of bacterial secretion of these effectors or the process whereby they enter host cells remains undetermined, we note that the N-terminal of otherwise unrelated PVC encoded effectors show strong predicted amino acid similarity (Figure 4.15) and a conserved hydrophillicity (Figure 4.16), suggesting a potentially conserved export motif for export from the bacterial cell.

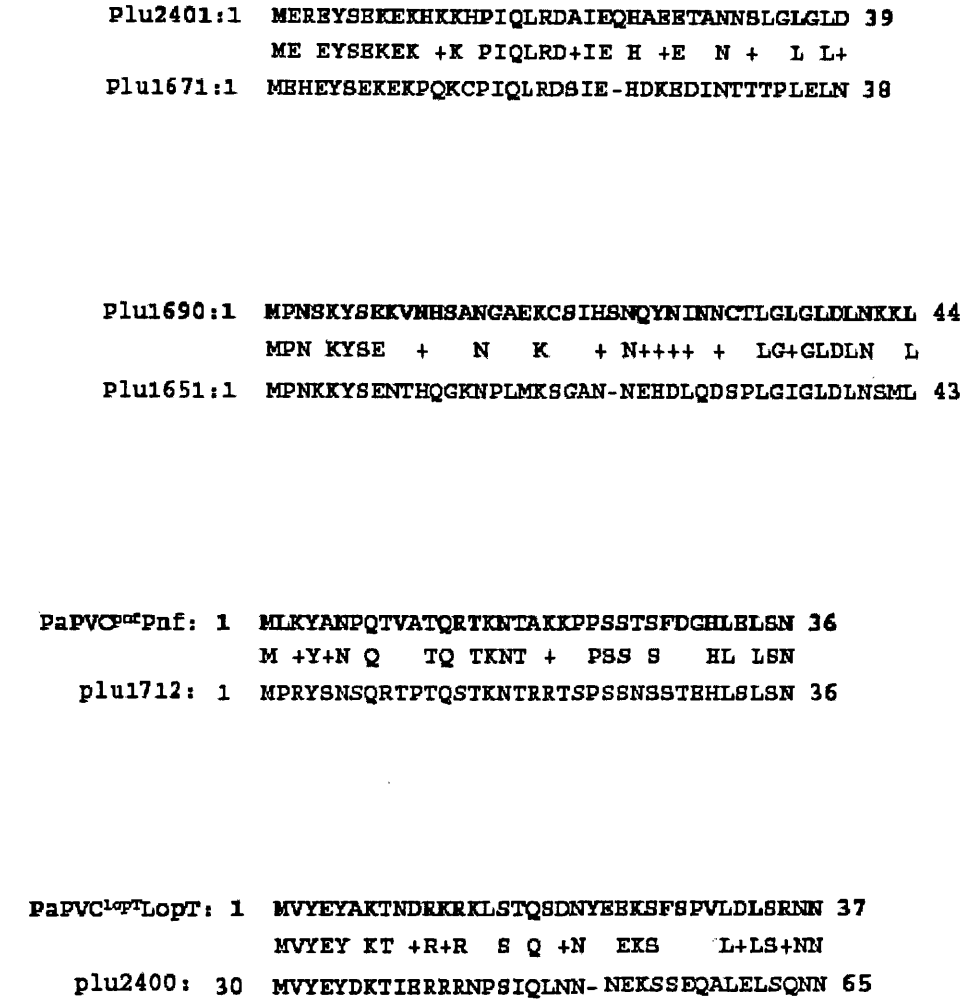

Figure 4.15 Alignments of the predicted N-termini of pairs of different PVC encoded effector proteins showing high predicted amino acid similarity between the pairs. This conservation of the N-terminal 35 to 45 amino acids suggests that they may represent a consensus sequence for PVC mediated delivery.

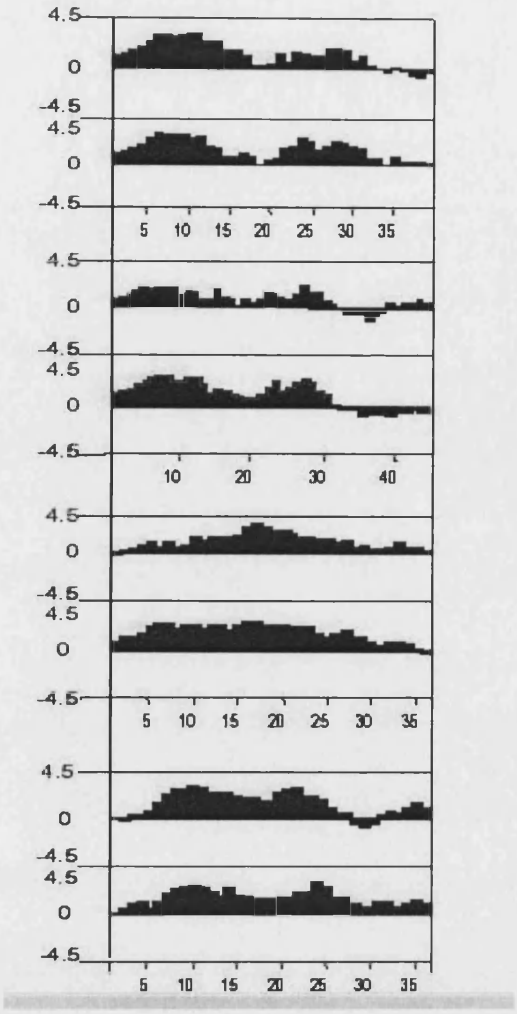

Figure 4.16 Hydrophobicity plots of the predicted N-termini of these effectors. Note that all are strongly hydrophilic.

At last, these data suggest that the PVCs may be bacteriocin-like structures modified to have activity against insect phagocytes. The role of these prophage-like elements in the ecology of different *Photorhabdus* species remains to be investigated.

CHAPTER 5

S15- A TEMPERATURE DEPENDENT SECRETED PROTEIN IN *PHOTORHABDUS*

5.1 Introduction

P. luminescens grown in a liquid culture secrete the large number of proteins into the supernatant. Some of these proteins have been well characterized, including the Tc toxins, proteases, and lipases and etc. Many secreted enzymes contribute to insect death and result in bioconversion of the insect cadaver (Bowen et al. 2000). However, most of the secreted proteins are poorly characterized, and, perhaps equally importantly, their mechanisms of export are not known.

P. asymbiotica has been associated with human infection in the USA and Australia (Fischer et al. 1999). The source of human infection remains unknown. The organism is not a human commensal and is not proven to exist as a nematode symbiont (although it is pathogenic to insects). *Photorhabdus* species have never been shown to live freely in soil, although they will survive in soil under laboratory conditions (Bleakley et al. 1999). Twelve cases of human infection with *P. asymbiotica* have been reported in the peer-reviewed literature-six from the USA and six from Australia (Farmer et al. 1989; Peel et al. 1999; Gerrard et al. 2003). A 13th case has been identified in a 29-year-old female from a smallholding near Beaudesert, Australia in February 2003. The true incidence of human infection is likely to be much higher than these reports would suggest (Gerrard et al. 2004).

The study of *Photorhabdus* pathogenicity has focused on insect models. Bacterial strains can be readily cultured in the laboratory and artificially introduced into experimental insect hosts by injection (Silva et al. 2002). The virulence of *Photorhabdus* species is manifest by very low LD50 values (the number of bacterial cells required to kill 50% of test animals). These values may be as low as five bacteria per insect for some strains. The relative pathogenicity of different strains, therefore, is

difficult to assess using this measurement. Thus, virulence is more accurately expressed as an LT50 value, that is, the time required to kill 50% of the test animals at a fixed dose of cells. Curiously, the *P. asymbiotica* strains so far tested have proven to be highly virulent in insect models, with LT50 values equivalent to or lower than those of symbiont strains. Whether specific virulence factors associated with human infection account for this high degree of insect pathogenicity is not known. There is currently no experimental vertebrate model for *P. asymbiotica,* and little is known regarding the pathogenic mechanisms specifically associated with human infection (Gerrard et al. 2004).

In addition, the full genome sequence of the USA clinical isolate *P. asymbiotica* ATCC43949 is near completion. These data provide an excellent opportunity for comparative genomics with the better-characterised entomopathogenic strains (ffrench-Constant et al. 2003). An examination of the genomic data from these strains has revealed that they possess an unusually large number of potential virulence factor genes, many of which are present in multiple copies. Furthermore, a comparison with the genome of the standard laboratory strain, *Escherichia coli* K12, suggests that the entomopathogenic *Photorhabdus* strains have approximately 1 Mb of extra coding available for virulence or symbiosis factors (Duchaud et al. 2003). We found two different toxins active against nematode worms in the supernatant of *P. asymbiotica*, one causes aggregation and the other causes paralytic killing (Figure 5.1). To isolate these two factors, the supernatant of *P. asymbiotica* grown at 30 °C and 37°C was examined via two-dimensional (2D) gel electrophoresis and subsequent MALDI-TOF analysis of the secreted *Photorhabdus* proteins (Figure 5.2). Visual examination of 2D gels of *P. asymbiotica* at 30 °C and 37°C showed several differences. S15 was identified as being expressed and secreted at 30 °C but not 37°C.

Over-expression *s15* in *E .coli* could form *E. coli* cell chains (Figure 5.7) and also make nematodes clamp together with the cells (Figure 5.6). This phenotype is very similar to the aggregation factor in the supernatant of *photorhabdus* (Figure 5.3). PCR

mutagenesis and gene knock out technology were used to investigate S15's function further.

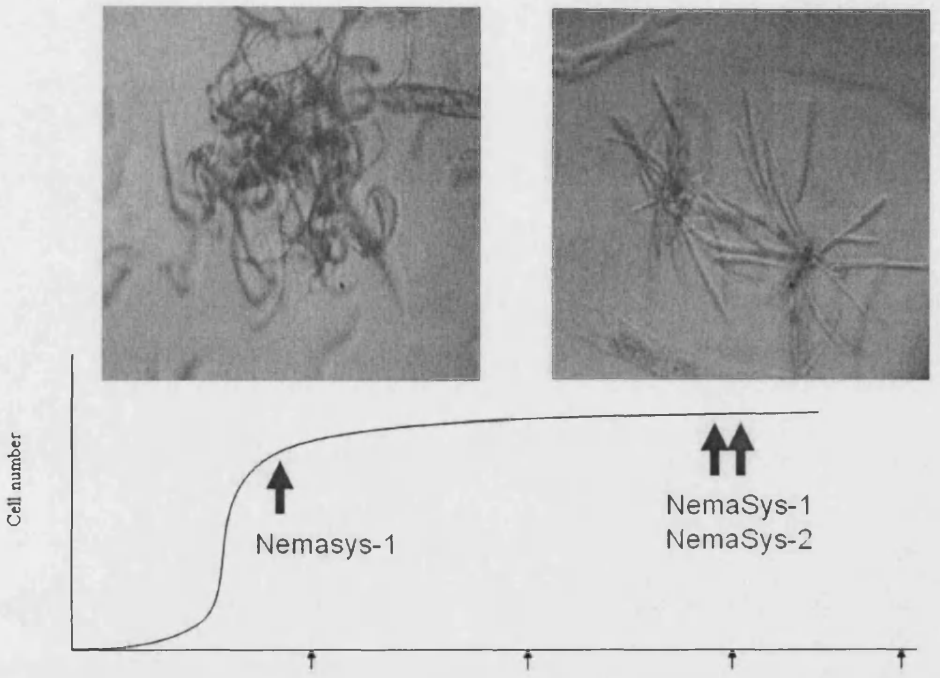

Figure 5.1 Aggregation and paralytic killing are caused by two distinct toxins produced at different times by the bacterium. Nemasys1 caused aggregation but worms do not die immediately, Nemasys2 kills worms rapidly.

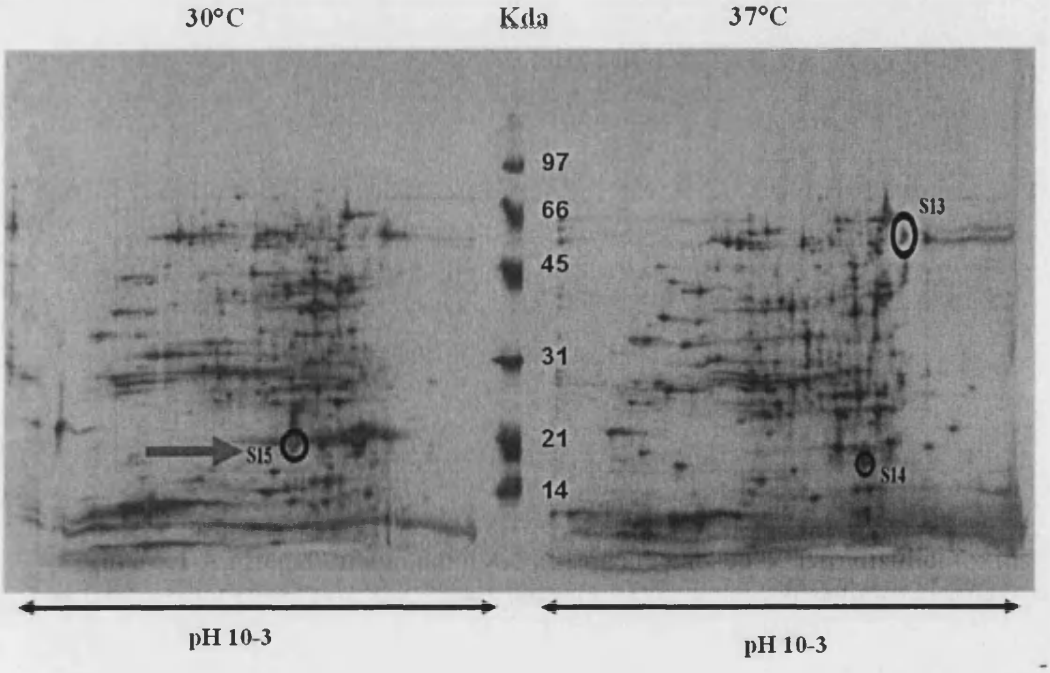

Figure 5.2 Identification of S15: 2D-gels of *Photorhabdus asymbiotica* ATCC43949 2 day supernatants. Note the presence of S15 at 30°C but not 37°C

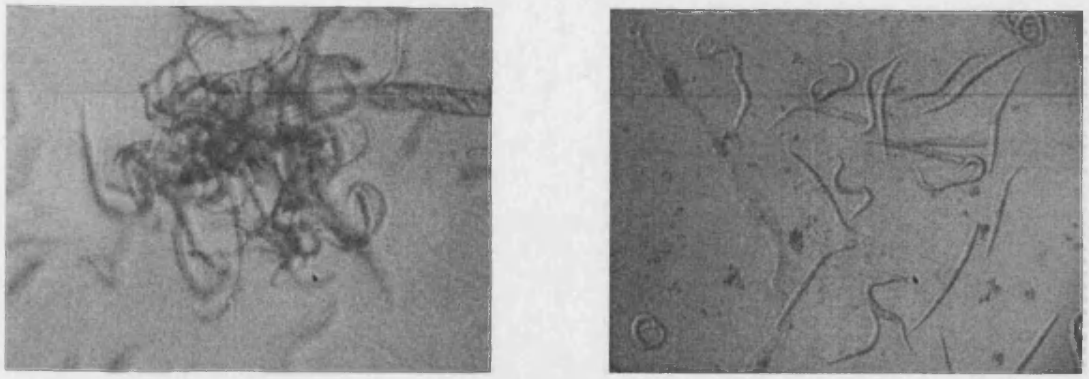

Figure 5.3 Aggregation factor in the supernatant of *photorhabdus* makes nematodes 'clamp' (Left). The right panel shows worms treated with heated supernatant.

5.2 Results

5.2.1 *E. coli* carrying induced pBAD30-s15 forms cell chains

The *s15* gene was PCR amplified from the genome DNA using the rTth DNA polymerise kit (Perkin-Elmer). Primers were synthesised by MWG biotech [primer sequences 5' to 3'.forward: TTAATCTTGGAATTCATTAAACACATT; reverse: TTAAAGCTTAGGTTACAATAGTATATTCT]. The resulting PCR products were restriction digested with *EcoR*I and *Hind*III and DNA-ligated (New England Biolabs) into the equivalent sites of the arabinose inducible expression plasmid pBAD30. Representative clones were fully sequenced to confirm the correct sequence of the cloned *s15* ORF. Induction produced a single protein with the predicted molecular weight-14980.83 Daltons (Figure 5.4). To produce the 'clamping' effect on worms, incubation induced culture at 4 °C for at least 2 days is required (Figure 5.5). TEM and SEM pictures showed that the induced *E. coli* cells formed chains due to an internal scaffold (Figure 5.6) and the cells are surrounded by a smooth matrix which binds them together (Figure 5.7). The cell-matrix surrounds the *C. elegans* worms that are aggregated by induced *E. coli* EC100 [pBAD30*s15*] and even extends into the mouth (Figure 5.8).

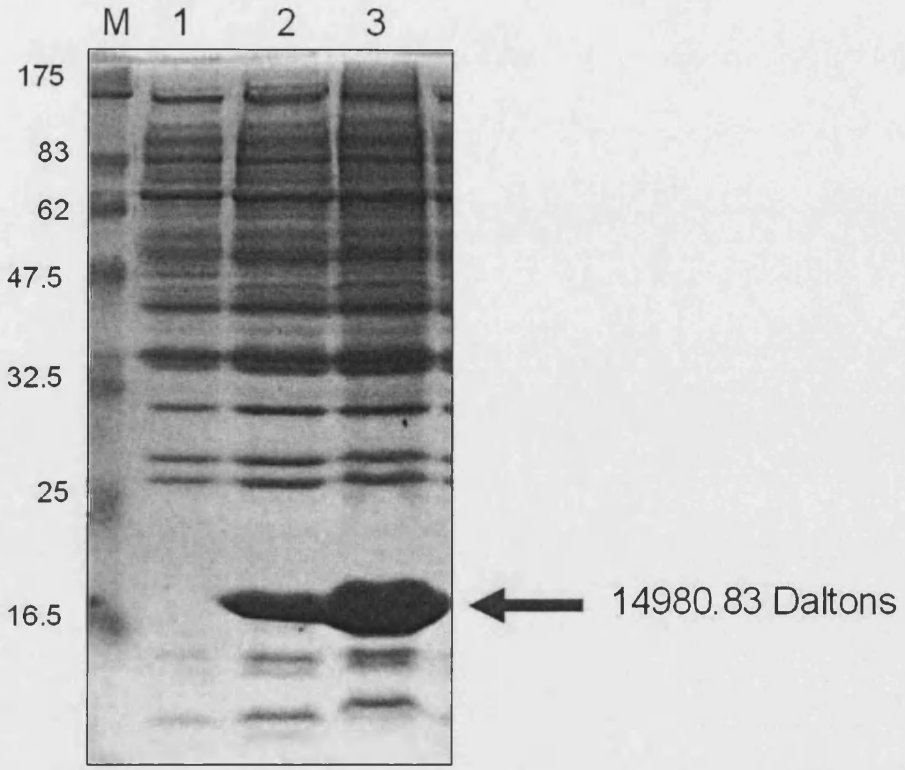

Figure 5.4 Expression of S15 in *E. coli* EC100 [pBAD30*s15*]. (M)=size marker; (1)=uninduced; (2)=+2 hours; (3)=+4 hours inductions. Arrow represents S15.

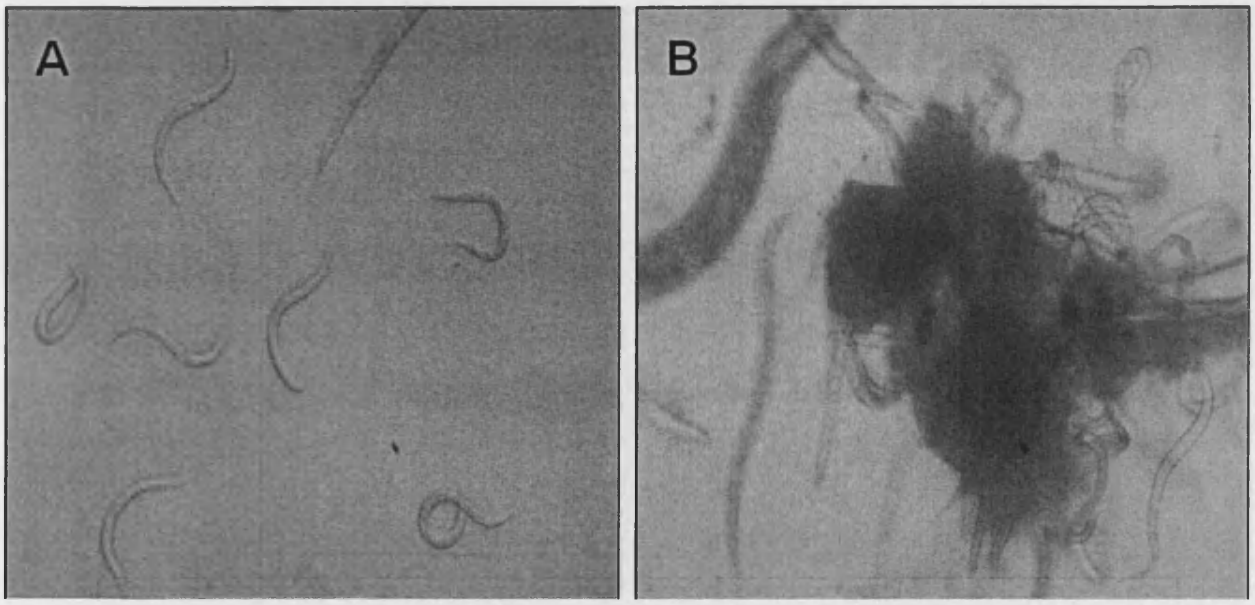

Figure 5.5 Effect of expression of S15 in *E. coli* EC100 [pBAD30*s15*] on *C. elegans*. (a) uninduced; (b) induced. Note how induced cells clot around the nematode worms forming dense aggregates.

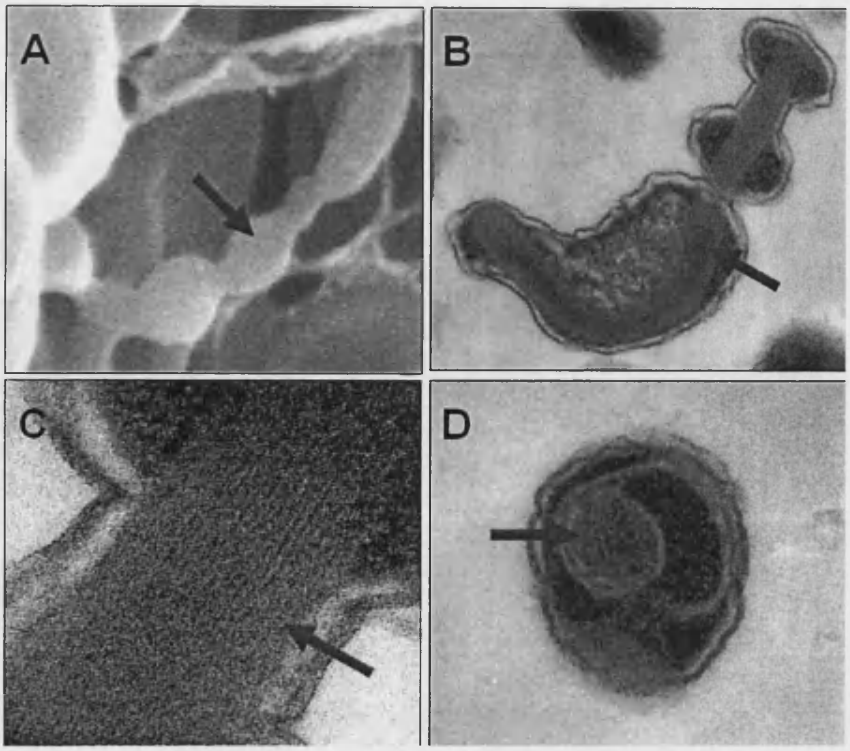

Figure 5.6 (a) an SEM view of induced *E. coli* EC100 [pBAD30*s15*] showing chains of bacterial cells. (b-d) TEM views of induced *E. coli* EC100 [pBAD30*s15*] showing that (b) bacterial chains are due to an internal scaffold (arrow) of self-assembled S15 protein, (c) that the protein is fibrilar/crystalline (arrow). (d) a S15 fibre- bundle in cross-section (arrow).

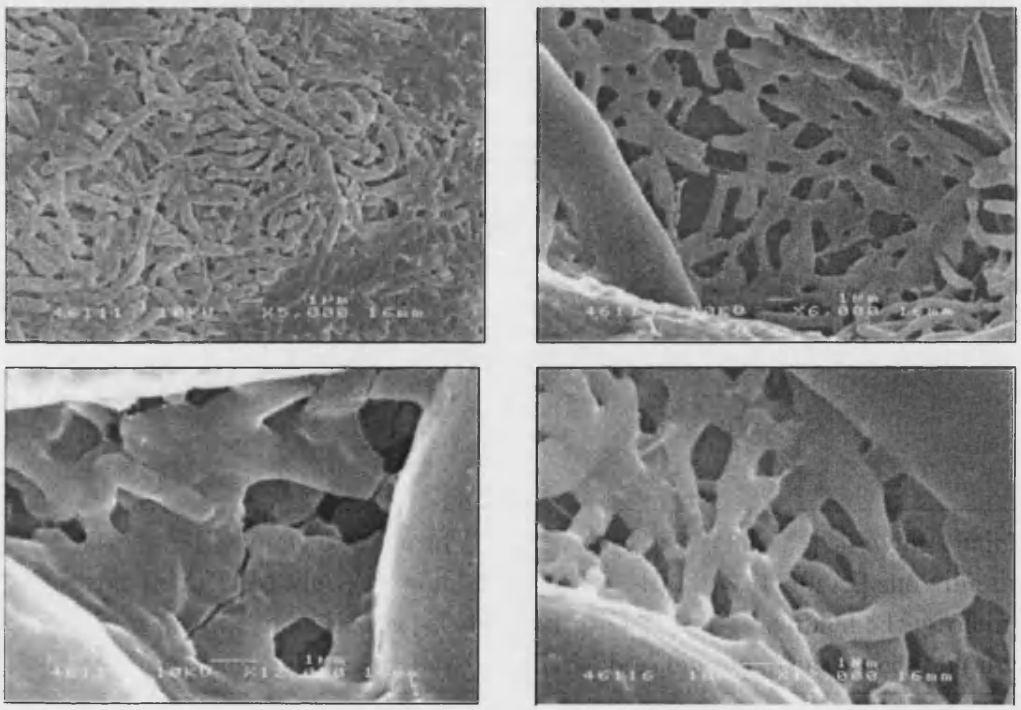

Figure 5.7 Four SEM views of induced *E. coli* EC100 [pBAD30*s15*] cells after exposure to *C. elegans*. Note how the cells are surrounded by a smooth matrix which binds them together.

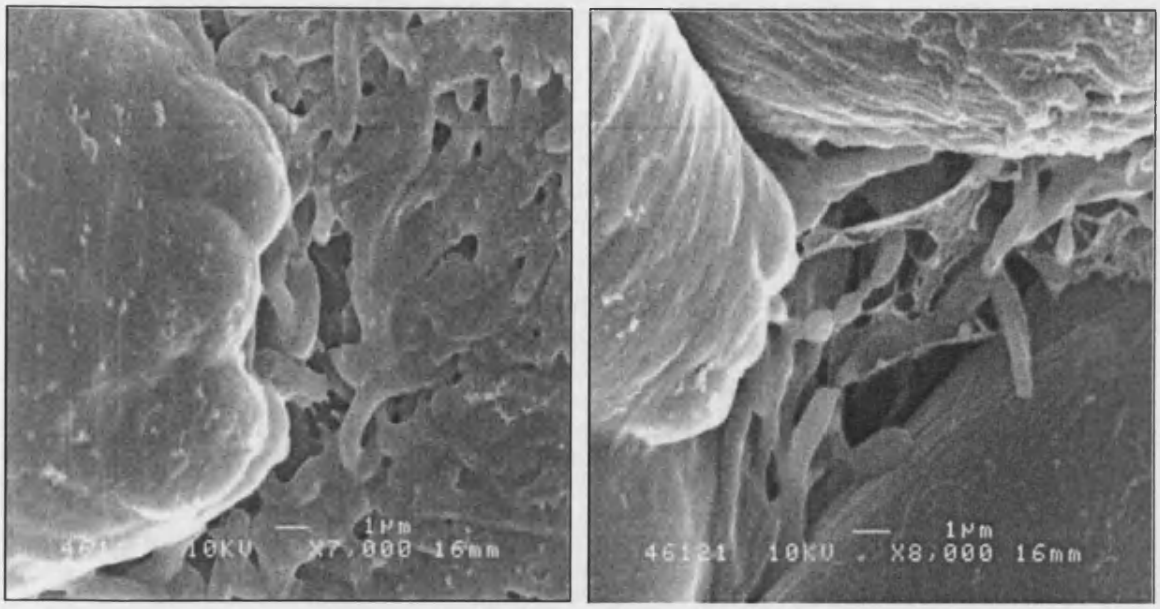

Figure 5.8 Two SEM views of the heads of *C. elegans* worms that are aggregated by induced *E. coli* EC100 [pBAD30*s15*]. Note how the cell-matrix surrounds the worms and even extends into the mouth.

5.2.2 PCR mutagenesis analysis

To study the structure function relationship of S15, PCR mutagenesis was used to mutate *s15* PCR products and re-clone them into pBAD30. Clones were sequenced and totally 98 mutant clones had single, double, triple or stop mutations (Figure 5.9 and 5.10). All mutant clones were induced as described above and the ability to form cell chains was tested. Some of the mutants failed to form fibres. Mutation mappings revealed that two regions are essential for fibre formation and nematode 'clamping' (Figure 5.11).

	site	cell chains		site	cell chains
C09	248 A-G	yes	8C09	40 A-C	yes
2D06	56 T-C	yes	8D03	181 A-G	yes
5B03	332 A-T	yes	8B09	161 A-G	yes
5B04	142 G-A	yes	8H09	286 A-G	yes
5C01	358 T-C	yes	8D08	94 G-A	yes
5G04	269 G-A	yes	8C03	101 T-A	yes
5C04	29 A-C	yes	8F04	124 A-G	yes
5F10	199 A-T	yes	8D11	114 A-T	yes

5H10	76 A-C	yes	8B11	175 A-T	yes
5D09	25 T-C	yes	8D10	196 T-A	yes
6A08	4 T-A	yes	8F01	280 A-T	yes
6G09	15 A-T	yes	8F09	322 T-A	yes
6A01	32 C-T	yes	8G02	359 A-G	yes
6H08	101 T-C	yes	7A05	214 G-A	yes
6D11	93 A-C	yes	F09	80 T-C	yes
6C06	106 T-A	yes	5 E04	28 A-C	yes
6 E10	157 A-G	yes	5B07	14 A-T	yes
6H04	164 A-G	yes	2 E01	211 A-G 248 A-G	yes
6B02	166 A-G	yes	5H08	22 A-T 114 A-T	yes
6B06	195 C-G	yes	6F04	25 T-A 167 C-G 365 C-T	yes
6G04	209 T-C	yes	6D03	31 G-A 106 T-C	yes
6A05	214 G-A	yes	6H06	43 G-A 280 A-G 358 T-A	yes
6B08	251 G-A	yes	6 E01	101 T-A 120 G-C	yes
6B01	331 T-C	yes	6G01	108 G-C 114 A-C	yes
7F01	92 A-C	yes	6A07	46 A-G 163 A-G	yes
7G05	119 A-T	yes	7C01	16 G-A 130 C-A	yes
7B02	176 A-G	yes	7G08	125 C-G 373 G-A	yes
7F02	332 A-T	yes	7G02	205 A-T 314 A-T	yes
7F05	335 A-G	yes	7H10	200 A-G 342 T-A	yes
7D07	335 GAA-GTG	yes	8G11	41 G-A 265 T-A	yes
7C09	349 C-T	yes	8H07	94 G-A 332 T-A	yes
7A09	351 T-A	yes	8C04	307 A-C 367 G-T	yes
7F07	356 C-A	yes	6H12	119 A-T 361 A-G	yes

Figure 5.9 Mutants that still could form cell chains

	site	cell chains		site	cell chains
A05	97 C-T	short	E08	127 C-A	no
6 E03	212 G-A 299 T-A	short	3B04	314 A-G	no
7C04	118 G-A 169 C-T	short	5F09	44 T-G 169 C-A	no
7C11	209 T-A 247 G-T	short	6H07	146 T-A	no
8 E12	160 G-T	short	6H10	91 C-T 269 G-T 296 T-C	no
			6B11	326 C-G	no
			6C10	170 C-A 307 A-G 320 T-A	no
			6G02	224 G-A 319 A-T 353 T-C	no
7D09	52 A-T STOP	no	7G11	4 T-C 316 T-A	no
6B12	242 T-G 253 A-T STOP	no	7D03	16 GCT-ACA 116 G-A	no

7A10	35 C-A 82 A-T STOP	no	7D01	38 T-A 46 A-T 242 T-C	no
5B05	276 T-A STOP	no	7G06	146 T-C 233 C-T 317 C-T	no
7 E11	187 A-T STOP	no	7D08	177 A-T 320 T-C	no
7B01	231 T-A STOP	no	7H01	278 T-A	no
8 E09	52 A-T STOP	no	8D06	77 A-G 254 A-G 317 C-T 322 T-A	no
6C05	185 G-A STOP	no	8A04	98 C-A	no
			8A08	248 A-T 329 A-T	no
			5F01	178G-A 217 G-C 255 A-T	no
			7 E03	323 C-T	no

Figure 5.10 Mutants that could form short cell chains or can not form at all, including stop mutants.

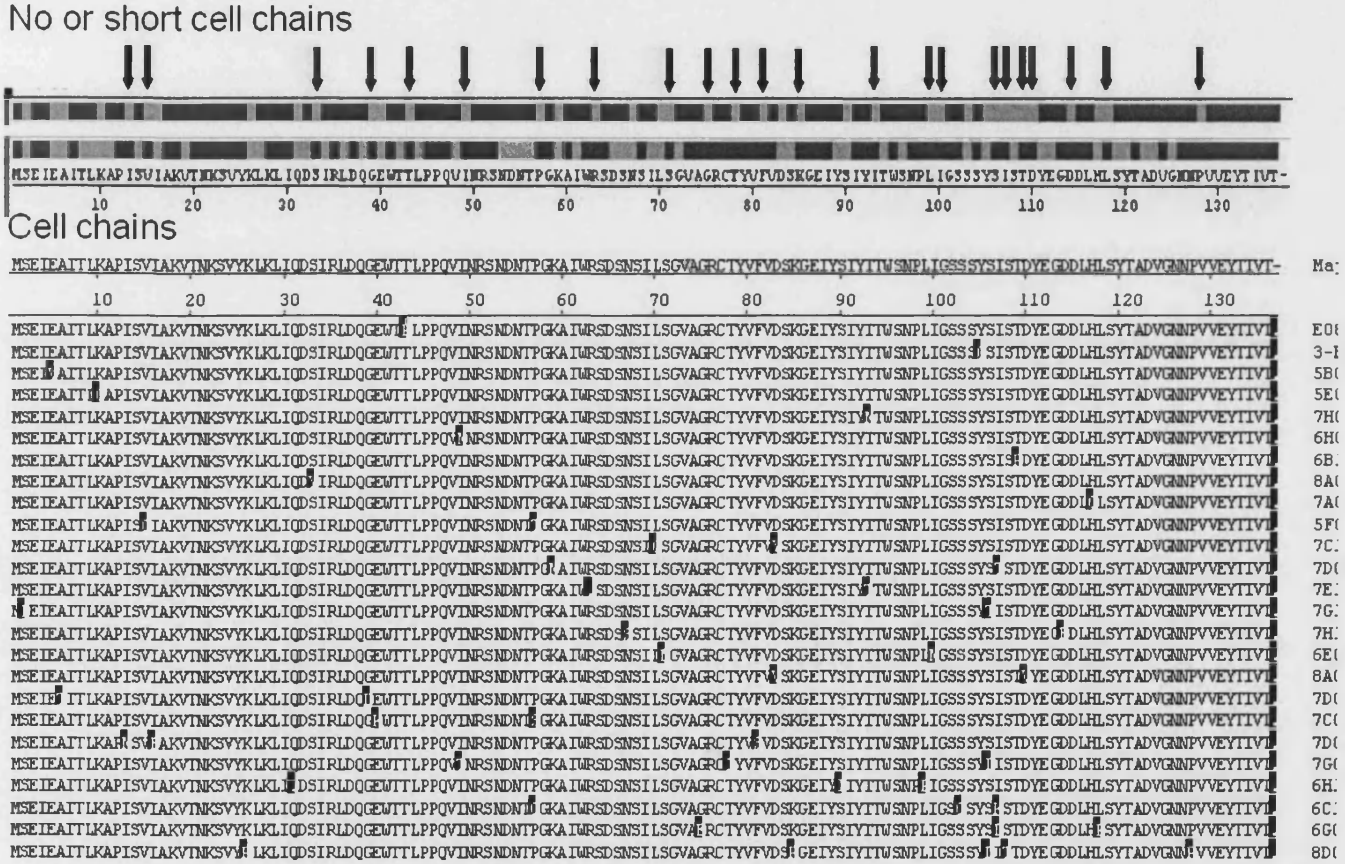

Figure 5.11 Mutation mapping of regions important in fibre formation, red arrows mean that just this single mutation could make S15 fail to form fibre, blue arrows mean 2 or 3 mutation sites could make S15 fail to form fibres.

5.2.3 *s15* knock-out using pDS132

To further analysis the function of *s15* in *Photorhabdus* biology, it is knocked out using the suicide vector-pDS132 (developed by Dr. Susan Joyce and Dr. David Clarke). There are still no good methods to knock out genes in *P. asymbiotica*, so the function of *s15* in *P. luminescens* strain TTO1 was analysed.

The fragments upstream and downstream of the target gene- *s15* were PCR amplified from the TTO1 genome DNA using the rTth DNA polymerise kit (Perkin-Elmer). Primers were synthesised by MWG biotech [primer sequences 5' to 3'.upstream forward: aattctagaGCTGATGGTTTTGTTGCTTTGC; reverse: ATATAAT GTAAGCTAATACTTAATCAC; downstream forward: aatgagctcCAGTTTACCAATACGTTCATTG; reverse: AGCTTAC ATTATATTCACTATAGGGAC]. The PCR products were ligated by primer extension. The resulting amplicon was restriction digested with *Sac*I and *Xba*I and DNA-ligated (New England Biolabs) into the equivalent sites of the suicide vector-pDS132.

After allelic exchange, we got picked 20 sucrose- resistant and chloramphenicol-sensitive colonies for PCR, using primers designed 100 bp upstream and downstream of the target region (primer sequences 5' to 3'.upstream: TGGGAACTGTTGCTAATACGG; downstream: AGCGACTTCCAGATCGGCAAC). The PCR results show that the target region is knocked out (Fig 5.12). The specific bands are purified and sequenced. The culture supernatant of KO strain and wild type strain were precipitated by TCA for SDS-PAGE gel, the gel shows the absence of S15 (Fig 5.13).

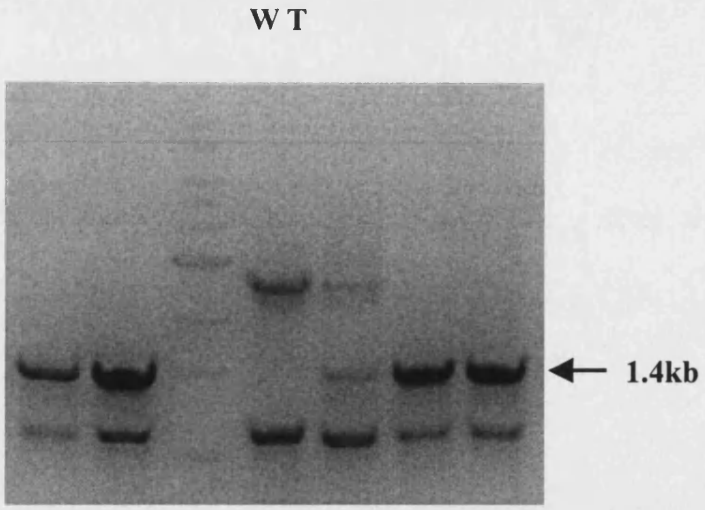

Figure 5.12 Colony PCR to confirm the *s15* knock out strain

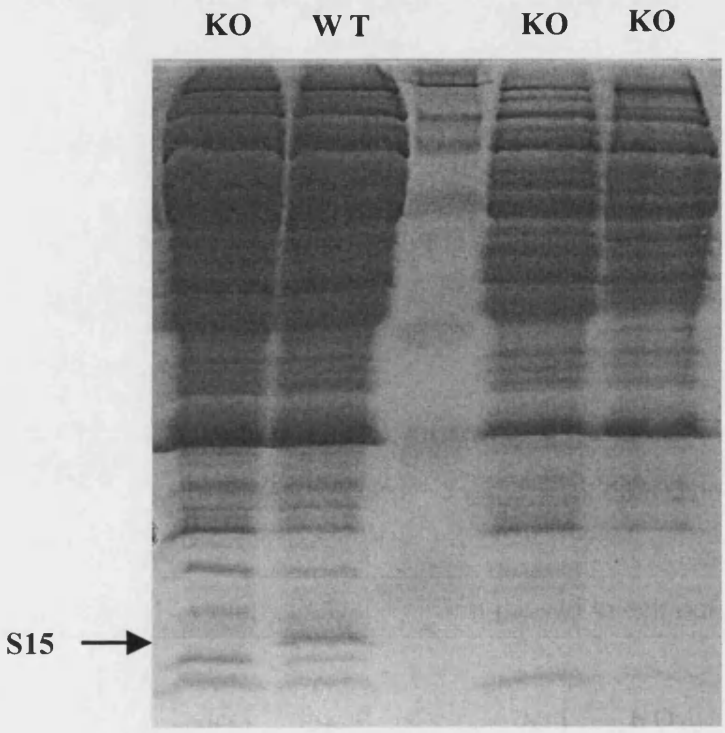

Figure 5.13 SDS-PAGE gel of culture supernatant of KO strain and wild type strain

5.3 Conclusion

The supernatants of several strains of *Photorhabdus* were able to induce "clumping" in *C. elegans* nematodes. Previous experiments had demonstrated that this was mediated by a heat-sensitive factor that was shown to be in the size range of 10 to 30 KDa (data not shown). Proteomic analysis of *P. asymbiotica* supernatants identified a

small protein designated S15 that was secreted at 30°C but not 37°C (human-infection temperature). This protein spot was picked from the gel and analysed using MALDI-ToF analysis of a trypsin digest. The MALDI-ToF profile allowed us to identify the *s15* gene from all predicted gene products revealed by the ongoing *P. asymbiotica* genome sequencing project. Cloning and expression of *s15* in the arabinose inducible plasmid-pBAD30, revealed good intracellular accumulation of the S15 protein.

These induced cultures induced "clumping" of *C. elegans*, suggesting that *s15* represents the clumping factor seen in the native *Photorhabdus* supernatants. Light and electron microscopy of induced cells revealed that *s15* produced fibres within the cells which gave rise to "chains" of bacteria. Random PCR mutagenesis identified 2 regions important in the formation of these chains. Further work is required to investigate this relationship, i.e.; does S15 have a specific nematode-binding receptor, or is the "clumping" and artefact arising as a result of the bacterial chains themselves. Nevertheless, it is interesting to note that chain formation described above is not sufficient to clamp nematode and that pre- incubation for at least 2 days at 4°C is required.

Appendix I

RANDOM KNOCK-OUT LIBRARY OF *PHOTORHABDUS LUMINESCENS* STRAIN TTO1

I.1 Introduction

Strain TTO1 possesses a single circular chromosome of 5,688,987 bp with an average GC content of 42.8%. No plasmid replicon was found. A total of 4839 protein coding genes, including 157 pseudogenes, seven complete sets (23S, 5S AND 16S) of ribosomal RNA operons and 85 tRNA genes, were predicted (Duchaud et al. 2003) (Figure I.1)

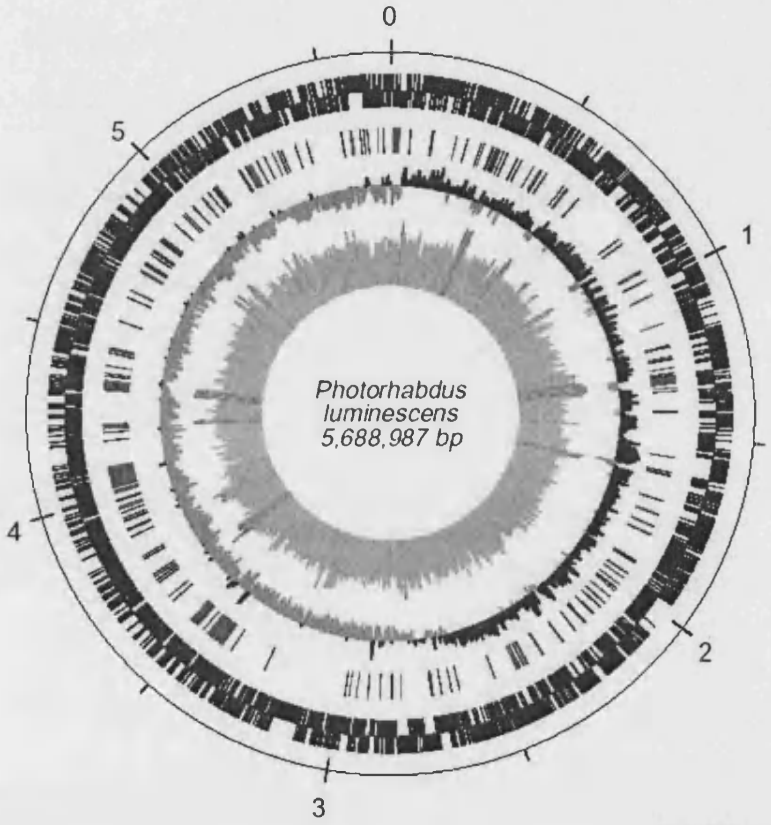

Figure I.1 Circular representation of the *P. luminescens* strain TTO1 genome. The outer scale is marked in megabases. Circle 1 and 2 (from outside to inside), genes transcribed clockwise and counterclockwise. Circle 3, transposases (red) and phage-related genes (green). Circle 4, GC bias (G-C/G+C). Circle 5, GC content with <32% G+C in light yellow. Shifts in GC bias correspond to positions of the predicted origin and terminus of replication or to putative prophage regions (green) (Duchaud et al. 2003).

P. luminescens has a life cycle which introduces it into a diverse array of environments, and in only one of these environments, the insect environment, is the bacterium pathogenic. The genomic sequence of strain TTO1 revealed sequences similar to the sequences of a diverse array of potential virulence factor-encoding genes, including the genes for several classes of toxins (*mcf1*, four toxin-complex loci- *tca*, *tcb*, *tcc* and *tcd* and some other toxins against insects), proteases, lipases, and LPS. The TTO1 genome contains 33 genes, clustered in 20 loci, encoding proteins similar to polyketide and nonribosomal peptide synthases that may be part of the biosynthetic pathway of antibiotics known to be produced by *P. luminescens* used as toxins against competitors (Duchaud et al. 2003). *P. luminescens* also gave us some indication of the diversity of the transport and metabolic systems present. Furthermore, *Photorhabdus* also seem to share potential virulence factors (Yops, a yersiniabactin-like siderophore, and the low-calcium-response stimulon) with distantly related vertebrate pathogens, such as members of the genus *Yersinia.*

P. luminescens encodes for complete type I, one type II and one type III secretion system. The *Photorhabdus* TTSS region is about 30 kb long and is very similar to the chromosome-encoded TTSS of *Pseudomonas* and the plasmid-encoded TTSS of pathogenic *Yersinia* (Duchaud et al. 2003; Brugirard-Ricaud et al. 2004). Comparisons of the genomic organization of the *Photorhabdus* TTSSs (Figure I.2) were performed with three strains: *P. luminescens* subsp. *laumondii* (strain TT01), *P. luminescens* subsp. *akhurstii*(strain W14), and *P. asymbiotica* (strain ATCC43949) (Brugirard-Ricaud et al. 2004). A TTSS-encoding locus is presented in all three strains analyzed. First, identical TTSS backbones, including all the genes predicted to encode the injectisome (Sct/Lss proteins): i.e., the basal body, the needle-like structure (*sctF*), and the translocator (*lopB*-, *lopD*-, and *lcrV*-like genes). *P. luminescens* subsp. *laumondii* and *P. luminescens* subsp. *akhurstii* as well as *P. asymbiotica* possess the same genetic organization required for the complete assembly of a functional TTSS machinery. Moreover, these three *Photorhabdus* species harbor genes similar to the *P. aeruginosa exsC* and *exsD* genes encoding transcriptional

regulators, which are absent from *Yersinia* spp., suggesting that the regulation of this system is more related to that performing regulation in *P. eruginosa* (Brugirard-Ricaud et al. 2004).

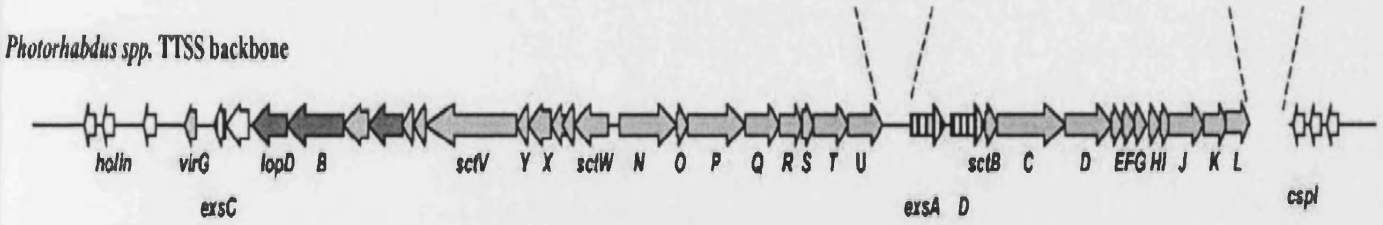

Figure I.2 Comparative genomics of TTSS organization in *Photorhabdus species* (Brugirard-Ricaud et al. 2004).

To further investigate some known and putative virulent factors, we construct a random knock out library of *P. luminescence* strain TTO1 using a suicide vector-pLOF, and tried to screen some interested KO strains by genomic PCR.

I.2 Results

I.2.1 Construct library

After conjugation, 3,300 colonies were streaked on kanamycin-containing LB agar plates and grow in 96-well plate. Genomic DNA was prepared by mixing 48 clones cell culture (Figure I.3). Clones were stored in a glycerol suspension at -80 °C.

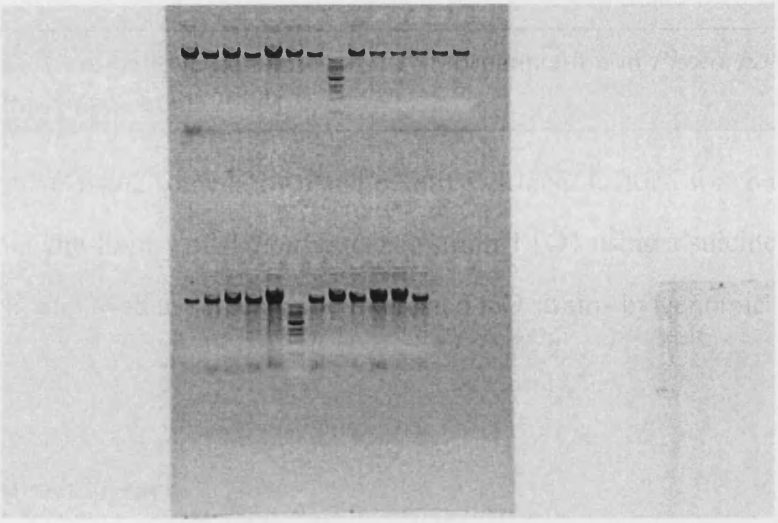

Figure I.3 Genomic DNA used for PCR screening

I.2.2 Design screen primers

Two primers were designed at the end of insert fragment (Figure I.4). Upstream and downstream primers are designed according to the genomic sequence of strain TTO1.

To screen *mcfl*, TTSS and some other interested target genes knock-out strain, primers were designed every 1kb in the interested region of strain TTO1 as follows:

Primers in insertion sequence: KanR: AGACGTTTCCCGTTGAATATGGCTCAT
KanF: GGTTGTAACACTGGCAGAGCATTACGC

Primers for TTSS screening: lopNF TGATATGACAGGGTAGACTATGGA
lscAR AAGACATAACACCAACAGATCCA
lscNR ACGATCATGAAGCTTTCCCTTGA
lscUF GCTGTTTGAGGACAGATTACGGCT
lscWR CATTCTGGATAACATGGCAAGGGA
sycTF ACCCGCACCAAGGAAGGCGGCGGA

Primers for Type IV screening: T4pilF AAGTATGTGAGTGATTCATCGGCA
T4pilR GAGGGCAGAGATAACGACTGCTCA
midT4pilF GCCGGAAGTGTTGAAAATTCATGT
midT4pilR CACAACACCTCGTTCACTCCCTCT

primers for *mcfl* screening: mcf1-plof-1.0F CCACCATCCTTTCGCTCGCCGA
mcf1-plof-3.4F CGAAACTGCGCGGTGATGTGGA
mcf1-plof-5.7F CTTGGTGGGCTCGCGGTGGGCT
mcf1-plof-7.8F GGCGGTGTTCGGAATCAAGGGT
mcf1-plof-3.4R CCAAACCATCTGTCCATCTCGT
mcf1-plof-5.7R AAAGCCCACCGCGAGCCCACCA

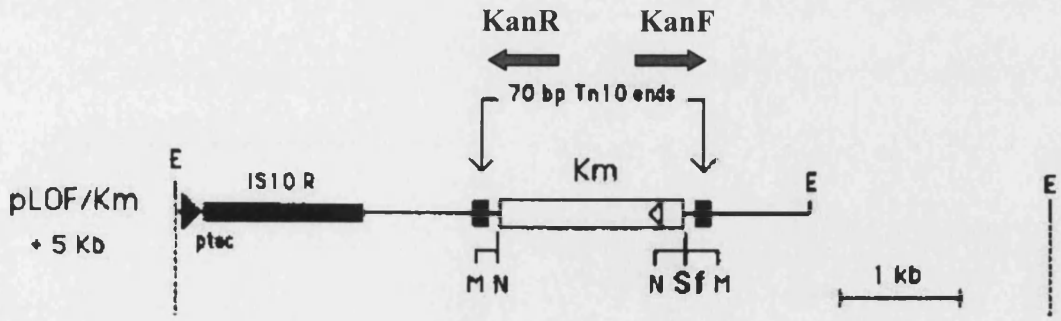

Figure I.4 primers located in insertion used to screen expected knock out

I.2.3 Pre-test

In pre-test, a known *flg*⁻ strain was used as positive control. Both the PCR product' size and sequence show that this system worked (Figure I.5).

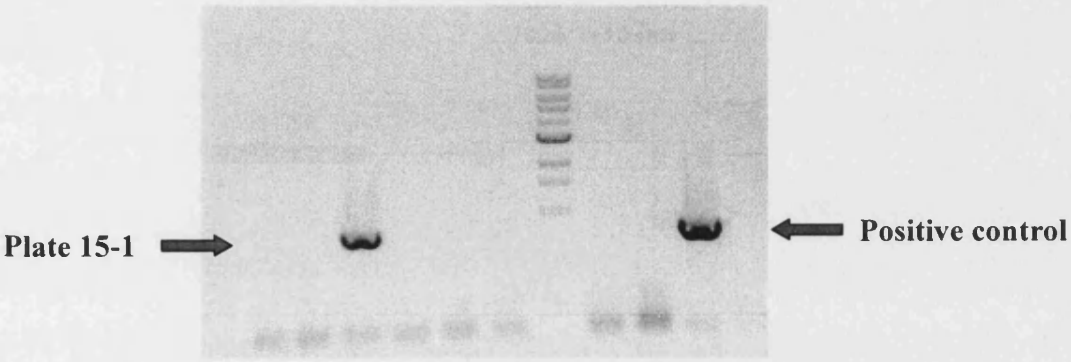

Figure I.5 PCR screening for the positive control

I.2.4 PCR screening

The PCR was performed by adding the following to a PCR tube: 0.5ul *Taq*, 5ul reaction buffer, 1ul 15uM forward primer, 1ul 15uM reverse primer, 5ul template DNA, 4ul 2mM dNTPs, 3ul 25mM $MgCl_2$, water to make up to 50ul. Start the PCR cycles according the following schemes: a) denaturation - 95 ° C, 30sec. b) annealing - 50 °C 0.5 min. c) extension - 72 °C 1min, repeat cycles 30 times. Add a final extension step of 10 min. to fill in any uncompleted polymerisation. Then cooled

down to 4- 25 °C.

Loading PCR products into 1.0% gel in TAE. After electrophoresis, cut the specific bands to purify and sequence.

I.2.5 TTSS knock-out strain

After sequencing the specific PCR products, genomic DNA of lanes and rows of that plate were prepared to isolate the target strain by PCR (Figure I.6). One TTSS knock-out strain, inserting at *lscA*⁻ a negative regulator in TTSS, similar to *Pseudomonas aeruginosa* ExsA transcriptional regulator, was isolated and named 3-7B.

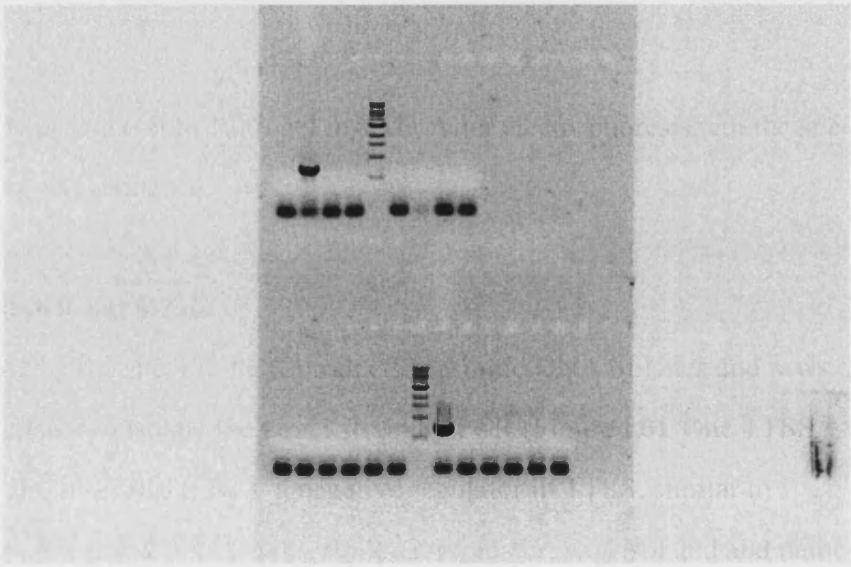

Figure I.6 PCR screening for TTSS knock-out

I.2.6 Bioassay of TTSS knock-out strain

Galleria were injected with TTO1 wild type strain and *lscA*⁻ strain. The result shows that there is no difference between these two strains in killing the insects (Figure I.7).

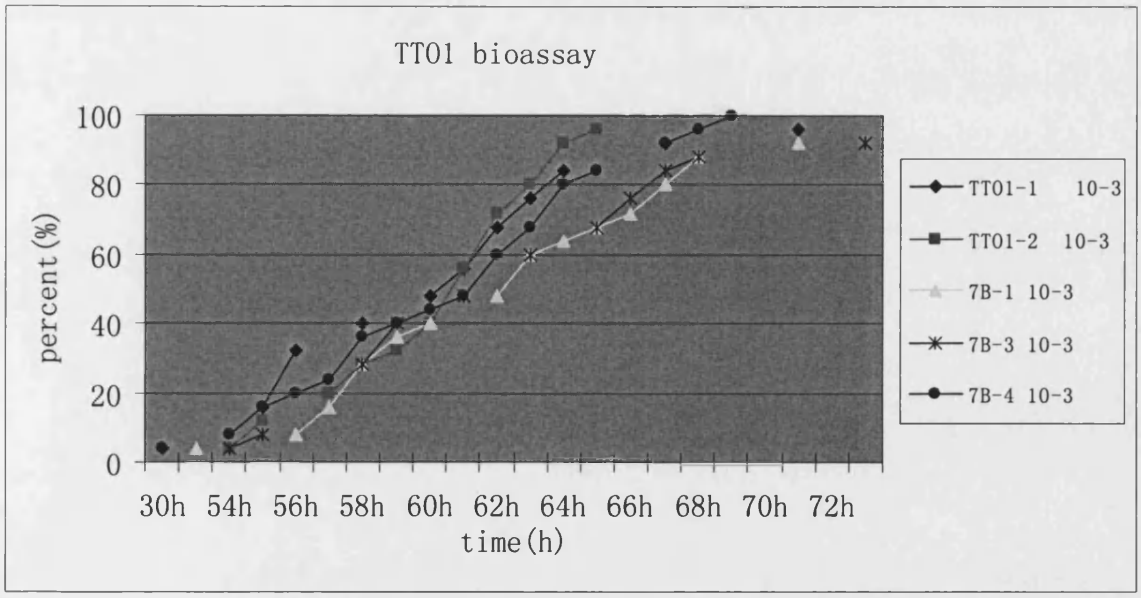

Figure I.7 Bioassay of TTO1 wild type strain and *lscA*⁻ strain

I.3 Conclusion

Although one knock out strain was isolated by PCR screening, in general, this method is not a sufficient one compared to targeted gene knock out technique.

Because mixed genomic DNA was used for PCR screening, concentration of genomic DNA from individual strain is quite low; therefore the frequency of false negative result is high. On the other hand, many unspecific bands will appear via genomic DNA PCR and it is hard to tell specific bands will cause the frequency of false positive result is high too.

GENERAL DISCUSSION

Photorhabdus encodes numerous toxins, the Toxin Complexes and Mcf1 are well characterized examples of these (Blackburn et al. 1998; Bowen et al. 1998; Waterfield et al. 2001; Daborn et al. 2002), and there are a whole host of other putative toxins whose mode of action and role in pathogenicity are yet to be determined (ffrench-Constant et al. 2000). Here, I showed some other virulence factors identified in the genome of *Photorhabdus*.

The Mcf1 encoding gene was discovered due to its ability to kill insects when expressed in *E. coli* and injected into caterpillars (Daborn et al 2002). Here the identification of a homologue of *mcf1*, termed *mcf2*, was described within the same *P. luminescens* W14 genome. The predicted amino acid sequence of Mcf2 is similar to Mcf1 but differs at its Nterminus. Comparison with TcaB from *C. diffcile* and a predicted Mcf-like homologue (ORF 4315) from the genome of *P. fluorescens* suggests that the Mcf proteins may belong to the same super-family as large clostridial toxins. In this family of toxins (Figure 3.2), a central predicted transmembrane domain is conserved whereas both the N-termini and C-termini are variable. The N-terminus appears to encode the putative effector domain in all four proteins: a BH3-like domain in Mcf1, an HrmA-like domain in Mcf2, and a glycosyltransferase domain in both *C. diffcile* TcaB and the novel homologue from *P. fluorescens*. The C-terminus of Mcf1 contains an RTX-like export domain whereas in TcaB there is a receptor-binding domain. The genomic context of *mcf2*, in an operon with type-I secretion machinery, suggests secretion of Mcf2 via the type-I pathway. Further, the low levels of expression achieved from cosmid W14-1C-G1, which contains a complete copy of this operon, suggests that the *mcf2* gene is regulated by its native promoter in *E. coli*. It is interesting to note that HrmA is secreted by the type-III pathway in *P. syringae pv. syringae* and therefore that the HrmA-like domain of Mcf2 may effectively be a fusion of a type-III effector with the high molecular mass Mcf1-like toxin.

Expression of Mcf1 in recombinant *E. coli* allows the *E. coli* both to persist within and also to kill caterpillars (Daborn et al 2002). It is therefore unexpected that *Photorhabdus* strains, both W14 and TT01, should require a second potent toxin also possessing the same properties. Knock out *mcf2* in strain W14 showed no different in killing the insect. There are several potential explanations for this observation. First, as insect death is a prerequisite for the lifecycle of *Photorhabdus*, individual strains may employ "functional redundancy" in toxins. In other words, they encode more than one toxin capable of killing the insect host. Secondly, Mcf1 and Mcf2 may have activities against different types of insects. Only the Mcf1 and Mcf2 toxins against larval lepidoptera (butterflies and moths) were tested and not, for example, coleoptera (beetles). Finally, and alternatively, Mcf1 and Mcf2 may have very different sites of action within the insect. The Mcf1 toxin can destroy the insect gut and hemocytes by triggering massive programmed cell death (Dowling et al. 2004). However, the site and mode of action of Mcf2 is unknown and is currently under investigation.

In this thesis, the first functional studies on phage-like PVC structures found as repetitive cassettes in two different genera of entomopathogenic bacteria, *Photorhabdus* (Waterfield et al. 2004) and *Serratia* (Hurst et al. 2004) was described. These prophage-like loci were described both as an anti-feeding locus on the pADAP plasmid of *S. entomophila* (Hurst et al. 2004) and as repetitive loci in the genomes of *P. luminescens* TT01 (Waterfield et al. 2004) and *P. asymbiotica* ATCC43949. Each PVC unit is predicted to encode 15 to 20 proteins, each with predicted similarity to phage tail, phage base plate assembly, fimbrial usher and one or more different putative effector proteins from other pathogenic and in *S. entomophila* this effector sequence has been implicated in the anti-feeding phenotype, suggesting it may be a virulence factor. Given that the *S. entomophila* pADAP plasmid is capable of conferring anti-feeding activity on insects in the absence of a described secretion system (Hurst et al. 2004), the genomic organization of the PVC loci in different *Photorhabdus* genomes was examined and tested if PVC containing cosmids were toxic to *Galleria* via injection.

Several points about the genomic organization of the PVCs in the different *Photorhabdus* genomes are worthy of discussion. First, these cassettes can either be found singly or in tandem repeats, suggesting that the *Photorhabdus* strains they occupy may have undergone lysogenic or polylysogenic conversion (Boyd et al. 2002). Second, within each of the repeated arrays, each PVC unit carries different putative effector sequences but always in the equivalent position (Figure 4.2), as documented for other prophage (Boyd et al. 2002). That the different PVC effectors are often flanked by transposons, suggests a possible mechanism for their insertion into the PVC or their movement between different PVCs. Importantly, the presence of multiple effectors within a single casette, or indeed multiple PVCs at a single locus (Figure 4.1), suggests that a single PVC containing locus may be able to confer several different phenotypes via the array of multiple effectors present. Thirdly, although several of the PVC encoded effectors can rearrange the actin cytoskeleton of cells, it is only a small proportion of the potential effector sequences identified have been tested in current study, and that the majority of putative effectors remain untested. Finally, one PVC element is consistently inserted adjacent to the *mukB* locus, a locus involved in plasmid maintenance and stability (Weitao et al. 2000). This suggests that *mukB* may either be a communal insertion point for these phage-like elements or that it may regulate the insertion of plasmids containing these elements. Interestingly, a type IV DNA conjugation pilus operon is found immediately 5' to this PVC element insertion site. A similar operon is also found on the pADAP plasmid where it is responsible for conjugative transfer of the plasmid. It is therefore temping to speculate that this operon in *Photorhabdus* is involved in horizontal movement of the PVC elements.

It is unexpected, that like the *S. entomophila* anti-feeding locus (Hurst et al. 2004), that these loci can confer insecticidal activity without a TTSS. Although the secretion mechanism of the PVCs is not certain, 2D-gel analysis of PVC expressing *E. coli* reveals the presence of proteins encoded by the phage tail-like genes within the PVCs in recombinant supernatants (Figure 4.4). Moreover, examination of these same cells

by electron microscopy reveals that the recombinant *E. coli* are intact and that these phage-like PVC proteins are not simply released into the bacterial supernatant following host cell lysis (Figure 4.8). Examination of supernatants of PaPVCpnf expressing recombinant *E. coli* via TEM revealed the presence of structures highly reminiscent of R-type pyocins (Figure 4.5)(Michel-Briand et al. 2002). Although the precise mode of action of R-type pyocins themselves is not known, it is suggested that their antibacterial activity is achieved by injection of the needle into bacterial cells via the contraction of the sheath (Michel-Briand et al. 2002). Unexpectedly, the PVCs have no anti-bacterial activity like well-documented R-pyocins but trigger rapid destruction of insect phagocytes following injection. This observation helps explain how PVC expressing *E. coli* can persist in the presence of the insect phagocytes or hemocytes. Moreover the fact that the actin cytoskeletons of the remnant hemocytes (Figure 4.13) are severely altered is consistent with the phenotypes observed upon direct expression of several different potential effector sequences directly inside mammalian cells (Figure 4.14). Finally, although the mechanism of bacterial secretion of these effectors or the process whereby they enter host cells remains undetermined, it is interesting to note that the Ntermini of otherwise unrelated PVC encoded effectors show strong predicted amino acid similarity (Figure 4.15) and a conserved hydrophillicity (Figure 4.16), suggesting a potentially conserved export motif for export from the bacterial cell.

In conclusion, taken together these data suggest that the PVCs, alongside the anti-feeding locus on pADAP of *S. entomophila* (Hurst et al. 2004), correspond to a novel family of phage-like elements capable of independent effector delivery into infected insect hosts. Whilst at this stage the mechanism whereby the effectors leave PVC expressing cells is still uncertain, that such cells remain intact and that PVC proteins are detected in the bacterial supernatant are confirmed. This suggests either that the PVCs themselves correspond to a novel secretion or effector delivery system, or alternatively that PVC derived effectors are exported via an uncharacterized system in *E. coli*. Finally, the role of these prophage-like elements in the ecology of different

Photorhabdus species remains to be investigated but they may well be important in conferring novel virulence properties either against different types of insects, or in the case of the *P. asymbiotica* strains isolated from human wounds (Gerrard et al. 2004), against man.

Proteomic analysis of *P. asymbiotica* supernatants identified a small protein designated S15 that was secreted at 30°C but not 37°C (human- infection temperature). Over-expression of *s15* in the arabinose- inducible plasmid- pBAD30, revealed good intracellular accumulation of the S15 protein. These induced cultures induced "clumping" of *C. elegans*, suggesting that S15 represents the clumping factor seen in the native *Photorhabdus* supernatants. Light and electron microscopy of induced cells revealed that S15 produced fibres within the cells which gave rise to "chains" of bacteria which is associated with the "clumping" of nematodes. Random PCR mutagenesis identified 2 regions important in the formation of these chains. Biological testing of these mutants suggested that "clumping" of nematodes was associated with the ability to form bacterial chains. Those are mutants that form shorter chains, such as a5, also gave "weaker" clumping effects. Analysis of the primary amino acid sequence of S15, gives no clues as to the mechanism of fibre formation, and as a result is interesting for this reason alone. Although there are several clues indicate that S15 is the clamping factor in the supernatant of *photorhadbus* such as previous experiments had demonstrated that this was mediated by a heat-sensitive factor that was shown to be in the size range of 10 to 30 KDa; *P. asymbiotica* grown at 30°C can clamp *C. elegans* but not 37°C; pre- incubation at 4 °C is required for the natural supernatant of *P. asymbiotica* same as induced *E. coli* pBAD30- *s15*, the function of S15 in *Photorhabdus* is still unknown.

Further work is required to investigate this relationship, i.e.; does S15 have a specific nematode-binding receptor, or is the "clumping" and artefact arising as a result of the bacterial chains themselves. Nevertheless, if S15 represents the *bona fide* "clumping" agent seen in *Photorhabdus* supernatants then it is a molecule secreted as a soluble

monomer, which is then able to "clot" around the nematode in response to a specific signal or ligand. Such molecule is of obvious interest both from a structural mechanistic perspective and also as a potential future target for nanotechnology applications.

PUBLICATIONS

G. Yang, A.J. Dowling, U. Gerike, R.H. ffrench-Constant and N.R. Waterfield
"Insecticidal pyocin-like structures from *Photorabdus* bacteria."
(submitted)

Waterfield N, Hares M, Yang G, Dowling A, ffrench-Constant R. (2005)
"Potentiation and cellular phenotypes of the insecticidal Toxin complexes of *Photorhabdus* bacteria." Cell Microbiol. **Mar;7(3):**373-82.

Waterfield NR, Daborn PJ, Dowling AJ, Yang G, Hares M, ffrench-Constant RH.
"The insecticidal toxin Makes Caterpillars Floppy 2 (Mcf2) shows similarity to HrmA, an avirulence protein from a plant pathogen."
FEMS Microbiol Lett. **2003 Dec 12;229(2):**265-70.

REFERENCES

Alfano, J.R., Klm, H.S., Delaney, T.P. and Collmer, A. (1997) "Evidence that the *Pseudomonas syringae* pv. *syringae* hrp-linked hrmA gene encodes an Avr-like protein that acts in an hrp-dependent manner within tobacco cells." Mol. Plant Microb. Interact **10**: 580-588.

Alfano, J.R., Charkowski, A.O., Deng, W.L., Badel, J.L., Petnicki-Ocwieja, T., van Dijk, K. and Collmer, A. (2000) "The *Pseudomonas syringae* Hrp pathogenicity island has a tripartite mosaic structure composed of a cluster of type III secretion genes bounded by exchangeable effector and conserved effector loci that contribute to parasitic fitness and pathogenicity in plants." Proc. Natl. Acad. Sci. USA **97**: 4856-4861.

Au, C., P. Dean, S. E. Reynolds and R. H. Ffrench-Constant (2004). "Effect of the insect pathogenic bacterium *Photorhabdus* on insect phagocytes." Cell Microbiol **6(1)**: 89-95.

Barbieri, J. T., M. J. Riese and K. Aktories (2002). "Bacterial toxins that modify the actin cytoskeleton." Annual Review of Cellular and Developmental Biology **18:** 315-44.

B.H. Bleakley, X. Chen, (1999) "Survival of insect pathogenic and human clinical isolates of *Photorhabdus luminescens* in previously sterile soil." Can. J. Microbiol **45**: 273–278.

Boemare, N.E., Boyer-Giglio, M.H., Thaler, J.O., Akhurst, R.J. and Brehelin, M. (1992) "Lysogeny and bacteriocinogeny in *Xenorhabdus* nematophilus and other *Xenorhabdus spp.*" Appl. Environ. Microbiol. **58:** 3032-3037.

Boemare, N. E., R. J. Akurst and R. G. Mourant (1993). "DNA relatedness between *Xenorhabdus spp.* (Enterobacteriaceae), symbiotic bacteria of entomopathogenic nematodes, and a proposal to transfer *Xenorhabdus luminescens* to a new genus, *Photorhabdus* gen. nov." International Journal of Systematic Bacteriology **43**: 249-255.

Boise, L. H. and C. M. Collins (2001). "*Salmonella*-induced cell death: apoptosis,

necrosis or programmed cell death?" Trends Microbiol **9(2):** 64-7.

Bowen, D., T. A. Rocheleau, M. Blackburn, O. Andreev, E. Golubeva, R. Bhartia and R. H. ffrench-Constant (1998). "Insecticidal toxins from the bacterium *Photorhabdus luminescens*." Science **280(5372)**: 2129-2132.

Bowen, D. J. and J. C. Ensign (1998). "Purification and characterization of a high molecular weight insecticidal protein complex produced by the entomopathogenic bacterium *Photorhabdus luminescens*." Appl. Environ. Microbiol. **64**: 3029-3035.

Bowen, D. J., T. A. Rocheleau, C. K. Grutzmacher, L. Meslet, M. Valens, D. Marble, A. Dowling, R. Ffrench-Constant and M. A. Blight (2003). "Genetic and biochemical characterization of PrtA, an RTX-like metalloprotease from *Photorhabdus*." Microbiology **149(Pt 6)**: 1581-91.

Bowen , D., Blackburn, M., Rocheleau, T., Grutamacher, C. and ffrench-Contant, R.H. (2000) "Secreted proteases from *Photorhabdus luminescens*: separation of the extracellular proteases from the insecticidal Tc toxin complexes." Insect. Biochem. Mol. Biol **30**: 69-74

Boyd, E.F. and Brussow, H. (2002) "Common themes among bacteriophage-encoded virulence factors and diversity among the bacteriophages involved." Trends Microbiol **10**: 521-529.

Brugirard-Ricaud, K., Givaudan, A., Parkhill, J., Boemare, N., Zumbihl, R., and Duchaud, E. (2004) "Variation in the effectors of the *Photorhabdus* type III secretion system among species revealed by genomic analysis." J Bacteriol **186**: 4376–4381.882.

Buetow, L., Flatau, G., Chiu, K., Boquet, P. and Ghosh, P. (2001) "Structure of the Rho-activating domain of *Escherichia coli* cytotoxic necrotizing factor 1." Nature Structural Biology **8**: 584–588.

Coleman, M. L. and M. F. Olson (2002). "Rho GTPase signalling pathways in the morphological changes associated with apoptosis." Cell Death Differ. **9.**

Cornelis, G. R. and F. Van Gijsegem (2000). "Assembly and function of type III secretory systems." Annu Rev Microbiol **54:** 735-74.

Daborn, P. J., N. Waterfield, C. P. Silva, C. P. Y. Au, S. Sharma and R. H. ffrench-Constant (2002). "A single *Photorhabdus* gene makes caterpillars floppy (*mcf*) allows *Escherichia coli* to persist within and kill insects." Proceedings of the National Academy of Sciences USA **99**: 10742-10747.

Daborn, P. J., N. Waterfield, M. A. Blight and R. H. Ffrench-Constant (2001). "Measuring virulence factor expression by the pathogenic bacterium *Photorhabdus luminescens* in culture and during insect infection." J Bacteriol **183(20)**: 5834-9.

Debra l. Milton, Ronan o'toole, Per Horstedt, and Hans wolf-watz (1996) "Flagellin A is essential for the virulence of *Vibrio anguillarum*." J. Bacteriology p. 1310–1319

DeLeo, F. R. (2004). "Modulation of phagocyte apoptosis by bacterial pathogens." Apoptosis **9(4):** 399-413.

Denecher, G., W. Declercq, C. A. Geuijen, A. Boland, R. Benabdillah, M. van Gurp, M. P. Sory, P. Vandenabeele and C. G.R (2001). "*Yersinia enterocolitica* Yop-P-induced apoptosis of macrophages involves the apoptotic signaling cascade upstream of Bid." J. Biol. Chem **276:** 19706-19714.

Donnenberg, M.S., Kaper, J.B. (1991) "Construction of an eae deletion mutant of enteropathogenic *Escherichia coli* by using a positive-selection suicide vector." Infect. Immun **59**: 4310–4317.

Dove, C. H., Wang, S.-Z., Price, S. B., Phelps, C. J., Lyerly, D. M., Wilkins, T. D. and Johnson, J. L. (1990) "Molecular characterization of the *Clostridium difficile* toxin A gene." Infection and Immunity **58**: 480-488.

Dowling, A. J., Daborn, P. J., Waterfield, N. R., Wang, P., Streuli, C. H. and ffrench-Constant, R. H. (2004) "The insecticidal toxin Makes caterpillars floppy (Mcf) promotes apoptosis in mammalian cells." Cell Microbiol **6**: 345-53.

Duchaud, E., C. Rusniok, L. Frangeul, C. Buchrieser, A. Givaudan, S. Taourit, S. Bocs, C. Boursaux-Eude, M. Chandler, J. F. Charles, E. Dassa, R. Derose, S. Derzelle, G. Freyssinet, S. Gaudriault, C. Medigue, A. Lanois, K. Powell, P. Siguier, R. Vincent, V. Wingate, M. Zouine, P. Glaser, N. Boemare, A. Danchin

and F. Kunst (2003). "The genome sequence of the entomopathogenic bacterium *Photorhabdus luminescens*." Nat Biotechnol **21(11)**: 1307-13.

Ehrbar, K. and Hardt, W.D. (2005) "Bacteriophage-encoded type III effectors in *Salmonella enterica* subspecies 1 serovar Typhimurium." Infect Genet Evol **5(1)**: 1-9.

Etienne-Manneville, S. and A. Hall (2002). "Rho GTPases in cell biology." Nature 420(6916): 629-35.

J.J. Farmer, J.H. Jorgensen, P.A.D. Grimont, R.J. Ackhurst, G.O. Poinar, and E.Ageron. (1989) "*Xenorhabdus luminescens* (DNA Hybridization Group 5) from human clinical specimens." J. Clin. Microbiol 27: 1594–1600.

Fiorentini, C., L. Falzano, S. Travaglione and A. Fabbri (2003). "Hijacking Rho GTPases by protein toxins and apoptosis: molelcular strategies of pathogenic bacteria." Cell Death Differ. **10:** 147-152.

Fischer-Le Saux, M., V. Viallard, B. Brunel, P. Normand and N. E. Boemare (1999). "Polyphasic classification of the genus *Photorhabdus* and proposal of new taxa: *P. luminescens* subsp. *luminescens* subsp. nov., *P. luminescens* subsp. *akhurstii* subsp. nov., *P. luminescens* subsp. *laumondii* subsp. nov., *P. temperata* sp. nov., *P. temperata* subsp. *temperata* subsp. nov. and *P. asymbiotica* sp. nov." Int. J. Syst. Bacteriol. **49**: 1645-56.

Flatau, G., Lemichez, and E., Gauthier, M. (1997) "Toxin-induced activation of the G protein p21 Rho by deamidation of glutamine." Nature **387**: 729–733.

Forst, S. and Clarke, D. (2001) in: Entomopathogenic Nematology, Vol. (Gaugler, R., Ed.), pp. 57-77. CAB International, London.

Forst, S., B. Dowds, N. Boemare and E. Stackebrandt (1997). "*Xenorhabdus* and *Photorhabdus* spp.: bugs that kill bugs." Annu Rev Microbiol **51**: 47-72.

Forst, S. and K. Nealson (1996). "Molecular biology of the symbiotic-pathogenic bacteria *Xenorhabdus* spp. and *Photorhabdus* spp." Microbiol Rev **60(1)**: 21-43.

ffrench-Constant, R., N. Waterfield, P. Daborn, S. Joyce, H. Bennett, C. Au, A. Dowling, S. Boundy, S. Reynolds and D. Clarke (2003). "*Photorhabdus*:

towards a functional genomic analysis of a symbiont and pathogen." FEMS Microbiology Reviews **26**: 433-456.

ffrench-Constant, R. and D. Bowen (1999). "*Photorhabdus* toxins: novel biological insecticides." Curr Opin Microbiol **2(3)**: 284-8.

ffrench-Constant, R. H. and D. J. Bowen (2000). "Novel insecticidal toxins from nematode-symbiotic bacteria." Cell Mol Life Sci **57(5)**: 828-33.

ffrench-Constant, R. H., Waterfield, N. and Daborn, P. (2004) in Comprehensive Molecular Insect Science, Vol. 5, pp. 239-253.

ffrench-Constant, R. H., N. Waterfield, V. Burland, N. T. Perna, P. J. Daborn, D. Bowen and F. R. Blattner (2000). "A genomic sample sequence of the entomopathogenic bacterium *Photorhabdus luminescens* W14: potential implications for virulence." Appl. Environ. Microbiol. **66**: 3310-3329.

Fields, K.A., Nilles, M.L., Cowan, C. and Straley, S.C. (1999) "Virulence role of V antigen of *Yersinia pestis* at the bacterial surface." Infect. Immun. **67:** 5395-5408.

Gay, P., Lecoq, D., Steinmetz, M., Ferrari, E., and Hoch, J.A., (1983) "Cloning structural gene sacB, which codes for exoenzyme levansucrase of *Bacillus subtilis*: expression of the gene in *Escherichia coli*." J. Bacteriol **153**: 1424–1431.

J.G. Gerrard, S. McNevin, D. Alfredson, R. Forgan-Smith, and N. Fraser, (2003) "*Photorhabdus* species: bioluminescent bacteria as emerging human pathogens?" Emerg. Infect. Dis **9 (2)**: 251–254.

Gerrard, J., N. Waterfield, R. Vohra and R. ffrench-Constant (2004). "Human infection with *Photorhabdus asymbiotica*: an emerging bacterial pathogen." Microbes and Infection **6(2)**: 229-237.

Gillespie, J. P., Kanost, M. R. and Trenczek, T. (1997) "Biological mediators of insect immunity." Annu. Rev. Entomol **42**: 611-43.

Grassme, H., V. Jendrossek and E. Gulbins (2001). "Molecular mechanisms of bacteria induced apoptosis." Apoptosis **6(6):** 441-5.

Guzman Luz-maria, Dominique Belin, Michael J. Carson, and Jon Beck. (1995) "Tight Regulation, Modulation, and High-Level Expression by Vectors Containing the Arabinose PBAD Promoter." J. Bacteriology **p.** 4121–4130

Hilbi, H., J. E. Moss, D. Hersh, Y. Chen, J. Arondel, S. Banerjee, R. A. Flavell, J. Yuan, P. J. Sansonetti and A. Zychlinsky (1998). "*Shigella*-induced apoptosis is dependent on caspase-1 which binds to IpaB." J Biol Chem **273(49):** 32895-900.

Hacker, J. and Kaper, J.B. (2000) "Pathogenicity islands and the evolution of microbes". Annu. Rev. Microbiol. **54**: 641-679

Heu, S. and Hutcheson, S.W. (1993) "Nucleotide sequence and properties of the hrmA locus associated with the *Pseudomonas syringae* pv. *syringae* 61 *hrp* gene cluster." Mol. Plant Microb. Interact **6**: 553-564.

Hofmann, F., C. Busch, U. Prepens, I. Just and K. Aktories (1997). "Localization of the glucosyltransferase activity of Clostridium difficile toxin B to the N-terminal part of the holotoxin." The Journal of Biological Chemistry **272**: 11074-11078.

Hueck, C. J. (1998). "Type III protein secretion systems in bacterial pathogens of animals and plants." Microbiol Mol Biol Rev **62(2):** 379-433.

Hurst, M.R., Glare, T.R., Jackson, T.A. and Ronson, C.W. (2000) "Plasmid-located pathogenicity determinants of *Serratia entomophila*, the causal agent of amber disease of grass grub, show similarity to the insecticidal toxins of *Photorhabdus luminescens*." J. Bacteriol **182**: 5127-5138.

Hurst, M. R., T. R. Glare, T. A. Jackson and C. W. Ronson (2000). "Plasmid-located pathogenicity determinants of *Serratia entomophila*, the causal agent of amber disease of grass grub, show similarity to the insecticidal toxins of *Photorhabdus luminescens*." J. Bacteriol. **182(18)**: 5127-5138.

Hurst, M. R., Glare, T. R. and Jackson, T. A. (2004) "Cloning *Serratia entomophila* antifeeding genes--a putative defective prophage active against the grass grub Costelytra zealandica." J Bacteriol **186**: 5116-28.

Jarvelainen, H. A., A. Galmiche and A. Zychlinsky (2003). "Caspase-1 activation by *Salmonella*." Trends Cell Biol **13(4):** 204-9.

Joo Lee, P., J. Y. Ahn, Y. H. Kim, S. Wook Kim, J. Y. Kim, J. S. Park and J. Lee (2004). "Cloning and heterologous expression of a novel insecticidal gene (tccC1) from *Xenorhabdus* nematophilus strain." Biochem Biophys Res Commun **319(4)**: 1110-6.

M. Kageyama (1964) "Studies of a pyocin. I. Physical and chemical properties." J. Biochem. (Tokyo) **55**: 49–53.

Landraud, L., Pulcini, C., Gounon, P., Flatau, G., Boquet, P. and Lemichez, E. (2004) "*E. coli* CNF1 toxin: a two-in-one system for host-cell invasion." Int J Med Microbiol **293**: 513-8.

Liu, D., S. Burton, T. Glancy, Z. S. Li, R. Hampton, T. Meade and D. J. Merlo (2003). "Insect resistance conferred by 283-kDa *Photorhabdus luminescens* protein TcdA in *Arabidopsis thaliana*." Nat Biotechnol **21**: 1307-1313.

Lionel Ferrie` res, Anne Francez-Charlot, Je´ roˆme Gouzy, Ste´phane Rouille´ and Daniel Kahn (2004) "FixJ-regulated genes evolved through promoter duplication in *Sinorhizobium meliloti*" Microbiology **150**: 2335–2345

Marta Herrero, Victor de Lorenzo, and Kenneth n. Timmis. (1990) "Transposon Vectors Containing Non-Antibiotic Resistance Selection Markers for Cloning and Stable Chromosomal Insertion of Foreign Genes in Gram-Negative Bacteria." Journal of Bacteriology **p.** 6557-6567

McGaughey, W. H. and M. E. Whalon (1992). "Managing insect resistance to *Bacillus thuringiensis* toxins." Science **258**: 1451-1455.

Michel-Briand, Y. and Baysse, C. (2002) "The pyocins of *Pseudomonas aeruginosa*." Biochimie **84**: 499-510

Mirold, S., Rabsch, W., Rohde, M., Stender, S., Tschape, H., Russmann, H., Igwe, E. and Hardt, W.D. (1999) "Isolation of a temperate bacteriophage encoding the type III effector protein SopE from an epidemic *Salmonella typhimurium* strain." Proc Natl Acad Sci U S A **17;96(17)**:9845-50.

Morgan, J. A., M. Sergeant, D. Ellis, M. Ousley and P. Jarrett (2001). "Sequence analysis of insecticidal genes from *Xenorhabdus* nematophilus PMFI296." Applied and Environmental Microbiology **67(5)**: 2062-2069.

M. Ohsumi, T. Shinomiya, M. Kageyama (1980) "Comparative study on R-type pyocins of *Pseudomonas aeruginosa*." J. Biochem. **87:** 1119–1125.

Nonaka, T., A. Kuwae, C. Sasakawa and S. Imajoh-Ohmi (1999). "*Shigella flexneri* YSH6000 induces two types of cell death, apoptosis and oncosis, in the differentiated human monoblastic cell line U937." FEMS Microbiol Lett **174(1):** 89-95.

Parkhill, J., B. W. Wren, N. R. Thomson, R. W. Titball, M. T. Holden, M. B. Prentice, M. Sebaihia, K. D. James, C. Churcher, K. L. Mungall, S. Baker, D. Basham, S. D. Bentley, K. Brooks, A. M. Cerdeno-Tarraga, T. Chillingworth, A. Cronin, R. M. Davies, P. Davis, G. Dougan, T. Feltwell, N. Hamlin, S. Holroyd, K. Jagels, A. V. Karlyshev, S. Leather, S. Moule, P. C. Oyston, M. Quail, K. Rutherford, M. Simmonds, J. Skelton, K. Stevens, S. Whitehead and B. G. Barrell (2001). "Genome sequence of *Yersinia pestis*, the causative agent of plague." Nature **413(6855)**: 523-7.

Parret, A.H. and De Mot, R. (2002) "Bacteria killing their own kind: novel bacteriocins of *Pseudomonas* and other *Q-proteobacteria*." Trends Microbiol. **10:** 107-112.

Peel, M. M., D. A. Alfredson, J. G. Gerrard, J. M. Davis, J. M. Robson, R. J. McDougall, B. L. Scullie and R. J. Akhurst (1999). "Isolation, identification, and molecular characterization of strains of *Photorhabdus luminescens* from infected humans in Australia." J. Clin. Microbiol. **37(11)**: 3647-53.

N. Philippe. (2004) "Improvement of pCVD442, a suicide plasmid for gene allele exchange in bacteria." Plasmid **51**: 246–255

Schaller, A., R. Kuhn, P. Kuhnert, J. Nicolet, T. J. Anderson, J. I. MacInnes, R. P. Segers and J. Frey (1999). "Characterization of apxIVA, a new RTX determinant of *Actinobacillus pleuropneumoniae*." Microbiology **145(Pt 8)**: 2105-16.

Sharma, S., N. Waterfield, D. Bowen, T. Rocheleau, L. Holland, R. James and R. ffrench-Constant (2002). "The lumicins: novel bacteriocins from *Photorhabdus*

luminescens with similarity to the uropathogenic-specific protein (USP) from uropathogenic *Escherichia coli*." FEMS Microbiol Lett **214(2)**: 241-9.

Silva, C. P., N. R. Waterfield, P. J. Daborn, P. Dean, T. Chilver, C. P. Y. Au, S. Sharma, U. Potter, S. E. Reynolds and R. H. ffrench-Constant (2002). "Bacterial infection of a model insect: *Photorhabdus luminescens* and *Manduca sexta*." Cellular Microbiology **6(4)**: 329-339.

Sugai, M., Hatazaki, K., Mogami, A. (1999) "Cytotoxic necrotizing factor type 2 produced by pathogenic *Escherichia coli* deamidates a gln residue in the conserved G-3 domain of the rho family and preferentially inhibits the GTPase activity of RhoA and rac1." Infection and Immunity **67**: 6550–6557.

Tascon RI, Rodriguez-Ferri EF, Gutierrez-Martin CB, Rodriguez-Barbosa I, Berche P, and Vazquez-Boland JA. (1993) "Transposon mutagenesis in *Actinobacillus pleuropneumoniae* with a Tn10 derivative." J Bacteriol **175(17)**:5717-22.

Thaler, J.O., Baghdiguian, S. and Boemare, N. (1995) "Purification and characterization of xenorhabdicin, a phage tail-like bacteriocin, from the lysogenic strain F1 of Xenorhabdus nematophilus." Appl. Environ. Microbiol. **61:** 2049-2052.

Y. Uratani, T. Hoshino (1984) "Pyocin R1 inhibits active transport in *Pseudomonas aeruginosa* and depolarizes membrane potential." J. Bacteriol. **157**: 632–636.

Valens, M., Broutelle, A.C., Lefebvre, M. and Blight, M.A. (2002) "A zinc metalloprotease inhibitor, Inh, from the insect pathogen, *Photorhabdus luminescens*." Microbiology **148:** 2427-2437.

Waterfield, N., Daborn, P. J., and ffrench-Constant R. (2002). "Genomic islands in *Photorhabdus*" Trends in Microbiology **Vol 10 No 12**: 541-545.

Waterfield, N., A. Dowling, and ffrench-Constant R. (2001). "Oral toxicity of *Photorhabdus luminescens* W14 toxin complexes in *Escherichia coli*." Appl Environ Microbiol **67(11)**: 5017-24.

Waterfield, N. R., D. J. Bowen, J. D. Fetherston, R. D. Perry and R. H. ffrench-Constant (2001). "The *tc* genes of *Photorhabdus*: a growing family." Trends Microbiol **9(4)**: 185-91.

Waterfield N, Hares M, Yang G, Dowling A, and ffrench-Constant R. (2005) "Potentiation and cellular phenotypes of the insecticidal Toxin complexes of *Photorhabdus* bacteria." Cell Microbiol. **Mar;7(3)**:373-82.

Waterfield N.R., Daborn, P. J. and R.H. ffrench-constant. (2004) "Insect pathogenicity islands in the insect pathogenic bacterium *Photorhabdus*." Physiological Entomology **29**: 240–250

Weinrauch, Y. and A. Zychlinsky (1999). "The induction of apoptosis by bacterial pathogens." Annu Rev Microbiol **53:** 155-187.

Weitao, T., Dasgupta, S. and Nordstrom, K. (2000) "Role of the mukB gene in chromosome and plasmid partition in *Escherichia coli*." Mol Microbiol **38**: 392-400.

Wood, M.W., Rosqvist, R., Mullan, P.B., Edwards, M.H. and Galyov, E.E. (1996) "SopE, a secreted protein of *Salmonella dublin*, is translocated into the target eukaryotic cell via a sip-dependent mechanism and promotes bacterial entry." Mol Microbiol **22**: 327-338.

Zumbihl, R., Aepfelbacher, M., Andor, A., Jacobi, C. A., Ruckdeschel, K., Rouot, B. and Heesemann, J. (1999) "The cytotoxin YopT of *Yersinia enterocolitica* induces modification and cellular redistribution of the small GTP-binding protein RhoA." J Biol Chem **274**: 29289-93.